87p

SUMMARY REPORT

PERIOD 8 MAY 1963 – 15 JUNE 1964

STUDY OF ENERGY CONVERSION SYSTEMS

Contract No. NAS8-5392

Request No. TP 3-84158

Prepared for

NATIONAL AERONAUTICS and SPACE ADMINISTRATION

GEORGE C. MARSHALL SPACE FLIGHT CENTER

HUNTSVILLE, ALABAMA

by

SPACE and DEFENSE SCIENCES DEPT.

RESEARCH DIVISION

ALLIS-CHALMERS
MILWAUKEE, WISCONSIN

JUNE 15, 1964

FOREWORD

This report was prepared by the Aerospace Power Systems Section, Research Division, Allis-Chalmers Manufacturing Company, Milwaukee, Wisconsin under NASA Contract NAS8-5392. The work was administered under the direction of the Electrical Components and Power Supplies Section, Astrionics Division, NASA, Huntsville, Alabama. Mr. Eugene Cagle and Mr. Richard Boehme were the technical supervisors for NASA.

This Summary Report covers the work completed from 8 May 1963 to 15 June 1964.

Management direction at Allis-Chalmers included Mr. Will Mitchell, Jr., Director of Research; Dr. P. A. Joyner, Mr. D. T. Scag and Mr. W. W. Edens, Assistant Directors of Research. The project was supervised by Messrs. J. L. Platner, P. D. Hess and D. P. Ghere. The Project Leader is Mr. R. W. Opperthauser.

The report was written by Messrs R. W. Opperthauser, J. F. Euclide and was edited by Mr. E. L. Laskey.

Dr. J. Huff was the consultant for the gas chromatography analysis.

ABSTRACT

32209

A Static Moisture Removal System for the capillary membrane hydrogen-oxygen fuel cell was tested for feasibility and various aspects of its operation and performance were investigated.

A gas chromatograph was used to measure water vapor at various places in operating fuel cells. It was also used to measure hydrogen diffusion through the water removal membrane.

Studies of the system were made to determine optimum system configuration. Computer programs were written to determine minimum weights for various missions and for systems made up of fuel cells alone or fuel cells combined with batteries.

Comparisons were made between fuel cell systems and low temperature expansion systems as well as those formed by the combination of the two.

Weight comparisons were made between Dynamic and Static Moisture Removal Systems.

A weight analysis was performed for a lunar surface vehicle electrical power supply.

Author

SUMMARY

The theory of operation of the Allis-Chalmers hydrogen-oxygen capillary membrane fuel cell is presented. Product water removal by means of Static Moisture Removal is also discussed.

To test the feasibility of the Static Vapor Pressure Control system, single cells and four-cell modules were operated. All the cells performed satisfactorily for the duration of the tests which varied in length from 60 to 220 hours. Peak current densities ran as high as 214 ma/cm^2.

A gas chromatograph has been applied to the measurement of vapor pressure within operating fuel cells to study the mechanism of water removal by the Static Moisture Removal system.

The gas chromatograph was also applied to the measurement of the rate of diffusion of hydrogen through the water removal membrane. Although a variety of water removal cavity pressures were studied, the observed diffusion rates were uniformly low. For a typical 2 KW unit, hydrogen lost through diffusion would amount to about 0.1% of the hydrogen consumed at rated load.

A general analysis has been performed for the optimization of fuel cell operating parameters to obtain the minimum weight of the fuel cell system. Analytical solutions were obtained for the special case of linearized cell voltage-current density characteristics and uniform power requirement. A significant reduction in system weight, particularly for long missions, was achieved through this optimization.

A digital computer program was developed for determining the optimum fuel cell operating parameters to obtain the minimum weight system for general mission requirements. This program was applied to a variety of missions, and it is apparent from the results that generalized conclusions regarding optimum operating conditions cannot be drawn. However, for 28 ± 2 volt systems which have a sufficiently uniform power output, an equation was derived by fitting curves to computer-calculated data.

Systems studies were performed on the low-temperature expansion cycle for space vehicle auxiliary power supplies. This system generates electrical power by expanding gas in a prime mover which drives an electrical generator. The working fluid is cryogenically-stored hydrogen, and the heat source is the energy dissipated in the vehicle electrical load. Studies were general in nature. Power ratings from 1 to 20 kilowatts and mission lengths to 500 hours were considered. Positive displacement expanders and turbines were studied in combination with both the super-critical and sub-critical storage of hydrogen. These systems were compared with fuel cell systems using static moisture removal and either evaporative coolers

or radiators. Hybrid systems incorporating fuel cells and low-temperature expansion cycles were studied for missions in which the energy dissipated by the electrical load and the waste heat from the fuel cell are assumed to be the total vehicle cooling load.

The lightest of these power systems for missions on the order of a lunar flight or longer was shown to be a fuel cell with a radiator used as a heat sink. Hybrid systems allow a relatively high degree of independence from the vehicle external environment and appear promising for missions involving extreme environmental conditions.

Power systems consisting of fuel cells combined with batteries for peak power requirements were considered in determining the minimum-weight system. For the simple case of a two power-level requirement, the duration of the peak power output was determined for which the combined system and the straight fuel cell system are equal in weight.

Comparison of the Static and Dynamic Vapor Pressure Control systems was made. A range of power levels from 1 to 10 kilowatts and mission durations up to 500 hours were included. The static system is lighter for all missions requiring 5 kilowatts or less and for systems up to 10 kilowatts with mission durations greater than three hours.

A weight analysis of an electrical power system for a lunar surface vehicle (the Mobile Laboratory) was made. The power system consisted of fuel cells for primary power and silver-cadmium batteries for fuel cell start-up and peak load power. Fuel cell water in sufficient quantity to supply crew requirements was considered. Excess water was used as a heat sink to decrease the radiator size.

TABLE OF CONTENTS

ILLUSTRATIONS

1.0 INTRODUCTION

This is the Summary Report submitted under Contract Number NAS8-5392. The purpose of the contract was to perform research and development to determine the optimum design approach for Energy Conversion Systems for Advanced Saturn Vehicle Missions.

To accomplish this purpose, studies and experimental investigations were conducted in the following general areas:

a. Experimental and theoretical investigations were performed on a hydrogen-oxygen capillary fuel cell employing Static Moisture Control for product water removal. The feasibility and performance characteristics of this system were investigated for possible application as a vehicle auxiliary power source.

b. A weight and feasibility study was conducted on a system combining a fuel cell and a cryogenic hydrogen-oxygen heat transfer cycle. The Lunar Logistics Mission concept will be used as a typical mission on which to base the study.

c. A study was made of other possible energy conversion systems which may compare favorably or may be used advantageously with the fuel cell system.

d. The Static Moisture Control fuel cell system was compared with the recirculating reactant Vapor Pressure Control fuel cell previously developed for MSFC. The study was made to show the advantages and disadvantages of each system considered as a complete vehicle subsystem.

The comparison studies were general in nature and pertained to weights, volumes, loads, duration of operation, and operational difficulties. These studies were performed after initial feasibility studies and experimental investigations were made for the fuel cell system employing Static Moisture Control.

2.0 STATIC MOISTURE REMOVAL CONCEPT

A fuel cell is an electrochemical converter that converts the chemical energy of fuels directly into electrical energy, reactant products and heat. In the case of the hydrogen-oxygen fuel cell the reaction product is water. Efficient and sustained operation of the hydrogen-oxygen fuel cell requires that the product water and excess heat produced be removed from the fuel cell system in a controlled manner.

Static Moisture Removal is a method whereby the product water formed in a capillary fuel cell is removed from the fuel cell stack entirely by diffusion mechanisms and is therefore static in nature. The water is removed from the cell stack in the vapor state and may be ejected directly to space, thereby significantly reducing the heat burden imposed upon a fuel cell cooling system. As an alternative, the water vapor may be condensed, and in this case, the advantages of the static system are applicable, but the overall system thermal advantage is not gained.

The following discussion describes the details of the Static Moisture Removal Concept.

2.1 Capillary Membrane Fuel Cell

The basic cell consists of two porous nickel electrodes separated by the capillary-membrane which holds the electrolyte. The most distinctive feature of this cell is the capillary membrane. The capillary potential of the membrane, defined as the differential pressure required to force liquid from its largest pore, is approximately 100 psi. This property enables the membrane to hold the electrolyte in its proper position between the electrodes, effectively separates the reactant gases and allows communication of water and hydroxyl ions between the electrodes.

When a cell is assembled, the asbestos membrane is filled with electrolyte and swells to a larger volume than when dry. During assembly, the associated electrodes are compressed against the asbestos membrane and some of the electrolyte is squeezed from the membrane into the electrodes, forming the necessary catalyst-electrolyte interfaces. The asbestos membrane remains filled with electrolyte.

In an operating hydrogen-oxygen cell, water is formed at the interface of catalyst, electrolyte and hydrogen. If not removed, the water dilutes the electrolyte until it fills the entire pore volume (overwetting). If the water is removed from the cell faster than it is formed, the electrolyte volume decreases to the point where the wetting front begins to recede into the asbestos (overdrying). Both overwetting and overdrying are accompanied by deterioration of cell performance.

The capillary membrane fuel cell is capable of satisfactory performance over a range of electrolyte concentrations and volumes. The range of controllable electrolyte concentrations is a function of thickness and porosity

of the fuel cell electrodes and the amount and concentration of the electrolyte added to the capillary membrane at the time of construction. Experiments have shown that the average electrolyte concentration should be maintained between 27% and 45% for adequate performance, with a concentration of 35% being near optimum. The typical performance of an individual cell as a function of average electrolyte concentration is shown in Figure 1. If the temperature is held constant, then the water vapor pressure of the electrolyte increases rapidly as the electrolyte becomes more dilute, as shown in Figure 2. This characteristic forms the basis for Static Moisture Removal.

2.2 Principle of Operation of Static Moisture Removal

Static Moisture Removal utilizes the principles of gas and liquid diffusion, the changing vapor pressure characteristics of the Allis-Chalmers fuel cell under load, and the capillary nature of the KOH impregnated membrane.

In this system, a second asbestos capillary membrane (the water transport membrane) containing concentrated KOH solution is placed adjacent to, but slightly separated from, the hydrogen electrode as illustrated in Figure 3. Hydrogen and oxygen reactants are dead-ended into the cell. The cavity located behind the water transport membrane is evacuated to a pressure corresponding to the vapor pressure of the desired maximum concentration of KOH solution to be maintained in the cell. A differential pressure of about 23 psi exists across the water transport membrane, but this presents no problem since pressure differentials approaching 100 psi are required to expel the KOH solution from the water transport membrane. Hydrogen will not flow through the water transport membrane because the pores of the membrane are completely filled with KOH solution. Water vapor is transported from the cell electrode to the water transport membrane by diffusion through the reactant gas due to the difference in vapor pressure between the cell electrolyte and the KOH contained in the water transport membrane. The water vapor condenses and tends to dilute the KOH in the water transport membrane. This causes the pressure in the evacuated cavity adjacent to the water transport membrane to increase. As the water vapor pressure rises, water vapor is removed from the cavity (and, hence, from the cell) to an external condenser where it may be condensed to potable water. If there is no need for the water, it may be vented directly to space and by so doing remove approximately 35% of the heat formed within the cell.

The controlled removal of water from the cell may be accomplished simply by maintaining a fixed pressure upon the water transport membrane corresponding to the vapor pressure of the maximum concentration of the electrolyte desired in the operating cell. The maintenance of the fixed pressure prevents excess water removal. When the cell operates under load and produces water, the subsequent dilution of the cell electrolyte and rapid rise in electrolyte vapor pressure provides the driving force for water removal.

REPRESENTATIVE FUEL CELL PERFORMANCE AT VARIOUS ELECTROLYTE CONCENTRATIONS

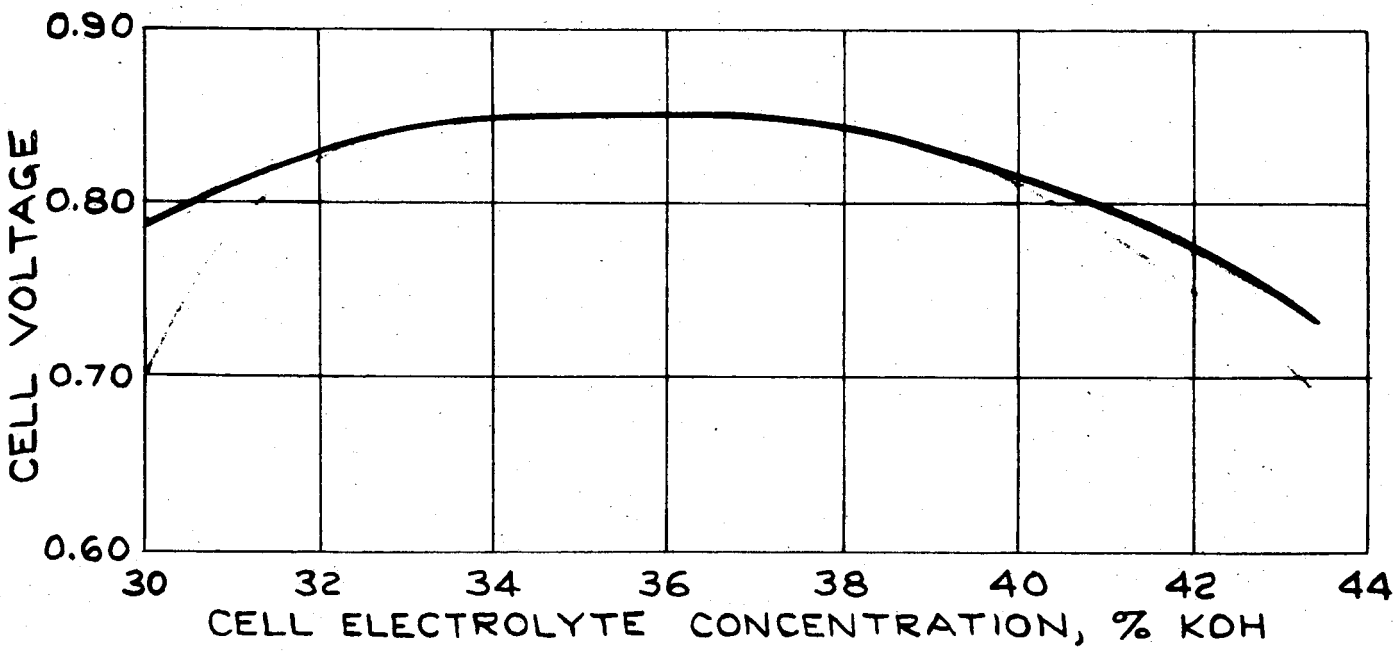

CELL PRESSURE = 30 PSIA
CELL TEMPERATURE = 200° F.

FIGURE 1

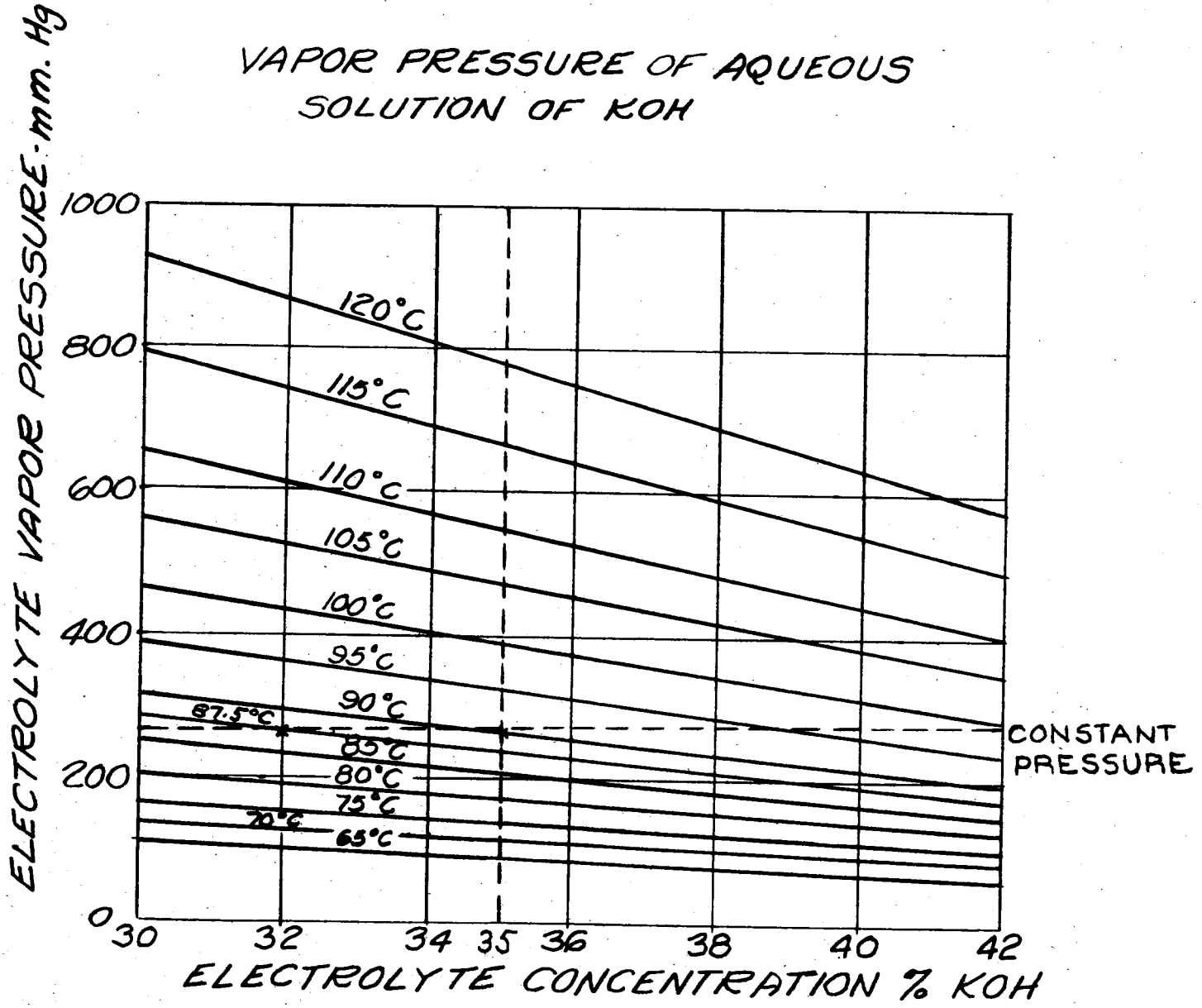
VAPOR PRESSURE OF AQUEOUS SOLUTION OF KOH
ELECTROLYTE VAPOR PRESSURE-mm. Hg
1000
800
600
400
200
0
120°C
115°C
110°C
105°C
100°C
95°C
90°C
87.5°C
85°C
80°C
75°C
70°C
65°C
CONSTANT PRESSURE
30
32
34
35
36
38
40
42
ELECTROLYTE CONCENTRATION % KOH

FIGURE 2

FUEL CELL CONSTRUCTION USING STATIC MOISTURE REMOVAL SYSTEM

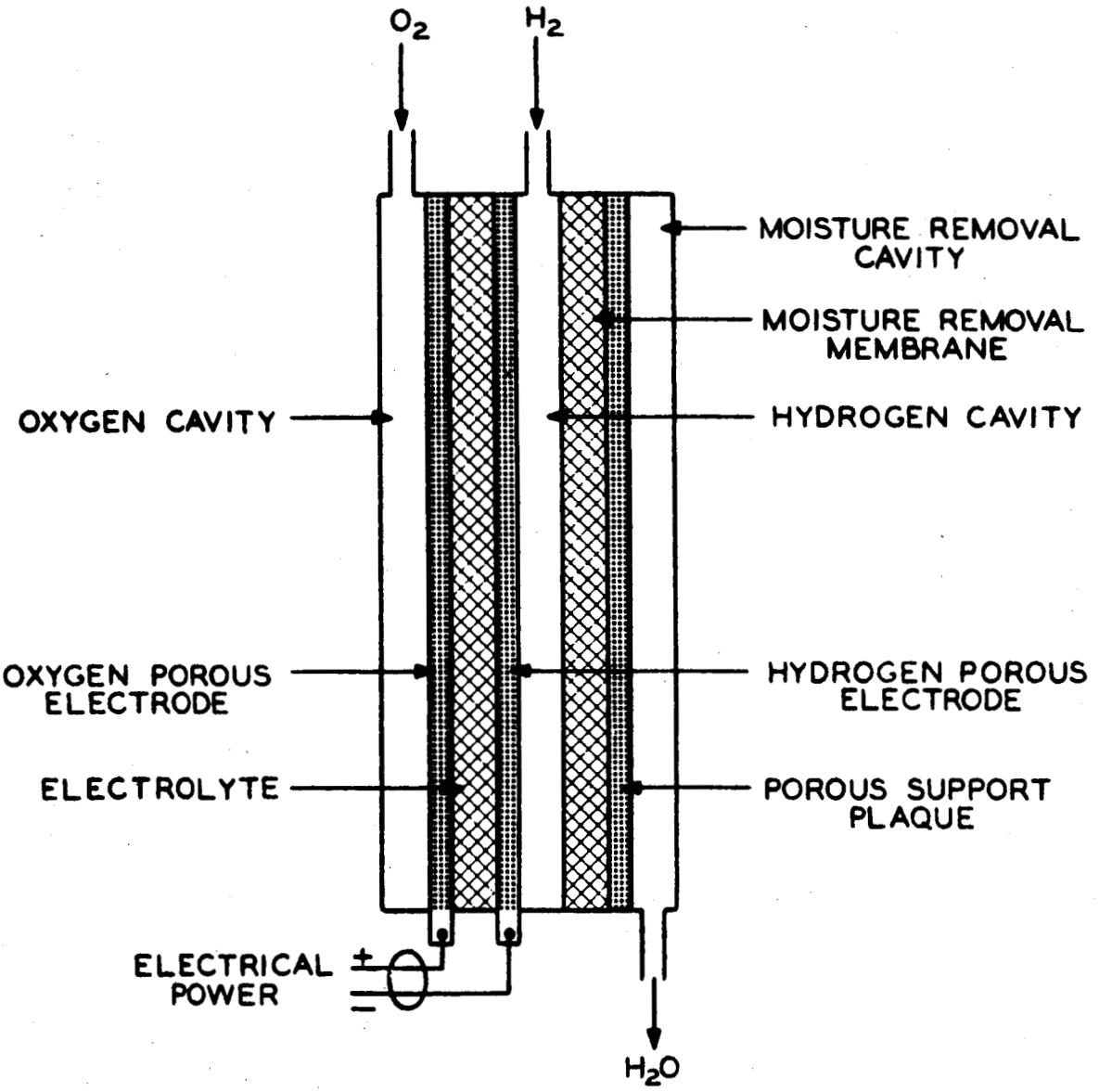

FIGURE 3

The transport of water through the water transport membrane and across the cell electrolyte membrane produces KOH gradients in the cell. The gradient existing in an operating cell is shown diagrammatically in Figure 4.

2.3 Thermal Considerations

A thermal advantage may be gained with the Static Vapor Pressure Control system as previously stated. Also, because the water vapor pressure exhibited by the water in the KOH solution is a function of temperature, the successful operation of this static system requires temperature control within acceptable limits.

The following discussion defines the thermal advantage that may be gained and predicts the allowable temperature variation in an operating cell.

Characteristic of fuel cell operation, some waste heat is produced during the fuel cell reaction. The amount of waste heat produced depends on the thermal efficiency and the power output as shown in the following analysis.

The thermal efficiency, assuming 100% current efficiency, is defined as:

$$\eta_t = \frac{\Delta F}{\Delta m \ \Delta H^o} \times 100 \qquad (2\text{-}1)$$

ΔH^o = Enthalpy of reaction per mole of product at the standard state *

ΔF = Observed free energy change (observed electrical work)

Δm = Determined moles of reactant consumed

* Standard state - H_2 at 1 atm

O_2 at 1 atm

25° C

Hydroxyl ion activity = 1

Explicit definition of ΔH and ΔF requires an explicit definition of reactions taking place in the fuel cell. Operating temperature must also be defined since the thermodynamic properties (ΔF and ΔH) are temperature dependent properties. Therefore, for the following discussions the efficiencies are based on the following defined reactions:

$$H_2 \text{ (aq.)} + 1/2\, O_2 \text{ (aq.)} \xrightarrow{25\,^\circ C} H_2O \text{ (liq.)}$$

DIAGRAM OF KOH GRADIENTS IN FUEL CELL
WITH STATIC VAPOR PRESSURE CONTROL

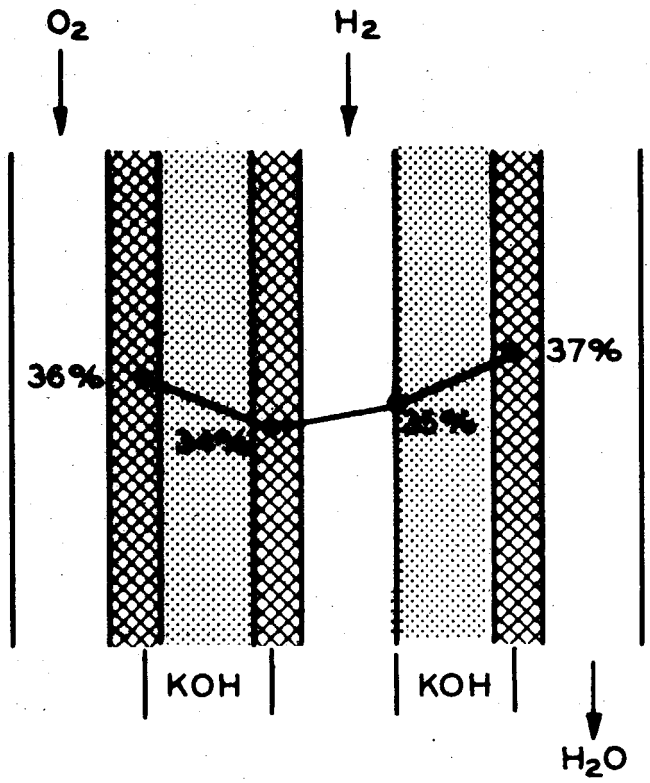

FIGURE 4

Since

$$\Delta F \approx - n \Delta m \mathcal{F} E, \qquad (2\text{-}2)$$

n	=	equivalents per mole of reactant
$\mathcal{F}$	=	Faradays constant (96, 500 coulombs per equivalent)
E	=	Observed voltage

ΔF is proportional to E and ΔF^{o} is proportional to E^{o} (1.23 volts). Thus, with reactants and products at 25° C and one atmosphere, the thermal efficiency may be determined from the relationship:

$$\eta_t = \frac{E}{1.23} \times \frac{F^{o}}{H^{o}} \qquad (2\text{-}3)$$

$$\eta_t = 0.67\ E \qquad (2\text{-}4)$$

ΔF^{o}	=	maximum theoretical free energy change per mole of product at standard state
E^{o}	=	theoretical open circuit voltage

E/1.23 is the ratio of the actual cell voltage to the theoretical cell voltage. The last term, F^{o}/H^{o}, is the maximum possible thermal efficiency at standard state. The total rate of heat production is dependent on the load and efficiency, as previously stated, and can be easily determined from the relationship:

$$Q = P \left(\frac{1}{\eta_t} - 1 \right) \qquad (2\text{-}5)$$

From Equation (2-4) and (2-5):

$$Q = P \left(\frac{1}{0.67\ E} - 1 \right) \qquad (2\text{-}6)$$

where

P	=	power in watts
Q	=	total rate of heat production in watts

In a space application, heat energy will be ejected from the system with the water vapor, if the water vapor is vented to space, thereby significantly reducing the heat burden to be dissipated by a vehicle cooling system. The amount of heat energy exhausted in this manner is in direct relationship to the amount of water produced in the cell and to the cell temperature.

The relationship for determining the amount of water produced in an operating cell is:

$$M = 0.337\ AN \qquad (2\text{-}7)$$

where

A = ampere hours

N = number of cells

M = mass of water, gms.

When the total heat energy of water at 93.3° C is taken as 0.757 watt-hours/gram, then the heat rejected with the vapor is:

$$Q' = 0.256\ AN \qquad (2\text{-}8)$$

where

Q' = heat rejected in the product water vapor in watt-hours

The heat rejected in this manner usually amounts to about thirty-five percent of the total heat burden.

If the water vapor is condensed and collected, the heat of condensation must be rejected from the fuel cell system by the fuel cell cooling system and the thermal advantage is no longer gained.

The maximum permissible temperature variation may be predicted by referring to Figure 2. Assuming an acceptable operating range of KOH concentration from 32 to 40 percent, the temperature can vary from 87.5° C to 95° C about the optimum operating point of 90° C (35% KOH).

3.0 STATIC MOISTURE REMOVAL FEASIBILITY STUDIES

From the discussion in the preceding section, it is apparent that the concept of Static Moisture Removal offers considerable advantages as a space vehicle auxiliary power system. A two phase program was undertaken to determine the feasibility of the system:

a. Performance tests were conducted to confirm the operation of the Static Moisture Removal method, and to establish operating characteristics of the system.

b. A system weight analysis was made and optimum operating parameters were determined.

The results of this program are presented in the following sections.

3.1 Performance Tests

Performance testing of the Static Vapor Pressure Moisture Removal system was conducted to accomplish the following:

a. Verify the diffusion transport of the product water from the cell.

b. Determine if the rate of water removal by static means is sufficient for practical current densities.

c. Evaluate and compare water removal from the hydrogen and from the oxygen electrode.

d. Evaluate the feasibility of controlling multi-cell units.

Testing was conducted in two steps. The first step utilized single-cell units. Although in some cases cell construction differed between tests, the same basic control system (Figure 5) was used for all tests. In the second step, four-cell modules were assembled and operated. A brief summary of the tests conducted follows:

Test Number 1

A single cell was constructed as shown in Figure 6. This cell operated for a total of 68 hours at a current density of 93.5 ma/cm^2 with an average voltage of 0.82 volt. Water was removed from the hydrogen side of the cell for 41 hours and the oxygen side for 27 hours.

Test Number 2

This single cell, with the same construction as in Test Number 1, operated for a total of 77 hours at a current density of 88 ma/cm^2 with an average

STATIC FOUR CELL MODULE SYSTEM SCHEMATIC

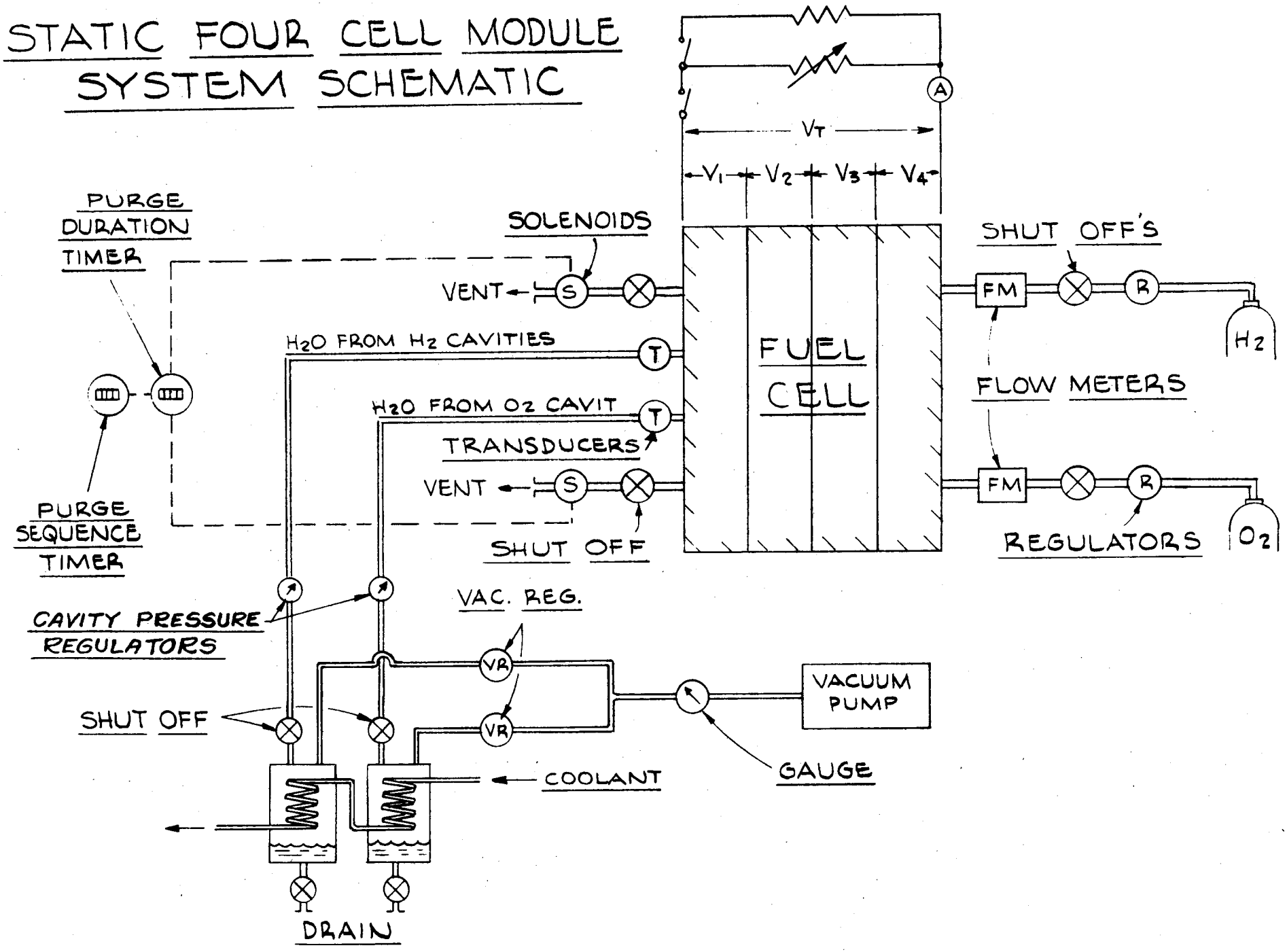

FIGURE 5

ISK63128-6
PLB 5-8-63

STATIC MOISTURE REMOVAL SYSTEM FOR THE H_2-O_2 FUEL CELL

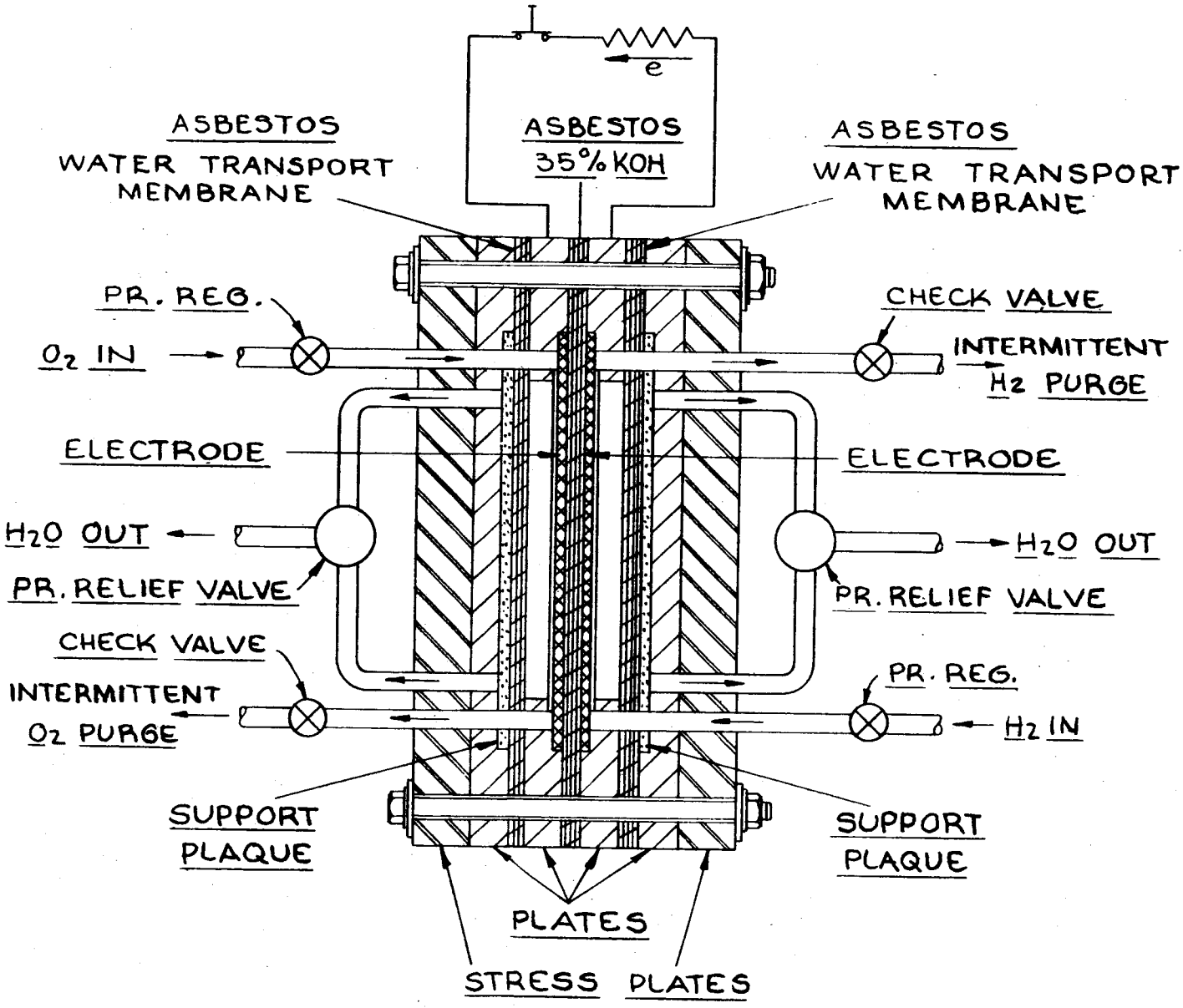

ALLIS-CHALMER MFG. CO.
APS-RESEARCH 12-11-62 EAG

FIGURE 6

voltage of 0.80 volt. Water was removed from both sides of the cell for the first 34.5 hours and from the oxygen side for the remainder of the test.

Test Number 3

A third cell, constructed in the same manner as the previous two cells, was operated for 135 hours at a current density of 88 ma/cm^2 with an average potential of 0.81 volt with water removal effected on the oxygen side (except for short periods at the beginning and end of the test).

Test Number 4

A four-cell module was assembled as shown in Figure 7. The module operated satisfactorily for approximately 115 hours. The load was increased in steps as shown in Figure 8. The capability of the Static Moisture Removal system to control a multi-cell module under a variety of load conditions was demonstrated in this experiment.

Test Number 5

This four cell module was operated for 220 hours with a cyclic load profile. Manifolding was altered to permit individual regulation of hydrogen and oxygen cavity pressures. Figure 9 illustrates the overall module performance with the cavity vapor pressure expressed in terms of equivalent KOH concentration. A summary of total module operating time at the various loads is shown in the following table:

TABLE 1

PERFORMANCE SUMMARY OF FEASIBILITY TEST NUMBER 5

Load Current (amperes)	Current Density (ma/cm^2)	Potential (volts)	Power (watts)	Time (hours)
20	47.3	3.51	70.3	77.0
30	70.9	3.38	101.4	74.5
40	94.5	3.28	131.0	68.5
		TOTAL TIME		220.0 hours

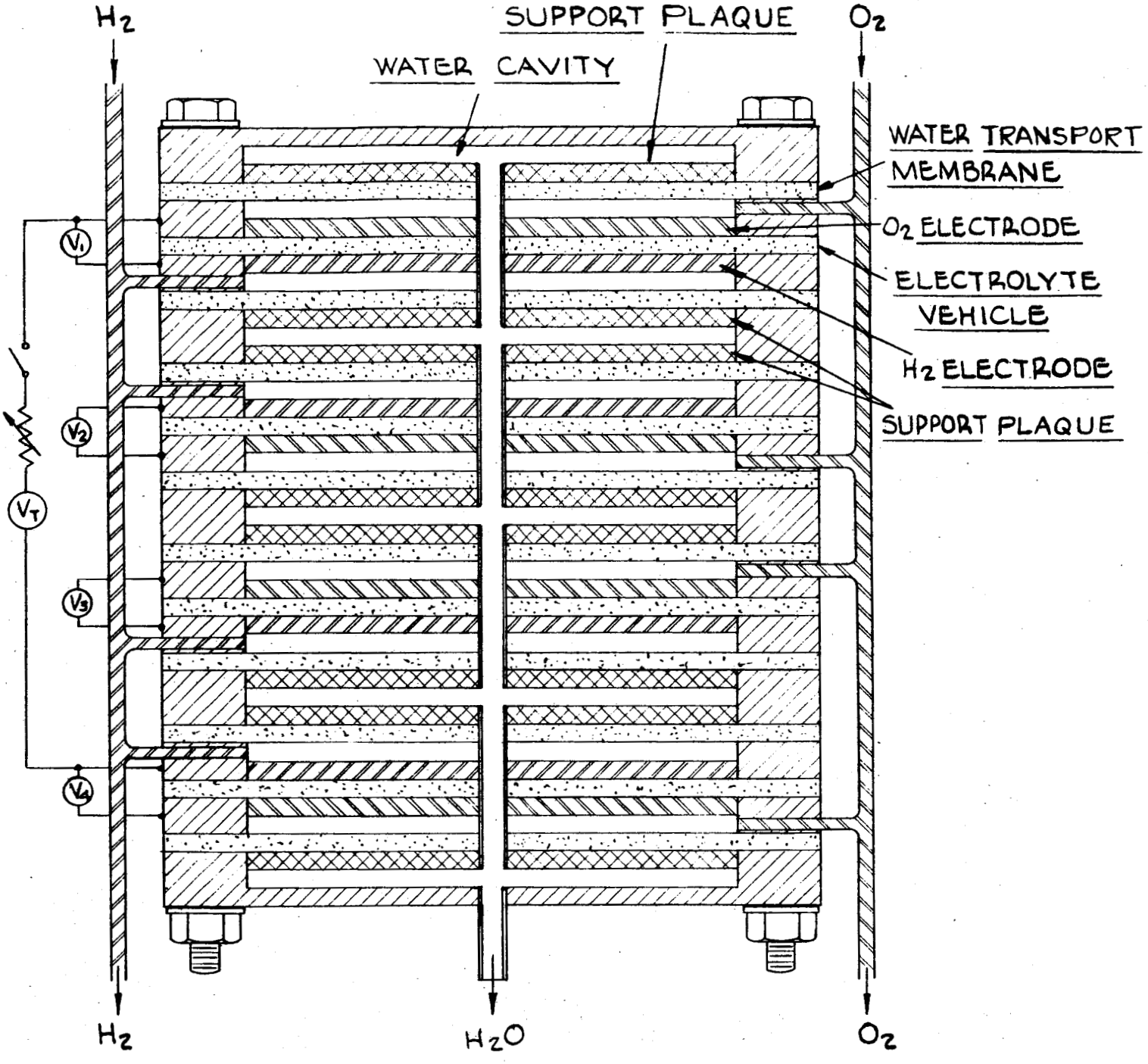

STATIC MOISTURE REMOVAL SYSTEM FOR THE H_2-O_2 FUEL CELL FOUR CELL MODULE

ALLIS-CHALMERS MFG. CO.
SADS- RESEARCH 2/11/63 PLB

FIGURE 7

FUEL CELL PERFORMANCE OF STATIC VAPOR PRESSURE CONTROL - FOUR CELL MODULE TEST NO. 4

MODULE TEMPERATURE = 85° C

MODULE PRESSURE = 2.02 ATMOS.

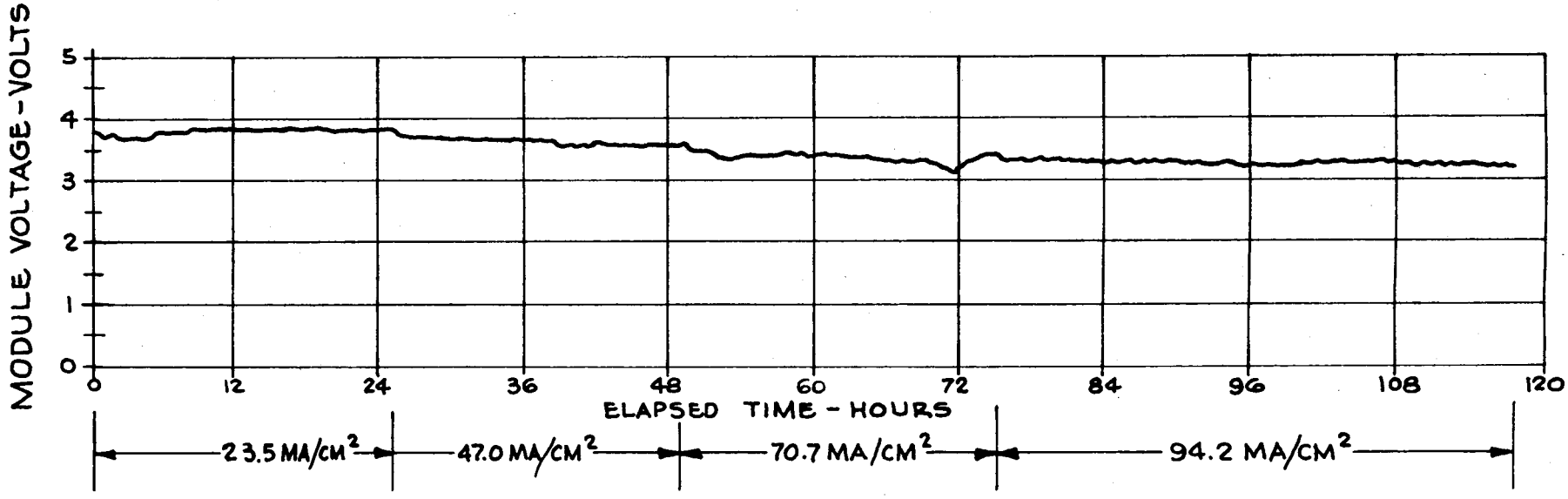

FIGURE 8

FOUR CELL MODULE TEST - Nº 5
STATIC VAPOR PRESSURE CONTROL

CELL PRESSURE = 2 ATMOS.
CELL TEMPERATURE = 79° C

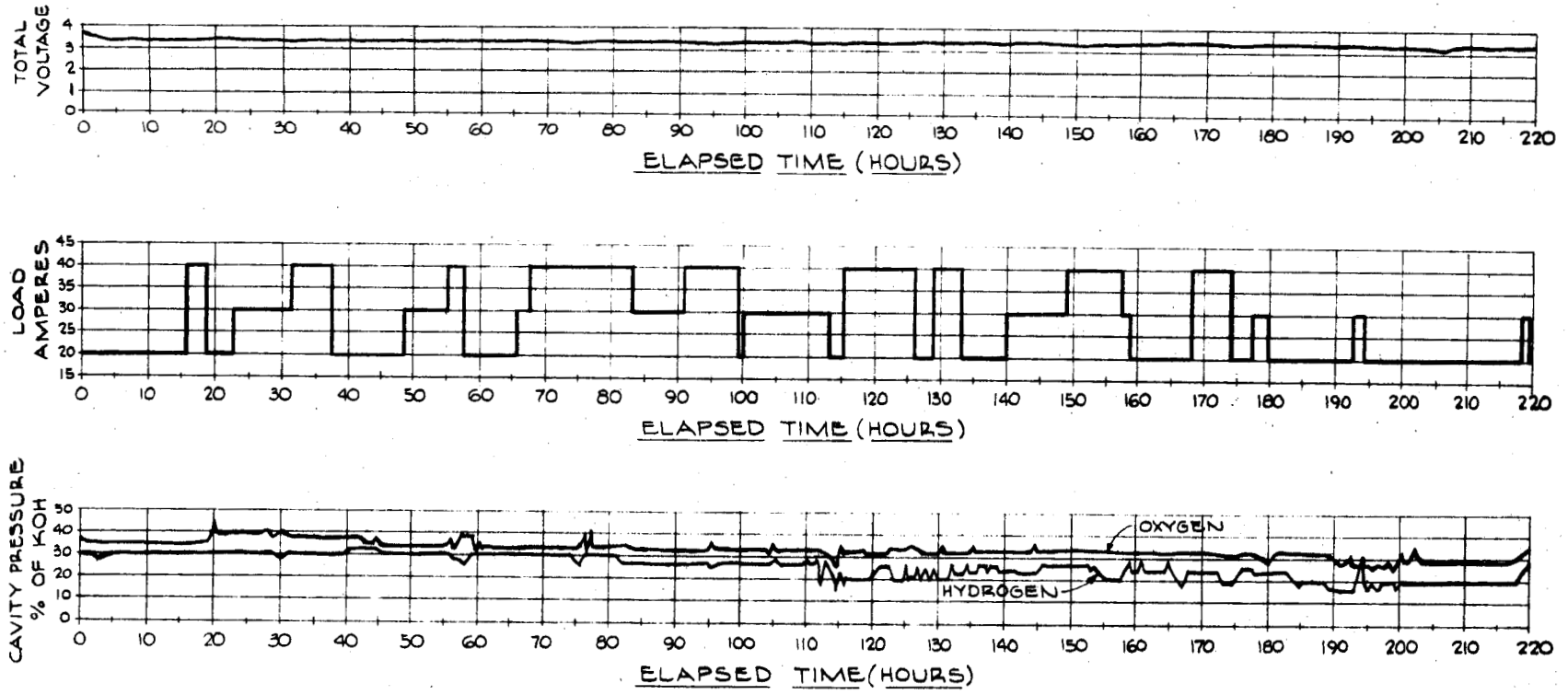

FIGURE 9

Test Number 6

This four-cell module was assembled using improved electrodes and a new plate designed specifically for the Static Vapor Pressure Control system. The new design provided improved heat removal, water removal and sealing. The module was operated for over 100 hours at various loads ranging from 10 amperes (24 ma/cm^2) to 90.5 amperes (214 ma/cm^2). Potential at 10 amperes was 3.70 volts; at 90.5 amperes it averaged 3.00 volts varying between 2.97 volts and 3.08 volts. The module performance is shown graphically in Figure 10. The performance of this module was definitely superior to previous modules.

3.2 Cell Vapor Pressure Tests

Fundamental studies of the Static Moisture Removal method were performed with the aid of a gas chromatograph. This instrument was calibrated to measure water vapor pressure in the hydrogen and oxygen cavities. The techniques developed for studying the Dynamic Vapor Pressure Control method (conducted under Contract Number NAS8-2696) were adapted to this study.

The test apparatus is shown schematically in Figure 11. The apparatus consists of four general sections:

a. The fuel cell with necessary controls and instrumentation.

b. A temperature-controlled sampling system.

c. The gas chromatograph with controls and carrier gas conditioner.

d. A calibration bath.

Gas samples are taken from either the hydrogen or the oxygen cavity and are analyzed with the gas chromatograph. The water removal cavity pressure is monitored by a pressure transducer. Operation of the cell is thus monitored while load, cavity pressure and cell temperature are varied in turn. The data obtained was reduced and plotted by a computer.

Initial experiments involved extracting gas samples from the end of the cell opposite the reactant inlet ports. These samples were analyzed by the gas chromatograph technique to determine the amount of water vapor contained in the gas. High water vapor measurements at this point indicated the presence of very dilute electrolyte solutions in the cell. Since the presence of such dilute solutions throughout the cell was inconsistent with other cell performance measurements, it was concluded that electrolyte concentration gradients must exist in the direction of reactant flow.

FOUR CELL MODULE TEST Nº6
STATIC VAPOR PRESSURE CONTROL

CELL PRESSURE = 254 ATM.
CELL TEMPERATURE = 93.4 °C

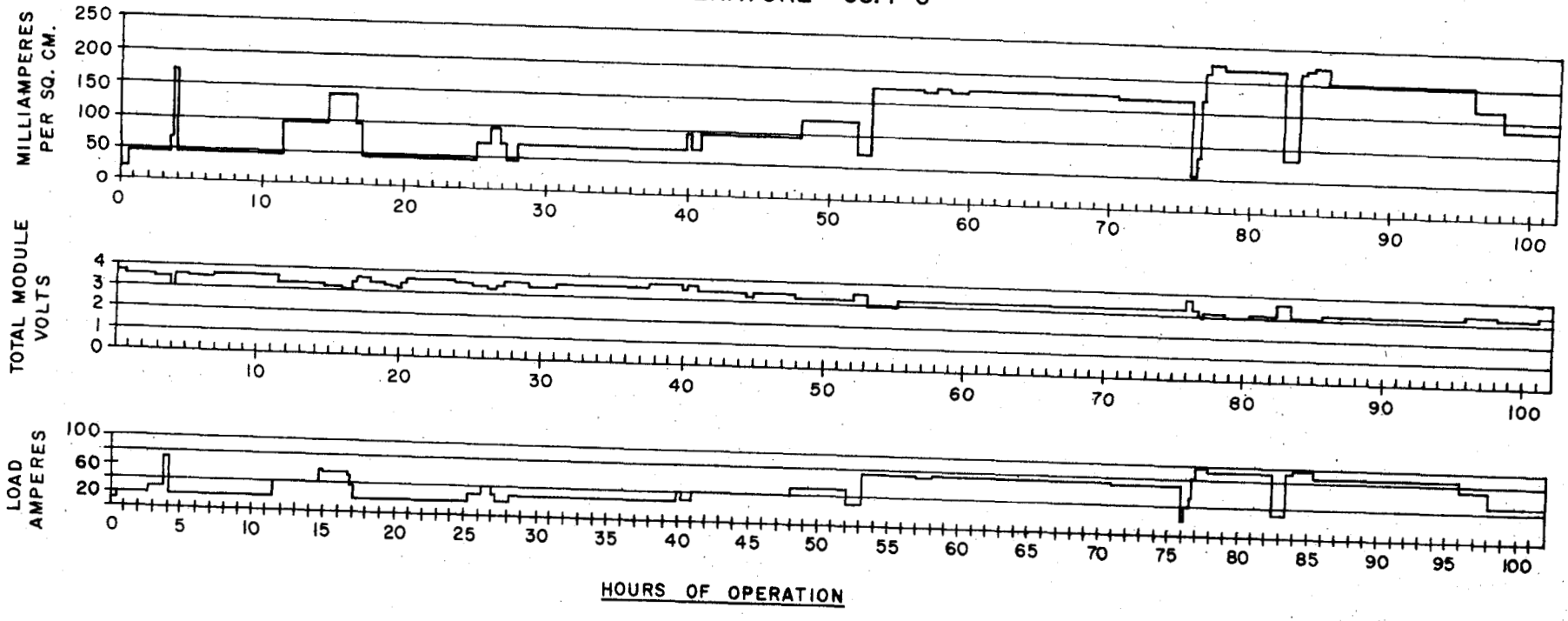

FIGURE 10

GAS CHROMATOGRAPH TEST SET UP
STATIC VAPOR PRESSURE CONTROL SYSTEM

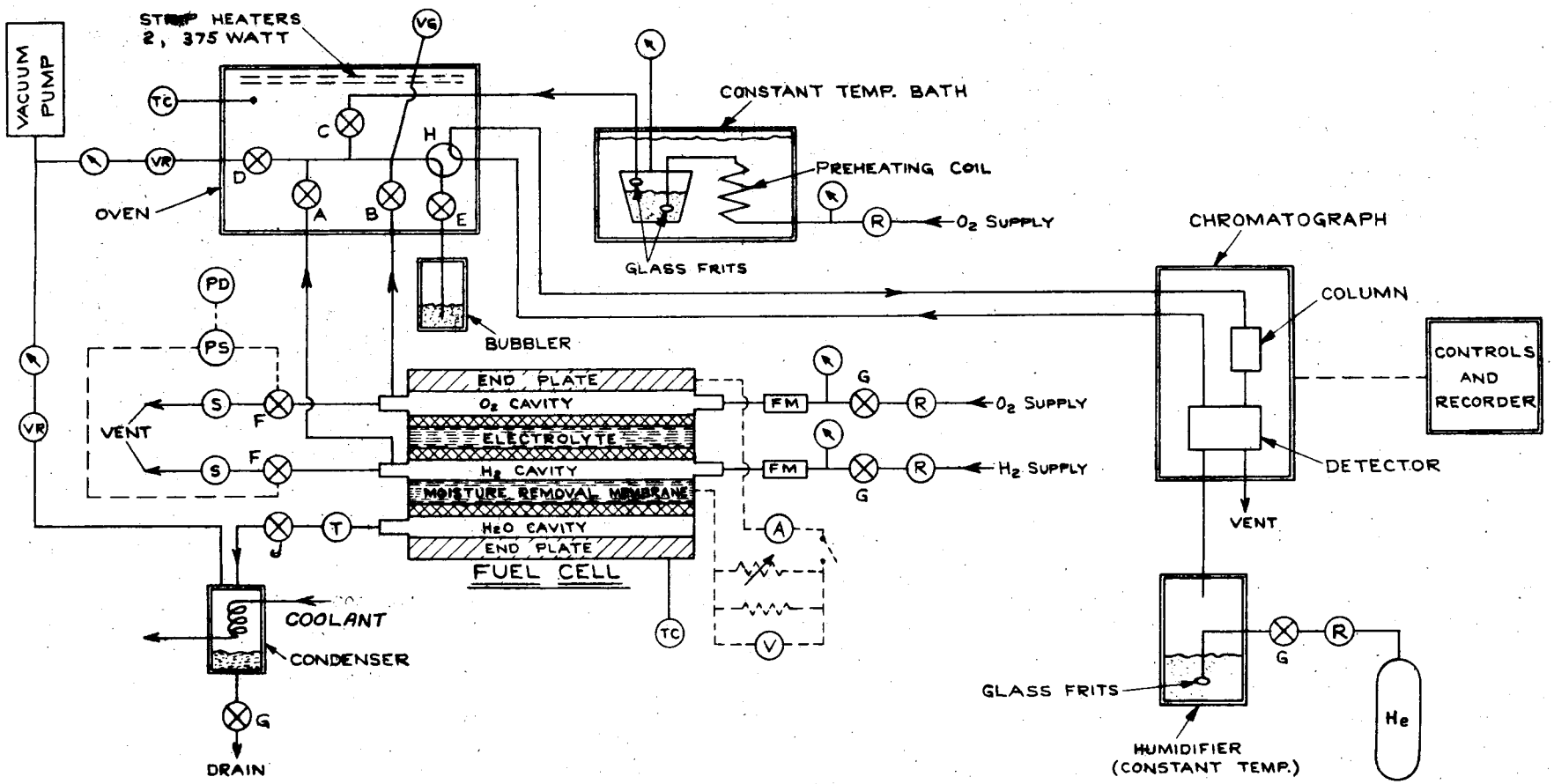

A - H_2 SAMPLING VALVE
B - O_2 SAMPLING VALVE
C - BATH SAMPLING VALVE
D - VACUUM VALVE
E - EXPANDER VALVE
F - PURGE RATE VALVES
G - SHUT OFF VALVES
H - SAMPLE VALVE
J - CAVITY PRESSURE REGULATOR

(PD) PURGE DURATION TIMER
(PS) PURGE SEQUENCE TIMER
(VR) VAPOR REGULATOR
(S) SOLENOID VALVE
(T) TRANSDUCER
(TC) TEMPERATURE CONTROLLER
(VG) VACUUM GAUGE
(R) REGULATOR

FM FLOW METER

(V) VOLTMETER
(A) AMMETER
⊗ NEEDLE VALVE
GAUGE

FIGURE 11

W.P.B. 5-16-63
2-SK-63154-1

To investigate electrolyte concentration gradients, three additional sample taps were located along the center line of the more accessible oxygen side of the cell. These taps were located as indicated in Figure 12A. Samples taken at these locations established an electrolyte concentration gradient as shown in Figure 12 B. At a current density of 116 ma/cm^2, the concentration varied from 53% KOH near the reactant inlet to 12% KOH at the opposite end. The concentration at the end opposite the reactant inlet has been found to decrease with increasing current density.

This gradient is believed to develop as a result of the dry inlet gases picking up water from the electrolyte near the inlet and depositing a portion of this water farther downstream. The test cell was arranged with parallel reactant flow; both reactant inlets were at the same end of the cell. Normal practice is to connect the cell for counterflow of reactants. Parallel flow was used in this instance so that samples from both reactant cavities could be obtained from the same end of the cell. A significant reduction in the electrolyte concentration gradient can be realized with the counterflow arrangement.

Starting from an open-circuit condition with uniform electrolyte concentration, about four hours of operation was required at 116 ma/cm^2 before a steady state condition was reached and the reported electrolyte concentrations were observed. During this time, cell voltage decreased by about 1.2%. Hence, the observed electrolyte gradients do not greatly affect cell operation at the tested current density. At higher current densities and at elevated operating temperatures, the gradients would increase, and the effects on cell performance would be more pronounced. For these conditions, the counterflow of reactants should significantly improve performance. Extreme conditions may require a modification in reactant manifolding design.

3.3 Hydrogen Diffusion Tests

Removal of the reaction-product water from a cell operating with Static Vapor Pressure Control is accomplished by diffusion of the water through a capillary membrane saturated with a solution of KOH. The water removal membrane has a capillary potential, defined as the differential pressure required to force liquid from the largest pore, approaching 100 psi. Operating conditions in the cell impose only about 30 psi differential pressure. Hence, saturation of the membrane will prevail as long as a sufficient volume of liquid is maintained in contact with it. Since all the pores are filled with liquid, there is no path for the flow of hydrogen through the membrane. Some hydrogen will reach the water removal cavity by diffusion through the liquid in the pores of the water removal membrane. However, the quantity of hydrogen lost in this manner should be very small.

During the performance tests reported in Paragraph 3.1, there was no measurable rate of hydrogen loss to the water removal cavity. Analyzing the exhaust from the water removal cavity of an operating cell with the gas chromatograph allows a more sensitive measurement of hydrogen diffusion. (A schematic diagram of the test apparatus used to check these results is shown in Figure 13).

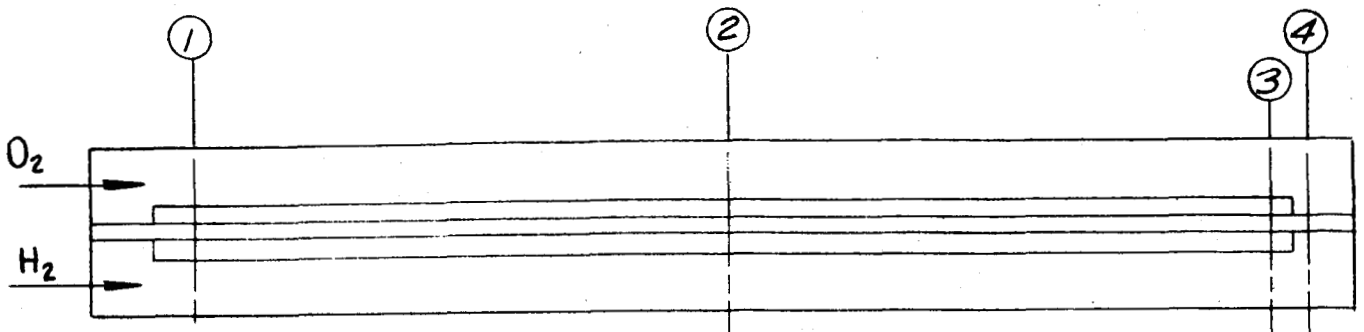

"A" LOCATION OF SAMPLE TAPS FOR CELL VAPOR PRESSURE CHROMATOGRAPH TESTS

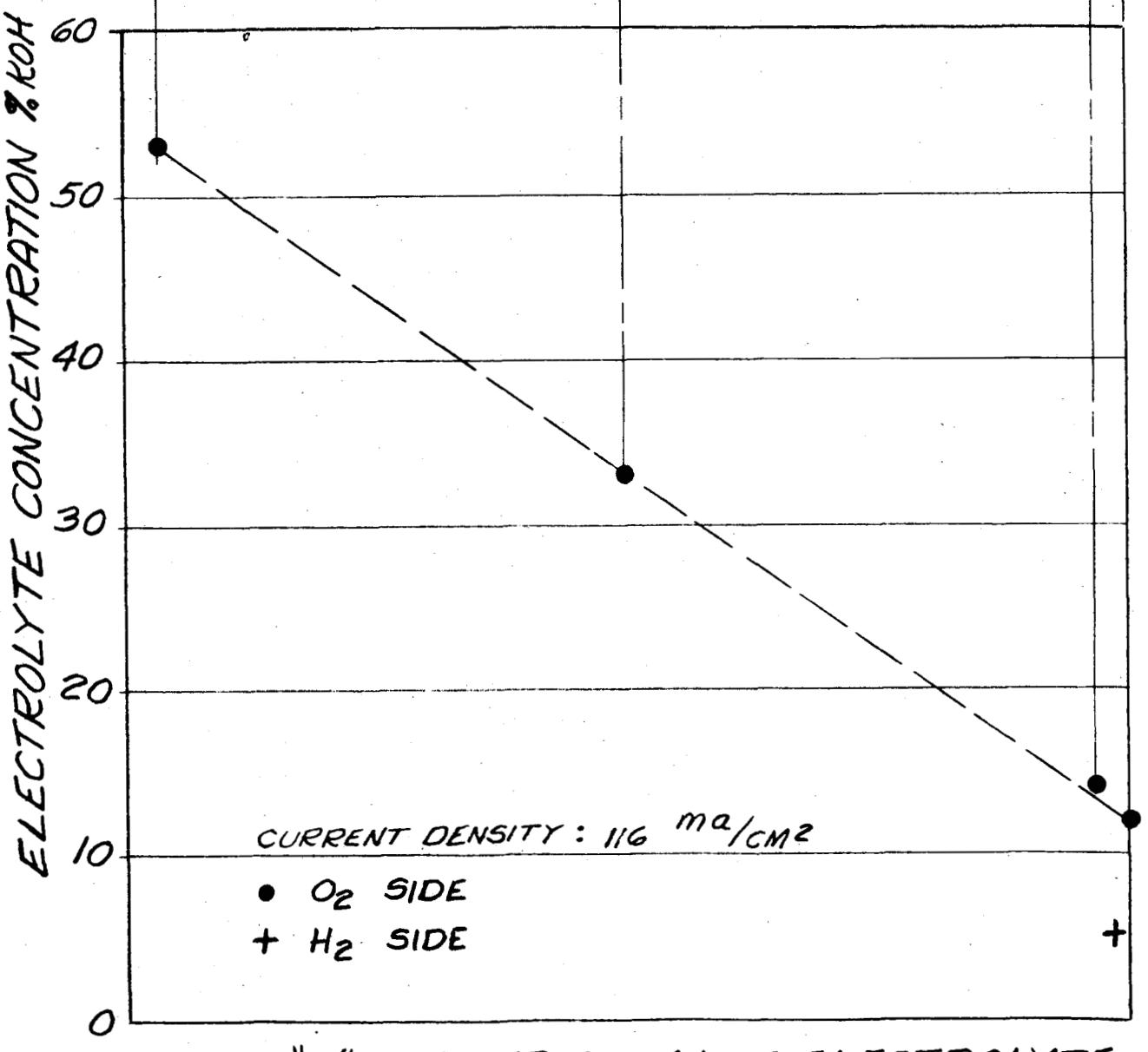

"B" DISTRIBUTION OF ELECTROLYTE CONCENTRATION IN A OPERATING CELL

FIGURE 12

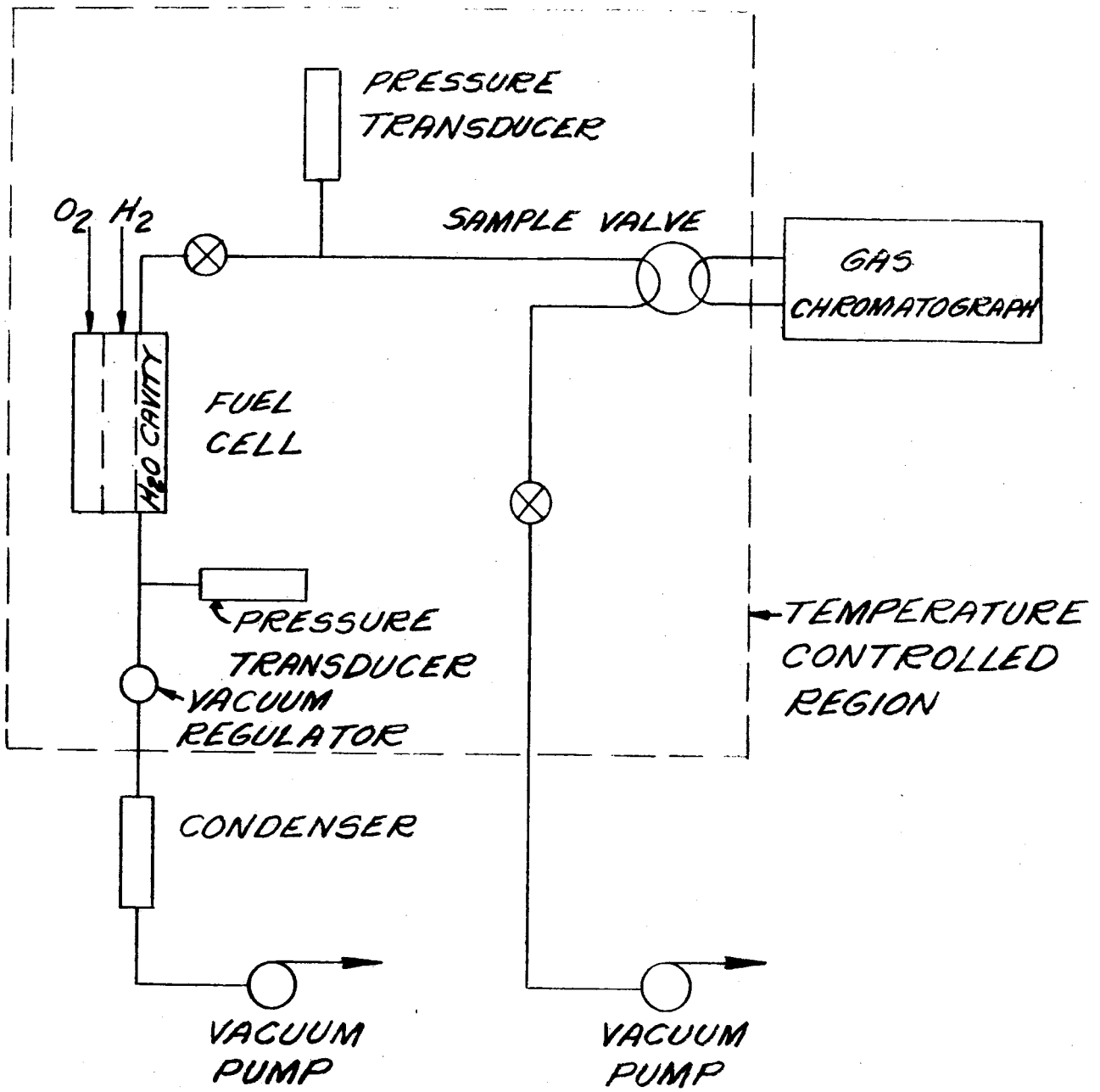

SCHEMATIC FOR HYDROGEN-DIFFUSION GAS CHROMATOGRAPH TESTS

FIGURE 13

Helium is commonly used as a carrier gas in the gas chromatograph but cannot be used to measure hydrogen diffusion because the thermal conductivity of hydrogen and helium are nearly identical. Nitrogen was used initially for this investigation but the chromatograph was later modified to operate with argon as a carrier. The sensitivity of the chromatograph is increased three times by changing from nitrogen to argon.

From results of feasibility tests on cells using Static Moisture Removal, it was apparent that hydrogen diffusion rates corresponding to 1% of stoichiometric consumption, or less, could be expected. This required calibration of the chromatograph for hydrogen partial pressures on the order of 2 mm of mercury. Calibration was accomplished by filling the sample loop with hydrogen and then evacuating the loop to the desired pressure as indicated on a McLeod vacuum gage. The calibration, shown in Figure 14, was quite linear over the range of zero to 5 mm of mercury.

Measurement of hydrogen diffusion through the membrane has been performed for water-removal cavity pressures corresponding to the vapor pressure of electrolyte solutions ranging from 33% KOH to 46% KOH. The cell temperature was 93° C and the reactant pressure was 2.5 atmospheres.

Observed diffusion rates have been so small (about 1/4% stoichiometric consumption) as to approach the limit of sensitivity of the gas chromatograph. Some scatter of data has resulted from this effect and from the variable rate of water vapor removal from the cavity due to the operation of the cavity vacuum regulator. However, the partial pressure of hydrogen observed in samples of the water-removal cavity vapor have consistently been below 1 mm, with the mean value about 0.5 mm.

There appears to be a tendency for increased diffusion of hydrogen as the KOH concentration is increased in the water removal membrane. This effect is shown in Figure 15. Data points shown in the figure are the mean values of at least eight measurements. This effect is explained by the lower volume (due to higher concentration) of electrolyte in the water removal membrane through which diffusion must occur. The rate of diffusion for a water removal cavity pressure corresponding to 46% KOH appeared to be about 50% greater than that observed at a pressure corresponding to 33% KOH. It should be noted that the 46% KOH setting is considerably "drier" than the optimum setting of 35% to 40% KOH.

For the range of cavity pressure normally used, the rate of hydrogen diffusion was found to be about 0.08gm/hr per square meter of active cell area. For a typical 2 KW unit design, hydrogen loss would amount to about 2.3 gm per day. This rate corresponds to 0.1% of hydrogen consumption at rated load.

If product water is condensed and collected, the condenser will require periodic purging of accumulated hydrogen. Only the liquid water will be transported to the site of consumption and the amount of hydrogen contained in the liquid water phase will be on the order of one part in ten

GAS CHROMATOGRAPH CALIBRATION FOR HYDROGEN WITH ARGON AS THE CARRIER GAS

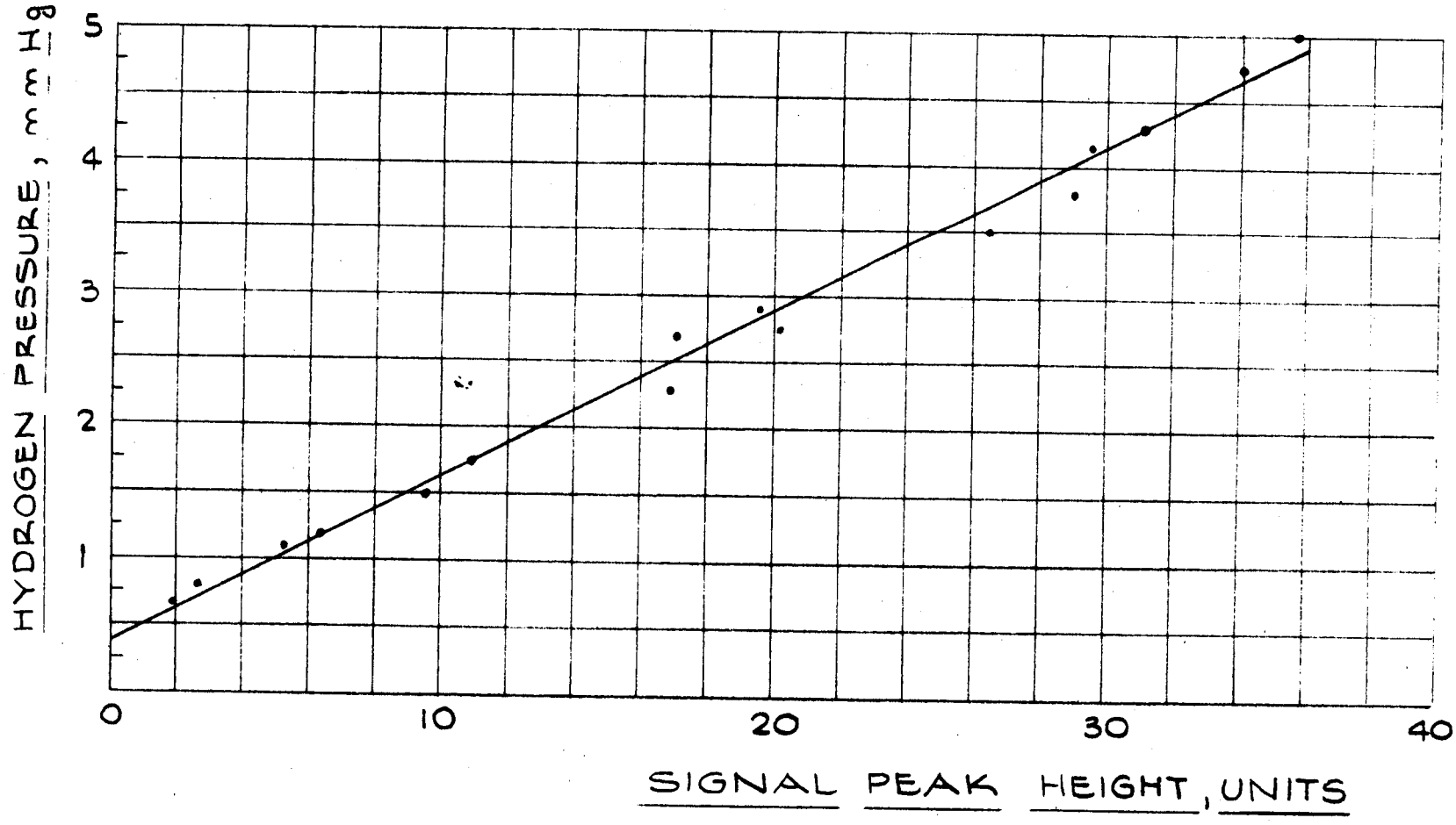

FIGURE 14

RATE OF HYDROGEN DIFFUSION THROUGH WATER REMOVAL MEMBRANE

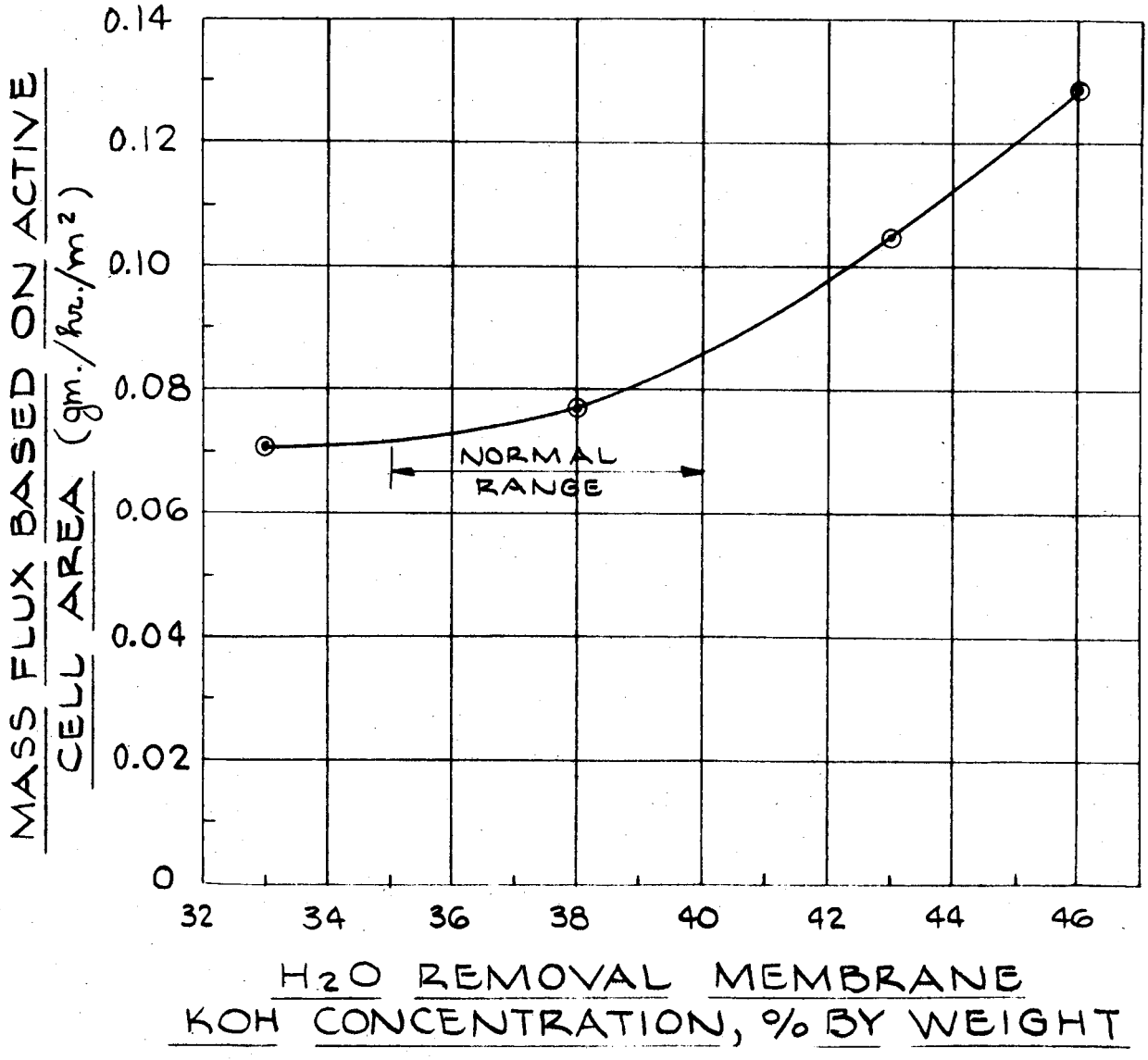

FIGURE 15

million. Hence there would be no hazardous accumulation of hydrogen in the cabin when the product water was used for crew consumption. Water can also be removed on the oxygen side of the cell to further reduce the possibility of any hydrogen entering the cabin.

3.4 Test Program Summary

Static Moisture Removal was shown to be sufficiently rapid to support current densities in excess of 214 ma/cm^2. Water removal from either the hydrogen or oxygen electrode is possible.

All performance was found to equal or exceed the performance obtained with the recirculating reactant system. Multi-cell stacks exhibited stable operation. Performance of individual cells within a stack was generally more uniform than obtainable with the recirculating system.

Diffusion of hydrogen through the water removal membrane occurs at a very low rate. Loss of hydrogen in this manner is far less than would be consumed to power parasitic loads for moisture removal in the recirculating reactant system.

3.5 Determination of Optimum Parameters

A fuel cell power system is composed of three major subsystems:

a. Fuel cell subsystem

b. Fuel storage and supply subsystem

c. Heat sink subsystem.

At a constant rate of power output, the weight of each subsystem can be expressed as a function of cell operating voltage. A value of cell voltage will exist for which the system weight is a minimum.

As the power requirement varies during a mission, the cell output voltage will also vary. It then becomes necessary to express the voltage at each power level in terms of the voltage at some convenient value of power (usually the maximum power level). Determination of optimum system weight may then be performed with respect to this voltage.

Generally, a power system is required to supply a range of loads while maintaining voltage regulation within tolerable limits. This requirement imposes additional restraints on the cell voltage which may prevent operation at the optimum value.

An analysis has been made for the determination of an optimum weight for the general hydrogen-oxygen fuel cell power system with non-uniform power

requirements, voltage tolerance limitations, and non-linear cell voltage vs. current density characteristics. The large number of computations required to determine the optimum system weight requires use of a digital computer and programming of the problem has been accomplished.

Before developing the program, useful results were obtained analytically by making certain simplifying assumptions:

a. The power output of the system is constant and continuous for the duration of the mission.

b. The cell voltage vs. current density characteristic of the cell may be approximated by a straight line.

c. The weight of a cell is proportional to the cell geometrical area.

The nomenclature used in the analysis is as follows:

A	=	Cell area, cm^2
$\mathcal{F}$	=	Faraday constant, amp-hr (number of cells)/kg H_2
J	=	Current density, amp/cm^2
K	=	Constant portion of the weight of auxiliaries, kg
P	=	Power, watts
S	=	Slope of linear approximation of voltage-current density curve, volt cm^2/amp (number of cells)
S_A	=	Auxiliary weight constant, kg/watt
S_C	=	Cell weight factor, kg/cm^2 (number of cells)
S_F	=	Fuel storage subsystem weight factor, kg/kg H_2
T	=	Mission time, hours
V	=	Voltage of a single cell, volts/cell
V_o	=	Open circuit voltage for linear approximation of voltage-current density curve, volts/cell
W_A	=	Weight of auxiliaries, kg
W_C	=	Weight of cell stack, kg
W_F	=	Weight of fuel storage subsystem, kg

W_R = Weight of radiator, kg

W_T = Total system weight, kg

3.5.1 Cell Weight

The linearized voltage vs. current density characteristic of the cell may be represented by:

$$V = V_o - S\,J \tag{3-1}$$

Cell weight is given by the product of the cell area and cell weight factor:

$$W_C = A\,S_C = \frac{P}{V\,J}\,S_C = \frac{P\,S}{V\,(V_o - V)}\,S_C \tag{3-2}$$

3.5.2 Fuel Supply Subsystem Weight

Weight of the fuel supply subsystem can be related to the weight of hydrogen consumed:

$$W_F = \frac{P\,T}{V\,\mathcal{F}}\,S_F \tag{3-3}$$

where:

$$S_F = \mathcal{f}\,(P,\ T,\ V)$$

An expression for S_F was obtained by fitting a curve to a plot of S_F for supercritical storage vs. weight of hydrogen required. Substituting the resulting expression in Equation (3-3) the weight of the fuel supply subsystem is:

$$W_F = \frac{36,500}{\mathcal{F}} + \frac{11.3}{\mathcal{F}}\,\frac{P\,T}{V} + \frac{.079}{\mathcal{F}}\,\frac{T^{\frac{5}{3}}\,P^{\frac{2}{3}}}{V^{\frac{2}{3}}} \tag{3-4}$$

3.5.3 Weight of Heat Sink Subsystem

The type of heat sink selected for a particular mission will depend upon such factors as mission duration, heat load, vehicle configuration, and vehicle environment. Studies of a general nature can adequately consider only the first two of these factors.

Deployed-type radiators were employed in this analysis. This type of radiator was chosen because of its light weight and the availability of optimized design information[1]. Based on an average coolant temperature of 280° K and a probability of successful mission completion of 0.9999, the weight of the radiator is given by:

$$W_R = 8.60 \times 10^{-6} \frac{P^{1.533} T^{0.50}}{V^{1.533}} \qquad (3\text{-}5)$$

3.5.4 Weight of Auxiliaries

The weight of the auxiliaries may be expressed as the sum of a constant term (representing such items as valving, controls, and structural components) and a term which is proportional to power output (representing such items as heat exchangers and plumbing capacity. Hence the auxiliary weight is given by:

$$W_A = K + S_A P \qquad (3\text{-}6)$$

3.5.5 Total System Weight

The weight of the complete system is the sum of the weights of all of the subsystems:

$$W_T = W_C + W_F + W_R + W_A \qquad (3\text{-}7)$$

$$W_T = \frac{P S S_c}{V (V_o - V)} + \frac{3.65 \times 10^5}{\mathcal{F}} + \frac{11.3}{\mathcal{F}} \frac{P T}{V} + \frac{0.079}{\mathcal{F}} \frac{P^{\frac{2}{3}} T^{\frac{5}{3}}}{V^{\frac{1}{3}}} + 8.60 \times 10^{-6} \frac{P^{1.533} T^{0.5}}{V^{1.533}} + K + S_A P \qquad (3\text{-}8)$$

3.5.6 Minimum System Weight

Differentiating Equation (3-8) with respect to V and equating the result to zero:

$$\frac{d W_T}{d V} = PSS_c \left[\frac{1}{V (V_o - V)^2} - \frac{1}{V^2 (V_o - V)} \right]$$

$$- \frac{11.3 PT}{\mathcal{F} V^2} - \frac{0.0527 T^{\frac{5}{3}} P^{\frac{2}{3}}}{\mathcal{F} V^{\frac{5}{3}}}$$

$$- 1.32 \times 10^{-5} \frac{P^{1.533} T^{0.5}}{V^{2.533}} = 0 \qquad (3\text{-}9)$$

Constants in Equation (3-8) have been evaluated for projected Static Moisture Removal fuel cell designs. The voltage vs. current density characteristic used, Figure 16, was obtained in tests on single cells and is expected to be representative of operating systems by 1968. Two straight lines were fitted to the voltage vs. current density curve in order to obtain more accurate representation over the entire range of voltages. The values are:

S_C = 2.96×10^{-3} kg/cm^2 (number of cells)

S_A = 9.0×10^{-4} kg/watt

$\mathcal{F}$ = 2.67×10^{-4} amp-hr (number of cells)/kg H_2

$V \geq 0.84$ volt

V_o = .985 volt/(number of cells)

S = .465 volt cm^2/amp (number of cells)

$V < 0.84$ volt

V_o = .900 volt/cell

S = .186 volt cm^2/amp (number of cells)

Substituting these values in Equation (3-9), the optimum voltage may be obtained for any mission duration and power requirement. Results for a wide range of these parameters are given in Figure 17.

Weight of the optimized system can be obtained by solving Equation (3-8) using the optimum voltage obtained from Equation (3-9). Optimized system weights are given in Figure 18. The weight reductions obtained through optimization are also illustrated. The non-optimized system weights are based on a cell potential which is the optimum voltage for a ten hour mission.

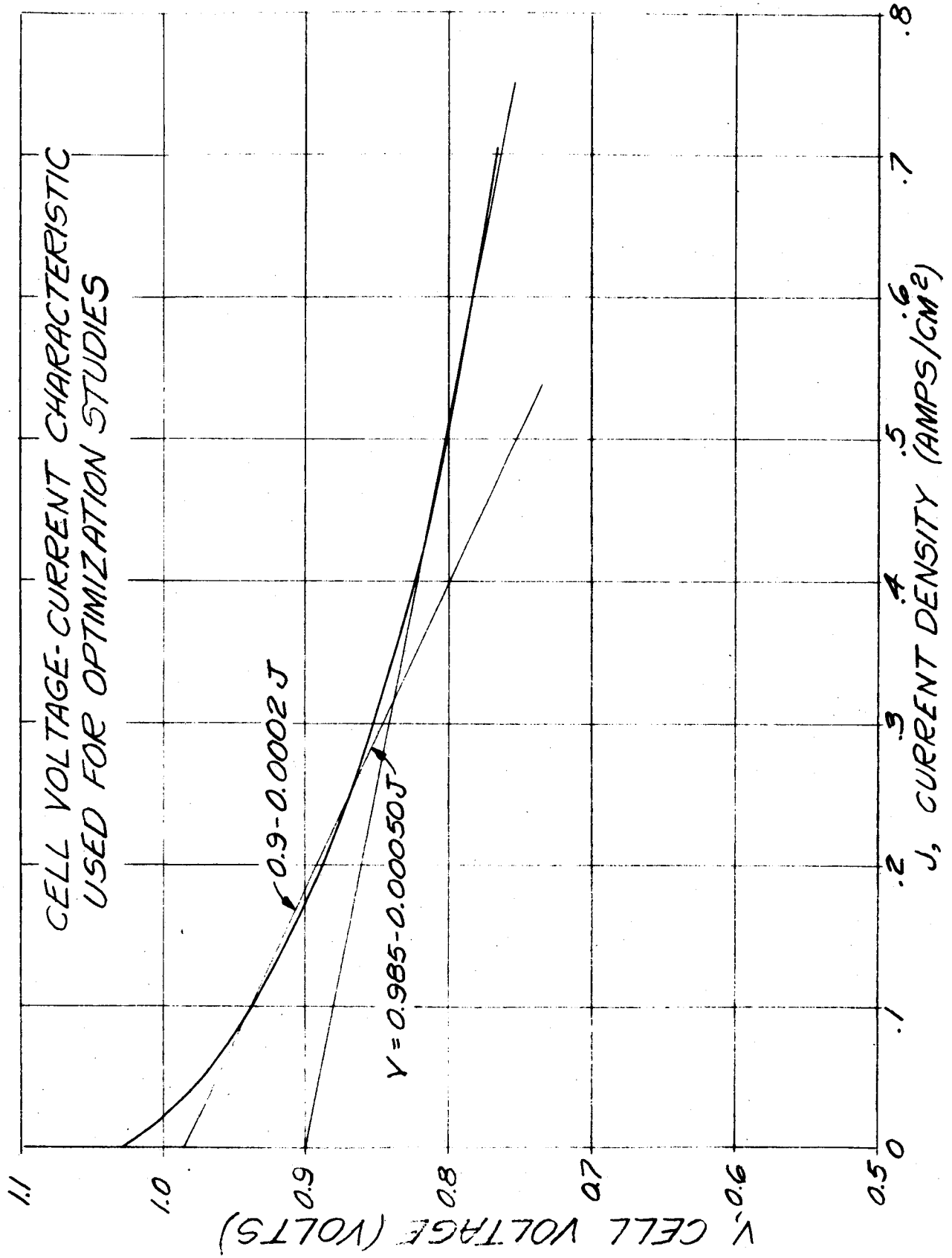
CELL VOLTAGE-CURRENT CHARACTERISTIC
USED FOR OPTIMIZATION STUDIES
V, CELL VOLTAGE (VOLTS)
J, CURRENT DENSITY (AMPS/CM²)
1.1
1.0
0.9
0.8
0.7
0.6
0.5
0
.1
.2
.3
.4
.5
.6
.7
.8
0.9-0.0002 J
Y = 0.985-0.00050J

FIGURE 16

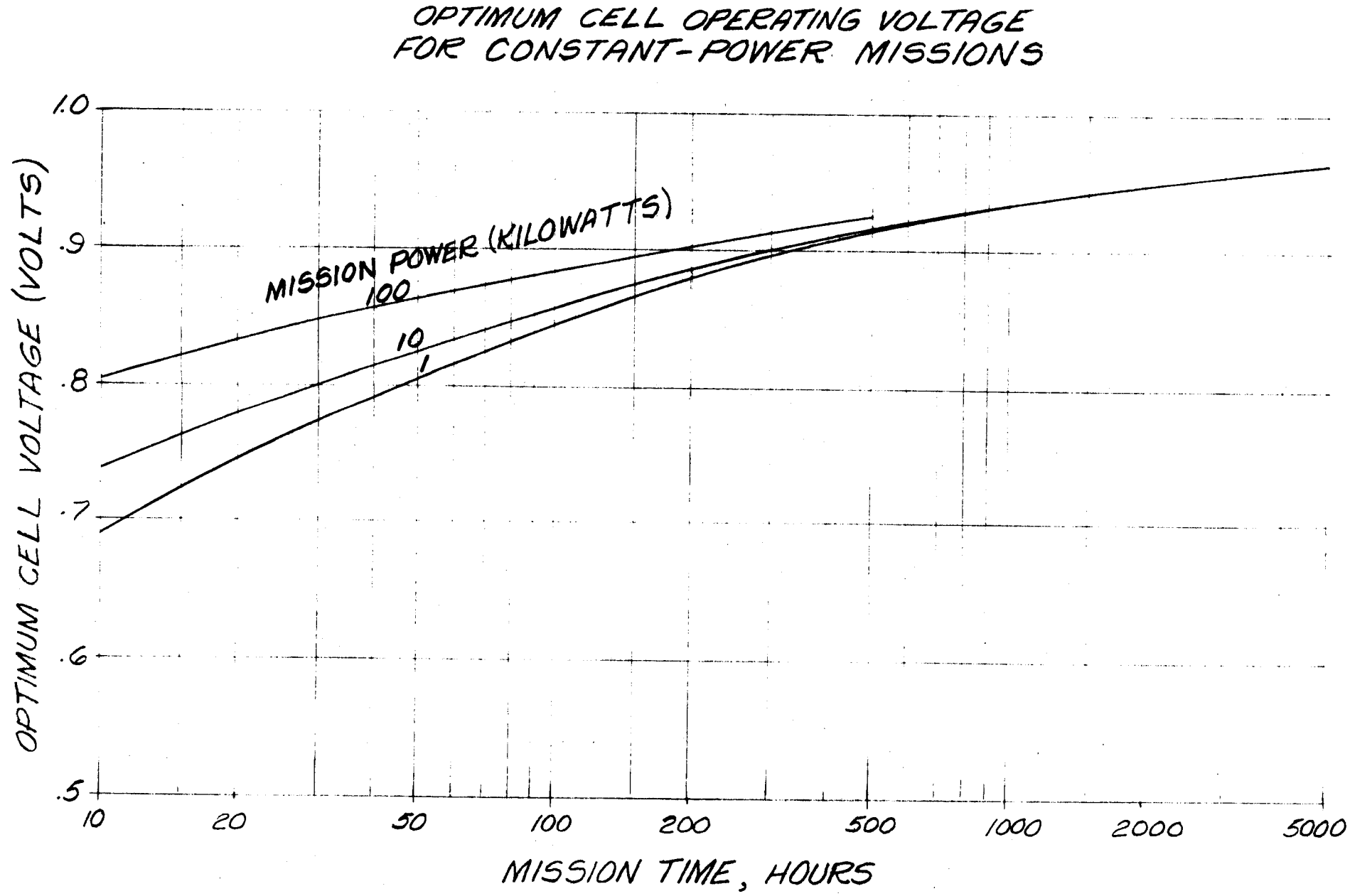
OPTIMUM CELL OPERATING VOLTAGE
FOR CONSTANT-POWER MISSIONS
OPTIMUM CELL VOLTAGE (VOLTS)
1.0
.9
.8
.7
.6
.5
MISSION POWER (KILOWATTS)
100
10
1
10
20
50
100
200
500
1000
2000
5000
MISSION TIME, HOURS

FIGURE 17

COMPARISON OF OPTIMIZED AND NON-OPTIMIZED FUEL CELL SYSTEM WEIGHTS.

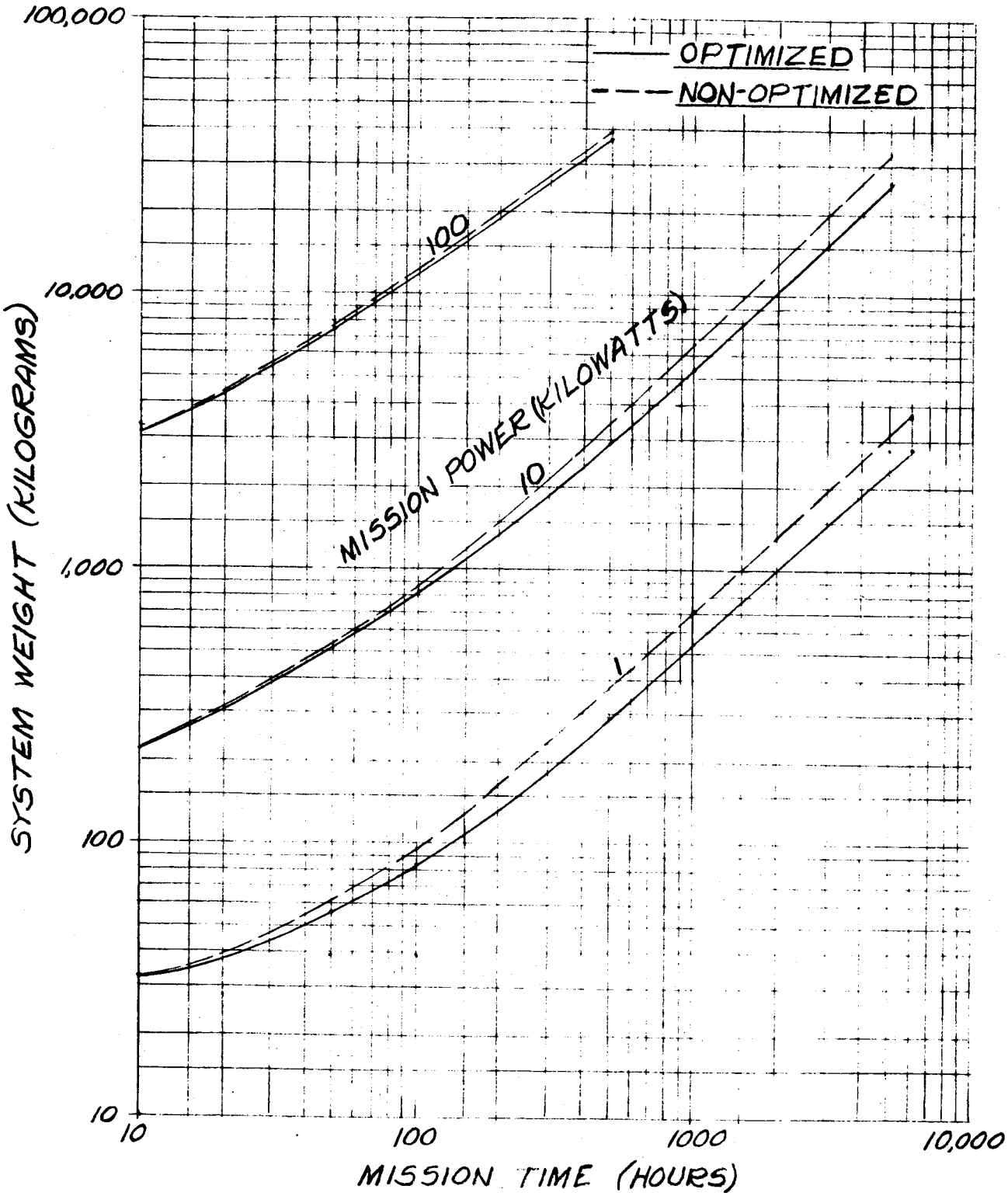

FIGURE 18

4.0 DIGITAL COMPUTER PROGRAM FOR DETERMINING OPTIMUM PARAMETERS FOR A FUEL CELL SYSTEM

A solution was given in the preceding section for the simple case of uniform power generation and a linearized cell voltage-current density characteristic. The analysis for the general hydrogen-oxygen fuel cell power system with non-uniform power requirements, voltage tolerances, and non-linear cell voltage-current density characteristic was programmed for an IBM-704 digital computer. The system considered in the program consists of the fuel cell and associated auxiliaries, a reactant storage and supply subsystem and a radiator heat sink. The use of primary batteries for peaking power is also considered and the optimum fuel cell-battery combination is determined.

4.1 Program Description

The computer program has been designed with sufficient flexibility that it may be applied to a wide range of fuel cell power systems. Reactant storage and heat sink weight calculations are performed in separate sub-routines. This facilitates program modifications if it is desired to consider design configurations different from those included. Portions of the input data may be changed independently, thus reducing the amount of input required when a number of related problems are to be run.

The polarization curve of the particular fuel cell to be studied is specified to the program in the form of voltage-current density coordinates. The program uses three-point interpolation to correlate values which fall between the input data.

The power profile is described to the program by means of power-time coordinates. The profile may be specified chronologically as it occurs during the mission, or it may be arranged in order of decreasing power levels. The latter method normally results in a decrease in the amount of the required input data.

Parasitic power requirements are represented by a linear equation with system maximum net power the independent variable. Constants in the equation are maintained as input, allowing representation of the requirements of various fuel cell systems. In comparing different fuel cell systems (such as the recirculating reactant and the static system), it is very important to base the comparison on systems with equal net power output.

A further feature of the program is the ability to specify the number of active and redundant units which comprise the system. A reliability figure is calculated for the fuel cell subsystem, and by specifying redundant units, a desired reliability may be obtained. This feature also allows tradeoffs to be made between weight and reliability.

Load sharing between primary batteries and fuel cells will be considered by the program if desired. Optimization of the combined system is limited to the case in which batteries supply all load power above some level which appears in the load profile. This is the situation which would exist if separate electrical bus were available for the peak power, or if power conditioning equipment were supplied to supervise the load sharing.

Calculation of the weight of fuel supply and heat sink subsystems is performed by the use of equations obtained by fitting curves to published data. Either supercritical or subcritical reactant storage may be considered, or the weight of tankage may be neglected completely. Radiator heat sinks which may be specified are the deployed type with bumper meteoroid shielding or a cylindrical configuration which also employs bumper shielding. Choice of the particular configuration is controlled by an input code symbol.

In addition to determining the operating parameters for the minimum-weight system, a tabulation of subsystem weights is prepared for a specified range of cell operating voltages. This feature allows some tradeoffs to be made manually and displays the sensitivity of the system weight to variations of operating parameters.

A tabulation is also prepared for the operating characteristics of the optimum fuel cell module. At each level of power output, the module voltage, current, current density, heat load, and reactant consumption rates are calculated.

This program has been applied to a variety of assumed mission requirements. Results obtained from these studies are discussed in the following section.

4.2 Applications

For missions in which the power requirement varies, the number of independent variables is too large to permit completely generalized conclusions regarding optimum operating voltages or minimum system weights. However, for the special conditions of a 28 ± 2 volt power requirement and for missions in which the following relation holds:

$$\sum_{i=1}^{N} P_i T_i \geq 0.4 P_{max} T \qquad (4\text{-}1)$$

where

P_i = the i'th value of N power levels (KW)

T_i = the duration of P_i (hr)

P_{max} = the highest power required (KW)

T = total mission time (hr)

the minimum weight system ($W_{T_{min}}$) may be represented by the formula:

$$W_{T_{min}} = 6.87\,(P_{max})^{0.834} + 0.09\left(\frac{P_{max}}{10}\right)^{0.956} \times$$

$$(T)^{0.44 + 0.0001\,T\left(\frac{2.5\sum_{i=1}^{N} P_i T_i}{P_{max}\,T}\right)^{0.063\,T^{\frac{1}{2}}}}$$

$$+ \frac{9.07}{P_{max}} \qquad (4\text{-}2)$$

$$1 \leq P_{max} \leq 25 \; ; \qquad 10 \leq T_m \leq 100$$

This formula was derived by fitting curves to data obtained from the computer program. Figure 19 shows the data and several points calculated by the formula. Maximum error of the formula in the specified range is 5%. Below a ratio of $\sum P_i T_i$ to $P_{max} T_m$ of 0.4, the curves become discontinuous because of limitations imposed by voltage regulation requirements. The equation is based on a system composed of Allis-Chalmers fuel cell with projected (1968) performance, supercritical reactant storage with 20% excess reactants and a deployable radiator with bumper meteoroid shielding designed to reject the heat dissipated in the electrical load as well as the fuel cell waste heat.

FUEL CELL SYSTEM OPTIMIZED WEIGHTS

ALLIS-CHALMERS FUEL CELL
SUPERCRITICAL REACTANTS (20% EXCESS)
DEPLOYED RADIATOR

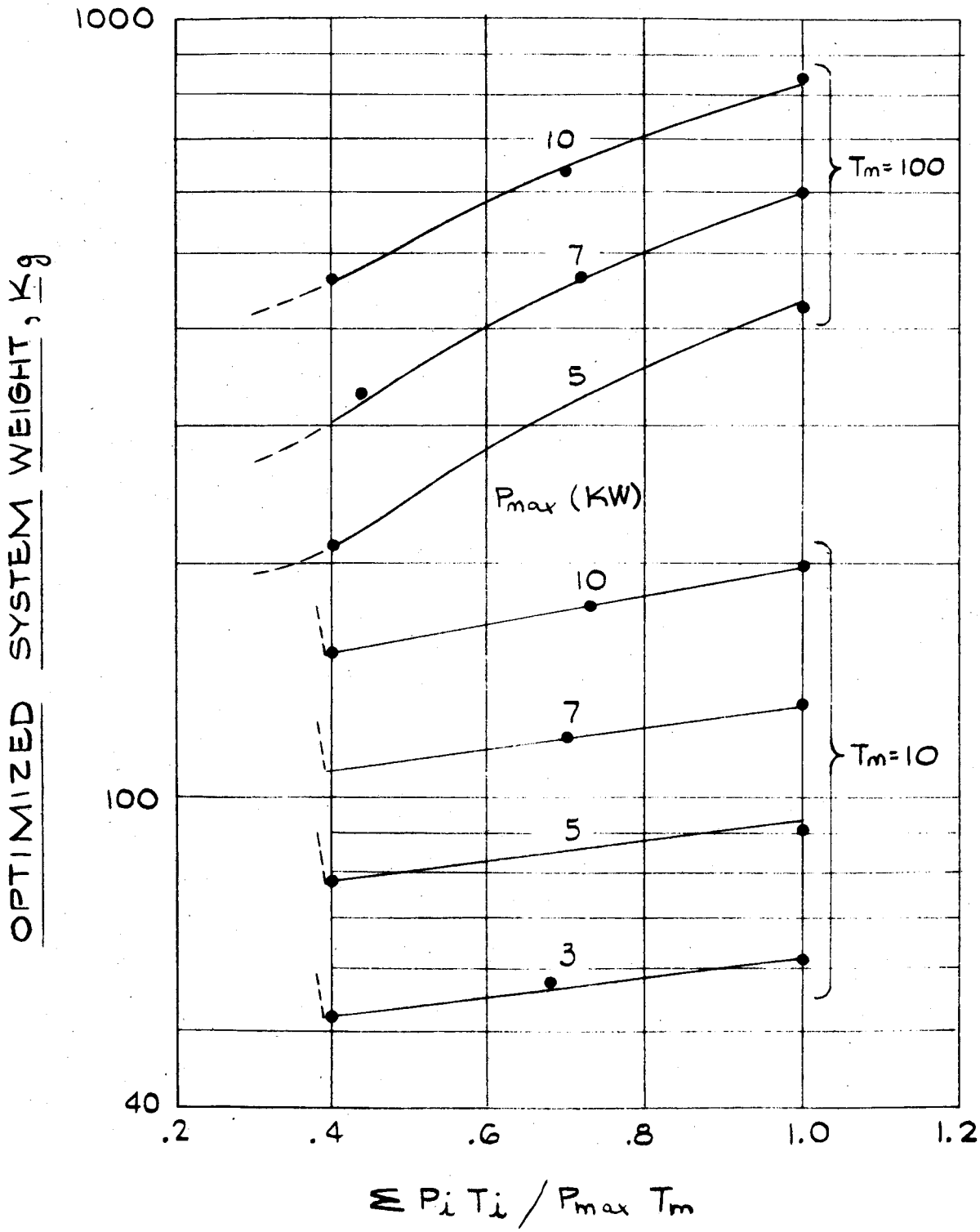

FIGURE 19

5.0 COMBINED POWER SOURCES

5.1 Combined Fuel Cell and Battery System

As previously mentioned, the computer program for system optimum parameter determination has been designed to consider the use of primary batteries (to supply peak power requirements) in combination with fuel cells (to supply the base power level). The optimization of the combined system has been limited to the case in which the batteries supply all load power above some level which appears in the load profile. This is the situation which would exist if a separate electrical bus were available for the peak power, or if power control equipment were supplied to supervise load sharing between the batteries and the fuel cells.

Much the same difficulties exist in drawing generalized conclusions for the combined system as for a straight fuel cell system. However, in the case of a two power level requirement it is possible to determine the duration of the peak power output for which equal weights are obtained for the combined system and for the straight fuel cell system. Figures 20 and 21 show the "break-even" times for mission durations of 10 and 100 hours, respectively, for voltage regulation of 28 ± 2 volts. Steps which occur in the curves are discontinuities caused by necessary changes in the number of cells in order to meet voltage regulation requirements.

To use these curves, consider the example of a 100-hour mission with a peak load requirement of 8KW and a base load of 2 KW. From Figure 21, with $P_{max} = 8$ and $p = 2$, the break-even time (t) is about 1.5 hours. Therefore, the lightest auxiliary power system consists of only fuel cells if the duration of the peak power is greater than 1.5 hours. Otherwise, the lightest system will consist of fuel cells for the base power and batteries for the peak power.

These curves can be used to establish the limiting conditions for which the minimum weight system will always consist of fuel cells alone. A similar limit can be established for which the minimum weight system consists of a combination of fuel cells and batteries. These limits are shown in Figure 22. For power requirements which correspond to points above the shaded area, the lightest power system will consist of fuel cells only; for power requirements which correspond to points below the shaded area, the lightest power system will consist of fuel cells combined with batteries for peaking power.

5.2 Combined Fuel Cell and Low Temperature Expansion System

The low temperature expansion system is an open cycle process which uses hydrogen as a thermodynamic fluid. Hydrogen is stored as a supercooled liquid and is passed through heat exchangers where it absorbs heat collected from the vehicle, equipment and crew. The heated hydrogen is then allowed to expand through a turbine or expansion engine and is exhausted to space vacuum. Electric power is developed in a generator driven by the heat engine.

BREAK-EVEN TIME VS. MISSION TIME
BASED ON PROJECTED V-J CURVE (1965)
VOLTAGE REGULATION 28 ± 2 VOLTS
MISSION TIME 10 HOURS
BATTERY SPECIFIC ENERGY 110 WATT-HR./KG.

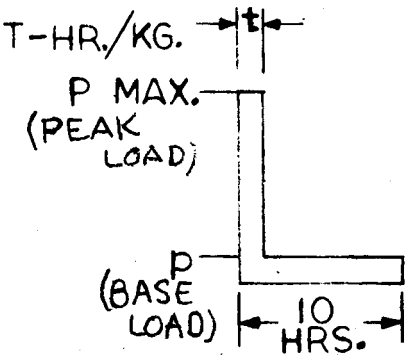

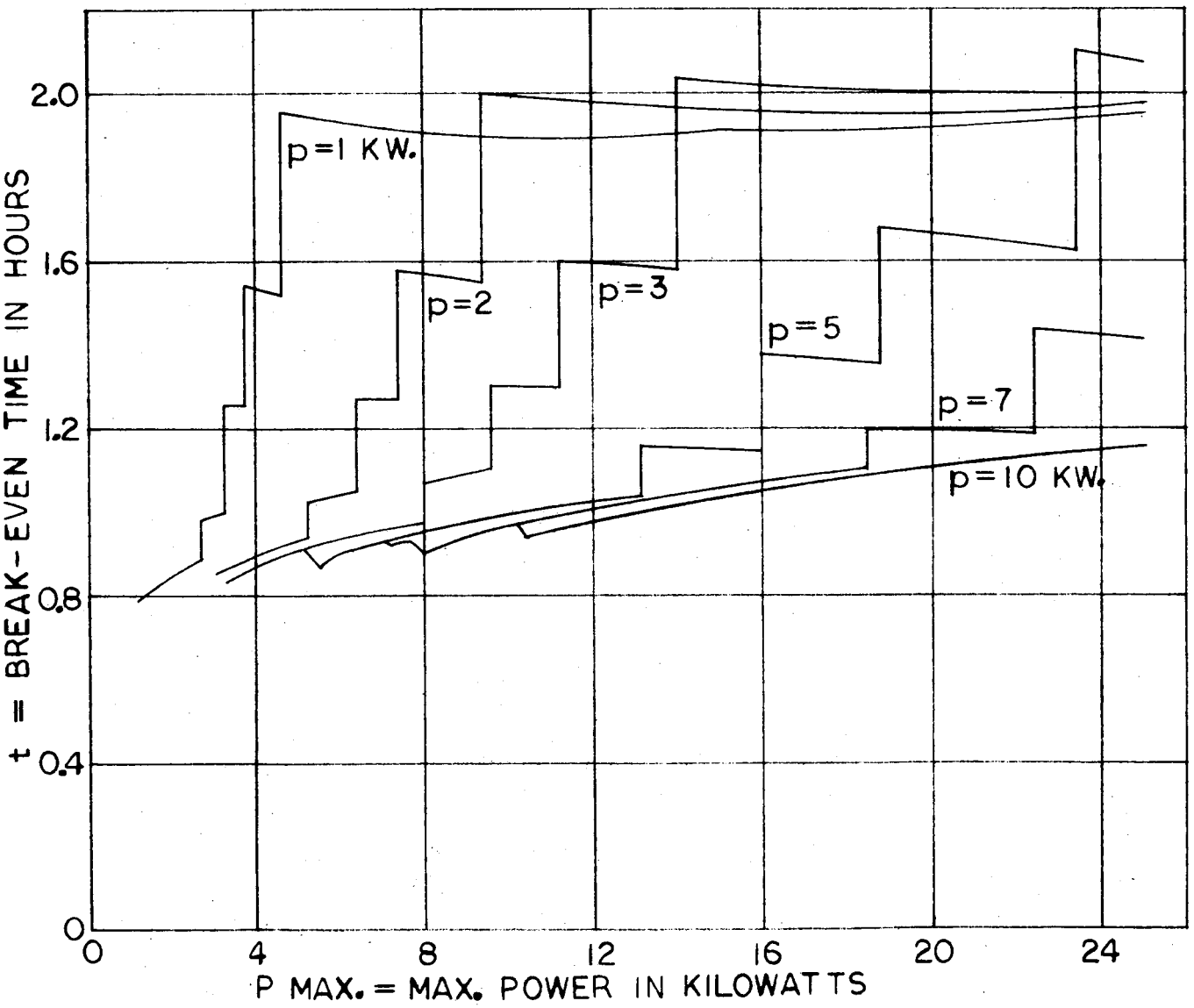

FIGURE 20

BREAK-EVEN TIME VS. MISSION TIME
BASED ON PROJECTED V-J CURVE (1965)
VOLTAGE REGULATION 28 ± 2 VOLTS
MISSION TIME 100 HOURS
BATTERY SPECIFIC ENERGY 110 WATT-HR./KG.

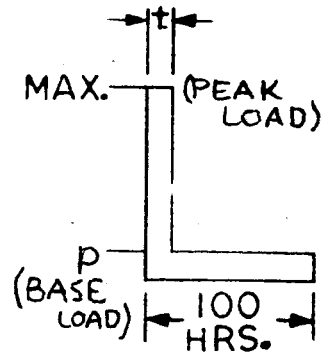

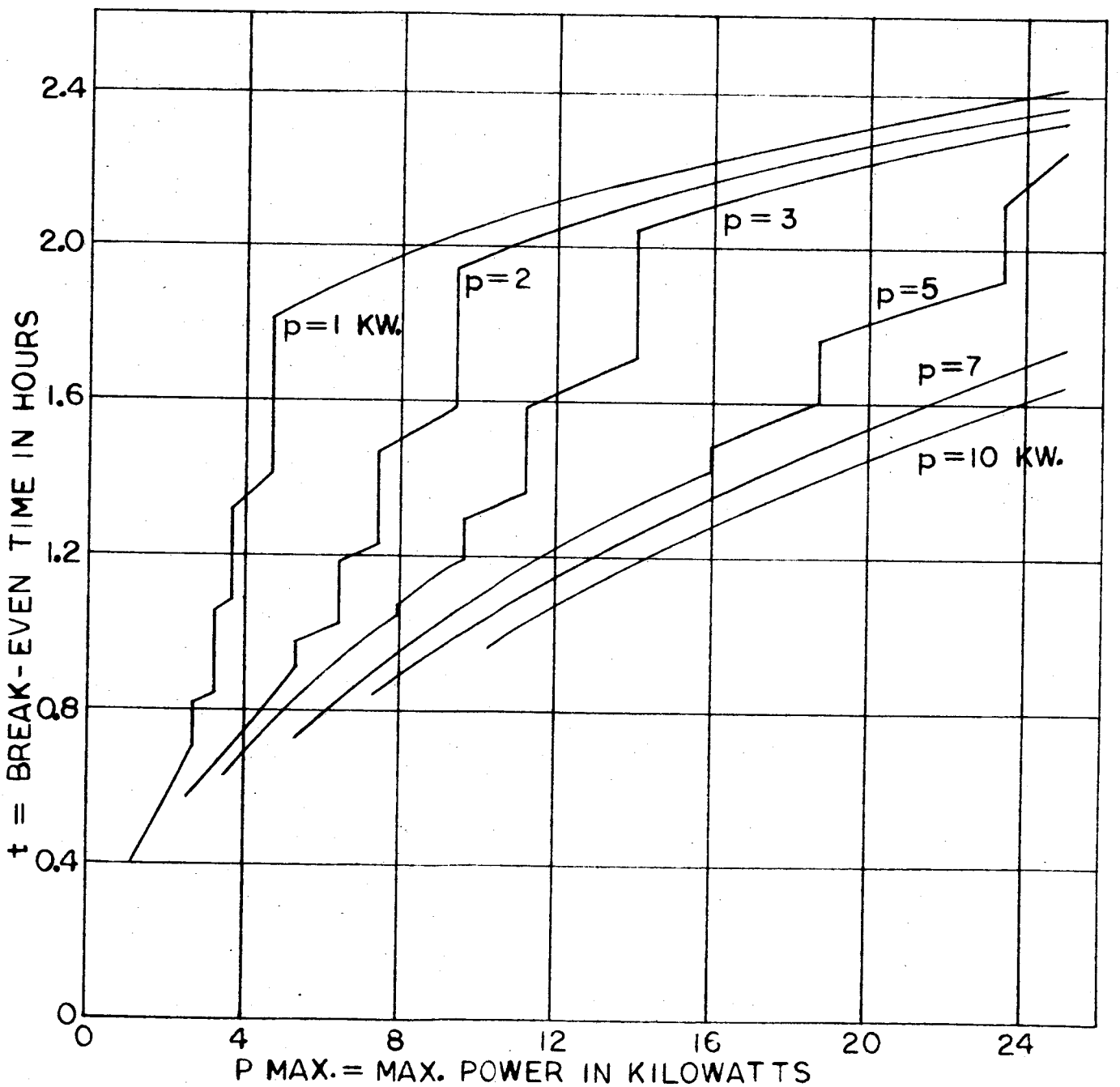

FIGURE 21

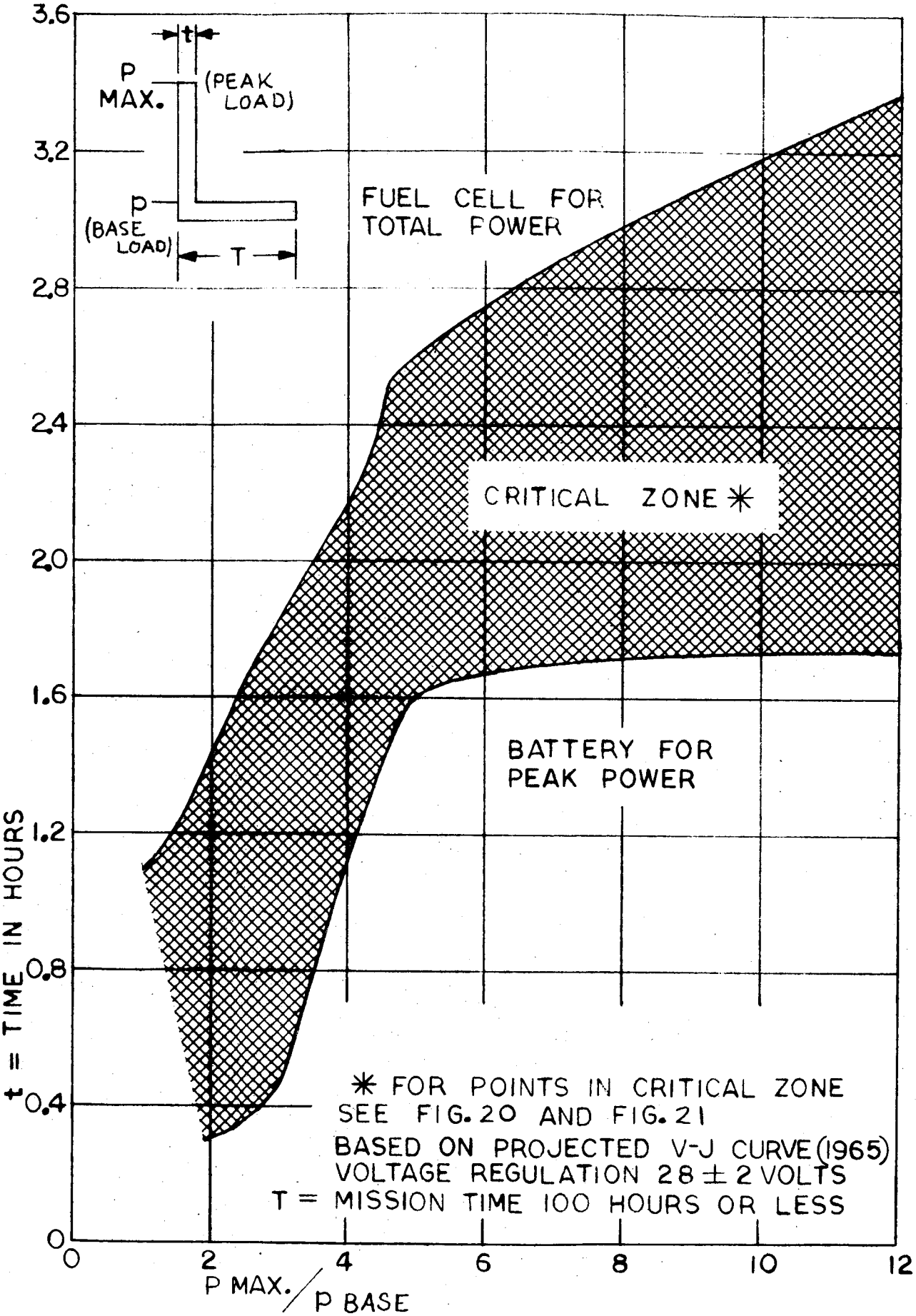
t
P MAX.
(PEAK LOAD)
P (BASE LOAD)
T
FUEL CELL FOR TOTAL POWER
CRITICAL ZONE *
BATTERY FOR PEAK POWER
* FOR POINTS IN CRITICAL ZONE SEE FIG. 20 AND FIG. 21
BASED ON PROJECTED V-J CURVE (1965)
VOLTAGE REGULATION 28 ± 2 VOLTS
T = MISSION TIME 100 HOURS OR LESS
t = TIME IN HOURS
3.6
3.2
2.8
2.4
2.0
1.6
1.2
0.8
0.4
0
0
2
4
6
8
10
12
P MAX. / P BASE

FIGURE 22

The heat energy used in the cycle is principally derived from sources which, with other systems, constitutes refrigeration loads. Waste heat from the electrical equipment, solar radiation, and crew metabolic heat is used. The vented hydrogen is capable of removing heat from the vehicle at a rate which exceeds power production by 50 percent or more. The amount of excess cooling will depend upon the temperature of the electrical equipment and the details of the thermodynamic cycle.

Under some circumstances, the available waste heat is not adequate for the cycle requirements. Additional heat is then provided by the combustion of a small amount of hydrogen. The need for supplementary heat suggests the possibility of using a fuel cell in combination with the low temperature expansion cycle. Waste heat from the fuel cell would be utilized in the thermal cycle and the fuel cell would supply a portion of the vehicle electrical power requirements.

The Cryhocycle, proposed by Sundstrand Aviation, is one type of low temperature expansion system. In 1962, Allis-Chalmers and Sundstrand performed a cooperative study of the feasibility of a combined fuel cell and Cryhocycle system. This study was based on a fourteen day mission with an average power of 1.4 kilowatts and a peak power of 3.0 kilowatts. Projected system performance for the year 1965 was used. Allis-Chalmers supplied data for the fuel cell system; Sundstrand Aviation supplied data for the Cryhocycle system.

Conclusions derived from the 1962 study were: [4]

a. A fuel cell system will weigh less than the corresponding Cryhocycle system or any combination of the two systems with the same combined power rating.

b. The parameters which most strongly influence the weight of the combined system are the specific hydrogen consumption of the Cryhocycle and the weight of the hydrogen tankage per weight of hydrogen contained.

c. Radiator weights did not significantly influence the problem, even though radiator specific weights ranging from 10 kg/kw (thermal) to 30 kg/kw (thermal) were used.

The fuel cell system which was considered in this early study used the recirculating reactant method to remove water from the cell. With the development of the Static Moisture Removal method, the recirculating reactant technique is now considered obsolete for use with the Allis-Chalmers cell. Also, operating parameters of both fuel cells and Cryhocycle systems have been improved since the time of that report. Accordingly, the present study was undertaken to determine the feasibility of the combined system based on technology predicted for the period 1968 - 1970.

Weight and feasibility have been determined for the lightest combination of fuel cells and low temperature expansion system. For comparison, the weights of each system operating independently have been calculated. All the systems compared are capable of rejecting the heat dissipated in the vehicle electrical load and the waste heat from the power supply unit. Constant power output throughout the mission duration was assumed. The use of redundant elements for improved reliability was not included in the weight analysis.

The Lunar Logistics Vehicle mission concept was considered a typical mission for purposes of this study. However, results of the study are general and may be applied to other vehicles and missions.

5.2.1 Hydrogen and Oxygen Storage and Supply Subsystem

Cryogenic storage of hydrogen (and oxygen for systems in which it is required) was assumed for these studies. Both subcritical storage and supercritical storage were considered.

In the subcritical system, hydrogen and oxygen are stored in the liquid state at pressures below the critical pressure for that gas. The low pressure results in light tankage, but a pump must be used to expel the fluid from the tanks and the energy requirement for the pump must be charged as a parasitic load to the system. In addition, there exists a potential problem of managing the liquid in a zero-gravity environment.

The supercritical storage system uses storage pressures greater than the critical pressure and makes it possible to avoid the existance of two phases in the fluid. The fluid density is essentially constant throughout the storage tank. Fluid is expelled from the tank by the addition of heat to the fluid. An electrical heater is usually used. This represents a parasitic load for the system.

In spite of its greater weight, the supercritical storage system is generally preferred for space applications because of its greater simplicity and reliability. Estimated weights of the two storage systems are given in Figures 23 through 26 inclusive.

5.2.2 Low Temperature Expansion System

The low temperature expansion system generates power by expanding gas in a prime mover which drives an electric generator. Expanded gas is vented to space. The working fluid is cryogenically stored hydrogen, and the heat source is the energy dissipated in the electrical load, net heat gain from solar radiation and metabolic heat from the crew. Waste heat is rejected from the vehicle in the form of internal energy of the exhaust hydrogen. In the event that the waste heat is less than the requirement of the expansion cycle, additional heat is obtained from the catalytic combustion of a small amount of hydrogen.

SUPERCRITICAL HYDROGEN STORAGE AND SUPPLY SYSTEM WEIGHT'

SPHERICAL TANK
24 ATM, SAFETY FACTOR = 2
INNER SHELL TITANIUM ALLOY
OUTER SHELL .076 mm NONRIGID PLASTIC
SUPER INSULATION 96 Kg / m^3
AMBIENT TEMPERATURE 290°K

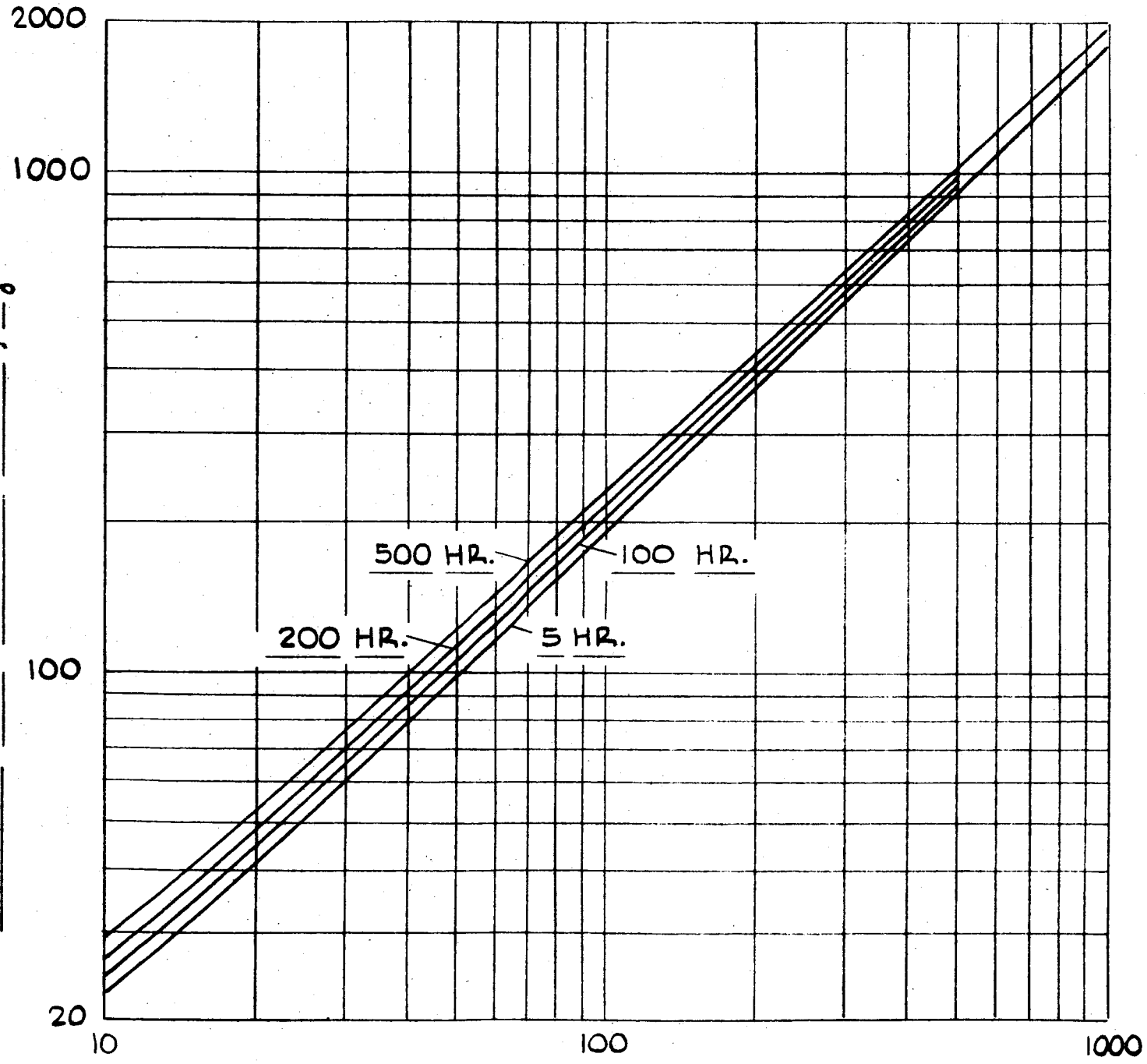

FIGURE 23

SUBCRITICAL HYDROGEN STORAGE AND SUPPLY SYSTEM WEIGHT'

SPHERICAL TANK
TANK FILLED TO 95% CAPACITY
INNER SHELL .64 mm ALUMINUM
OUTER SHELL .076 mm NONRIGID PLASTIC
AMBIENT TEMPERATURE 290°K

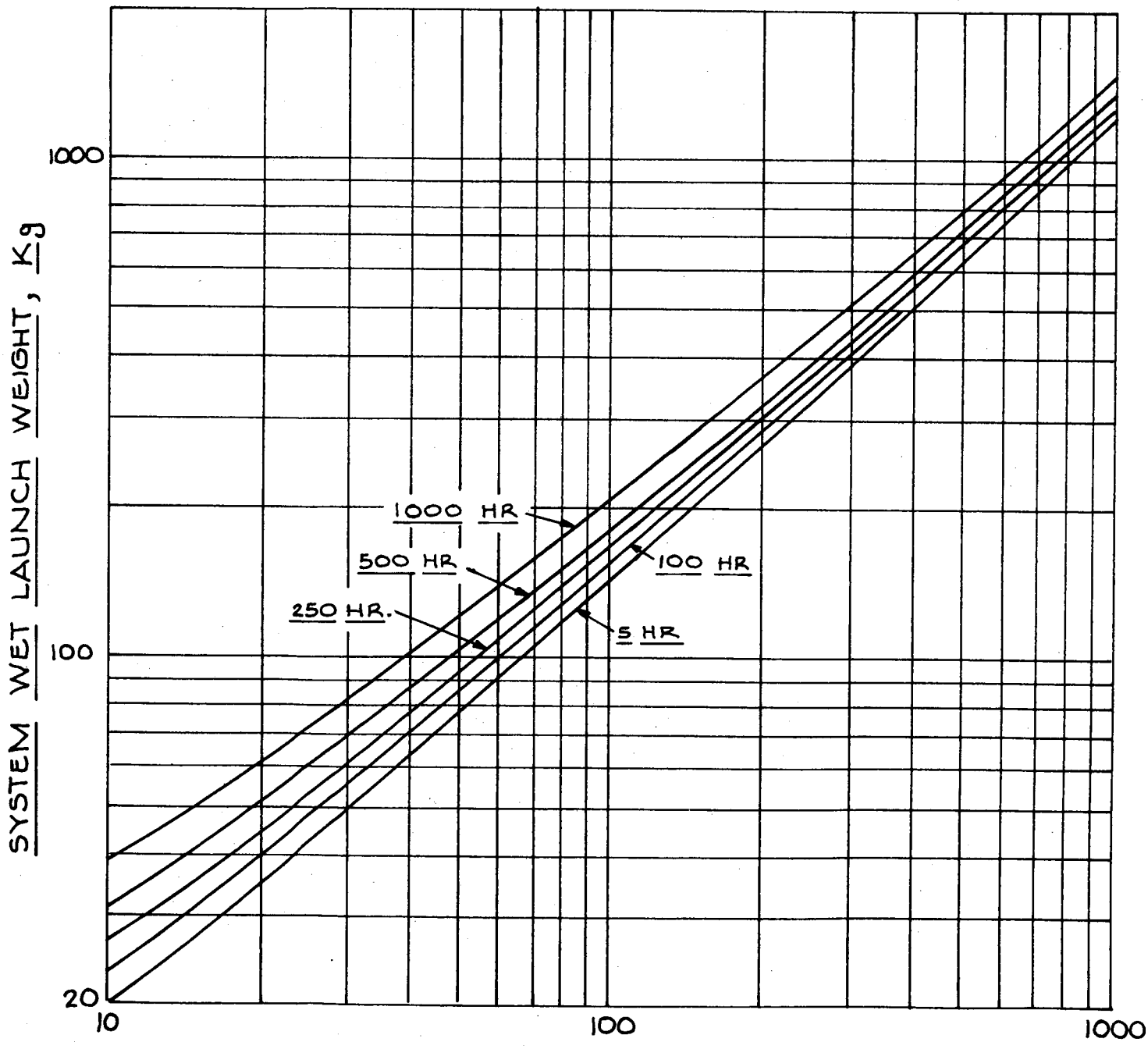

FIGURE 24

SUPERCRITICAL OXYGEN STORAGE AND SUPPLY SYSTEM WEIGHT

SPHERICAL TANK
58 ATM
INNER SHELL ALUMINUM ALLOY
OUTER SHELL .5 mm NONRIGID MAGNESIUM
INSULATION 256 Kg/m³

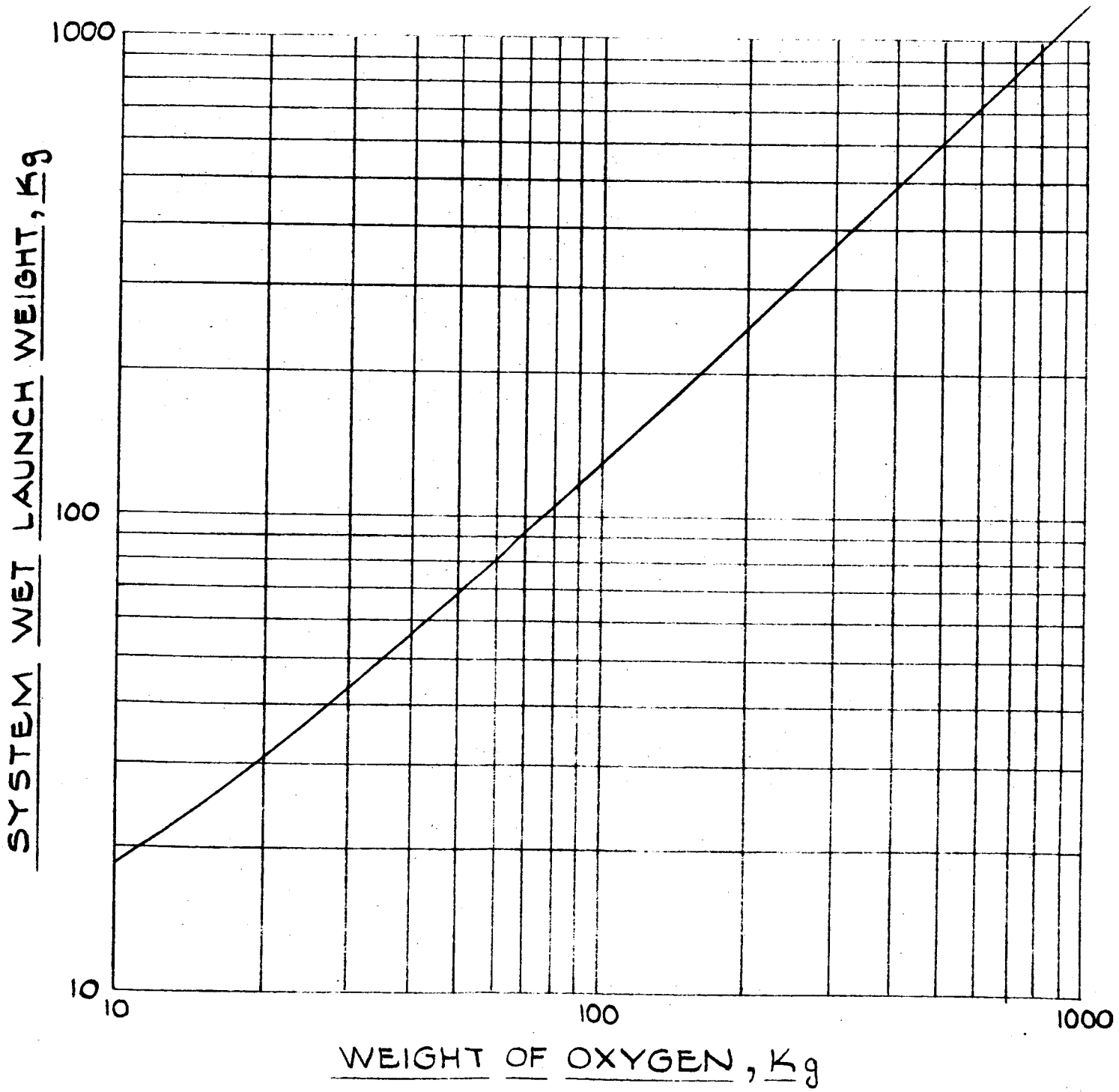

FIGURE 25

SUBCRITICAL OXYGEN STORAGE AND SUPPLY SYSTEM WEIGHT

SPHERICAL TANK
6.5 ATM
INNER SHELL ALUMINUM ALLOY
OUTER SHELL RIGID MAGNESIUM
SUPER INSULATION 112 Kg/m³

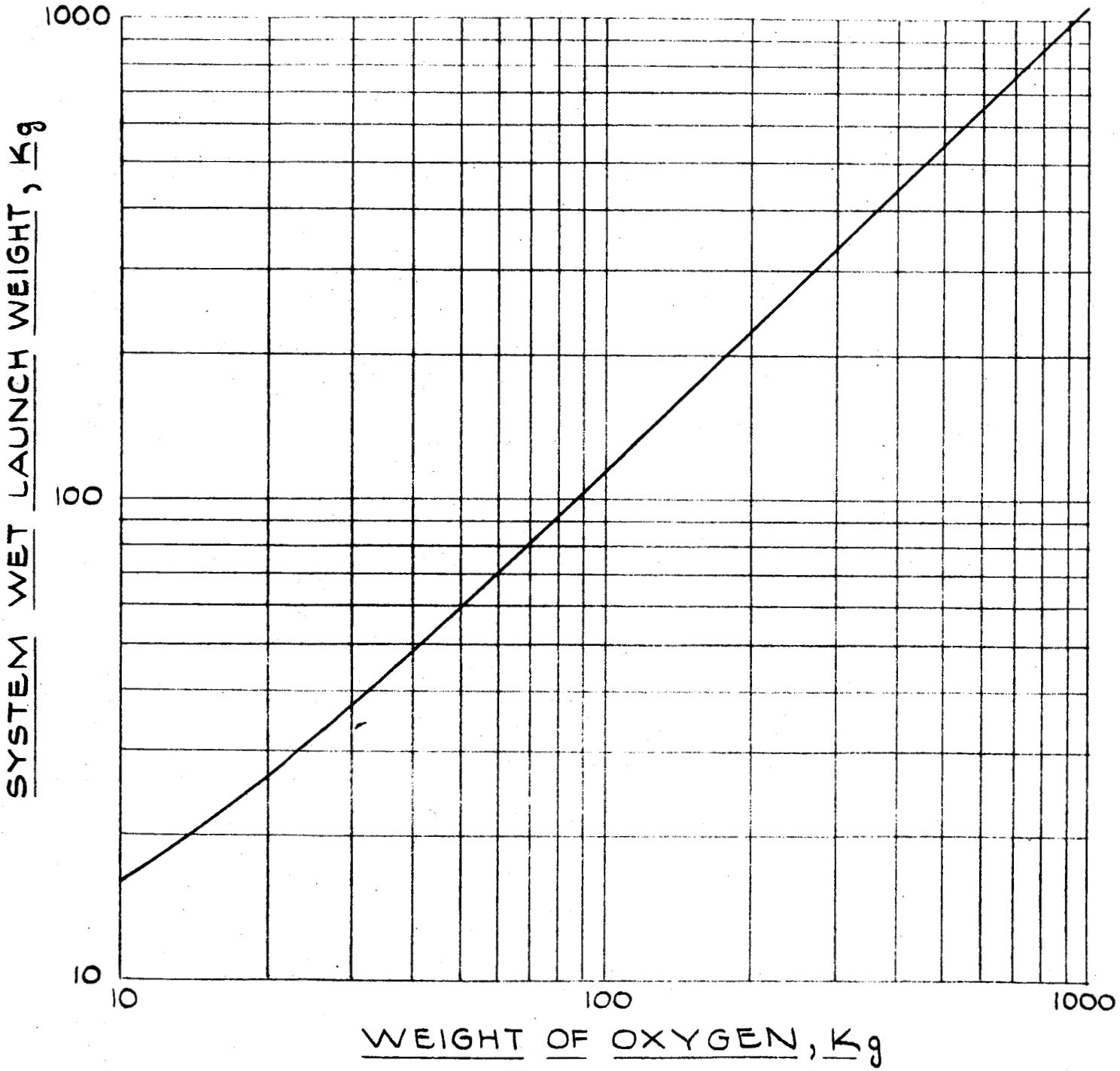

FIGURE 26

The vented hydrogen is capable of removing heat from the vehicle at a rate which exceeds power production by 50% or more. The amount of excess cooling will depend upon the temperature of the electrical equipment and the details of the thermodynamic cycle employed. For the purpose of this analysis, it was assumed that the total cooling load was the energy dissipated in the electrical loads driven by the auxiliary power system.

Refinements of the low temperature expansion system include several stages of expansion with reheating; recirculation of a portion of the hydrogen and the use of pumps or compressors to obtain lower specific hydrogen consumption rates by raising system pressure before heating.

Weights and performance of three representative low temperature expansion systems were obtained from predictions contained in the literature.[2] System No. 1 uses supercritical hydrogen and oxygen storage and a two-stage reciprocating expander with recirculation. System No. 2 used subcritical hydrogen and oxygen storage, a high pressure pump, and a three-stage reciprocating expander with recirculation. System No. 3 uses subcritical hydrogen and oxygen storage, a pump, and a four-stage turbine expander without recirculation.

Figure 27 shows the weights of the lightest of these systems for various mission times and power levels. No redundancy is assumed for any of the components, but hydrogen weights are based on a 10% residual and a 10 % safety factor. For all missions greater than 30 hours, System No. 2 is the lightest of the low temperature expansion systems. System No. 2 also requires less volume than the other expansion systems, as indicated in Figure 31.

Additional characteristics of the low temperature expansion systems are:

a. Ability to reject heat from the vehicle is not seriously affected by the vehicle thermal environment.

b. Low temperature operation avoids many materials problems associated with other dynamic power systems.

c. The large number of dynamic components in the system are expected to require appreciable redundancy.

d. Redundancy for improved reliability would usually require a complete engine system duplication.

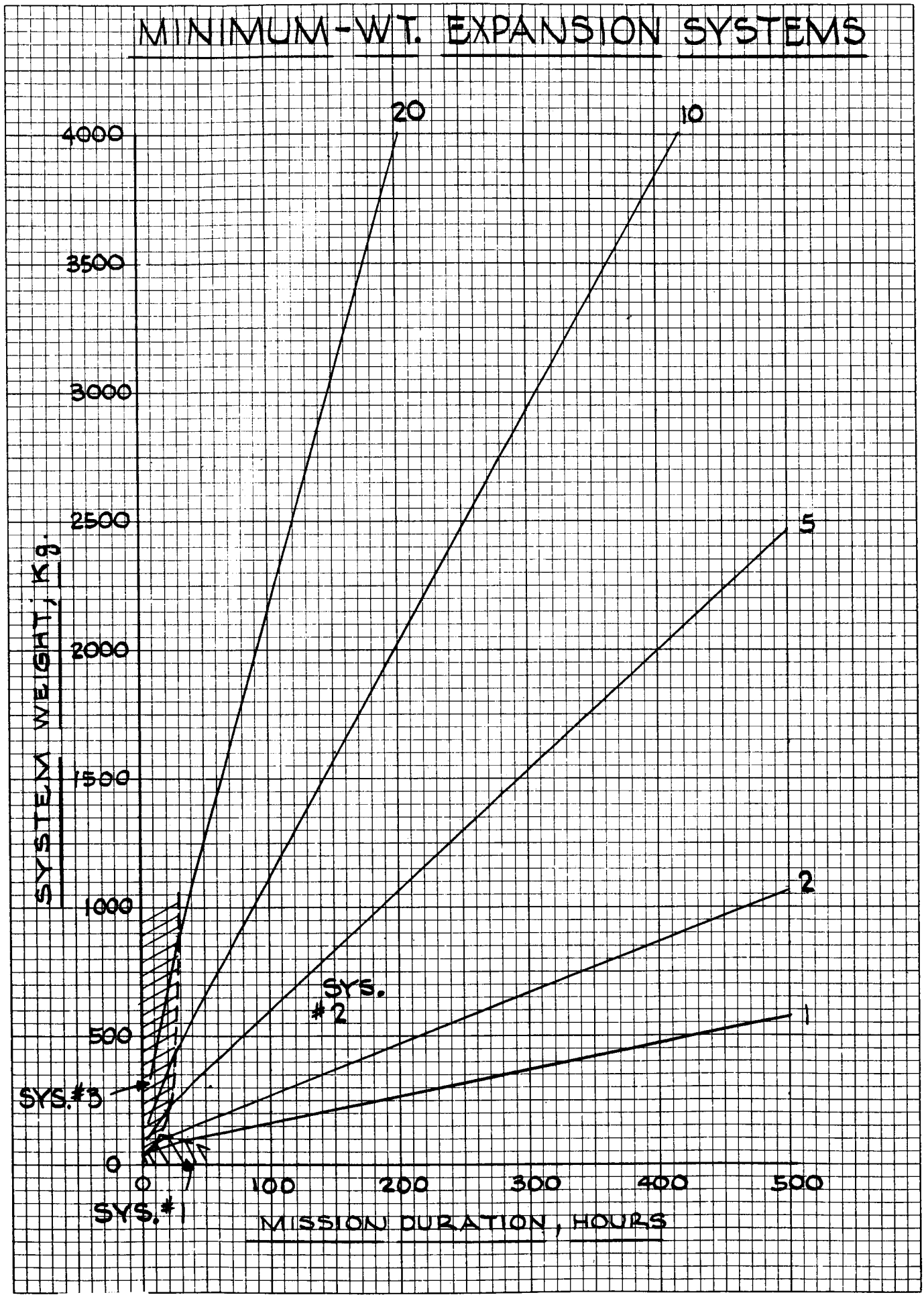
MINIMUM-WT. EXPANSION SYSTEMS
20
10
5
2
1
4000
3500
3000
2500
2000
1500
1000
500
0
SYSTEM WEIGHT, Kg.
SYS. #2
SYS.#3
SYS.#1
0
100
200
300
400
500
MISSION DURATION, HOURS

FIGURE 27

5.2.3 Fuel Cell Systems

Fuel cell power systems produce electrical energy through electrochemical reactions. Although the thermal efficiency of the fuel cell is high, some waste reaction heat must be rejected from the space vehicle. The fuel cell system requires an associated heat sink.

Fuel cell systems employing Allis-Chalmers fuel cells with Static Moisture Control were analyzed for comparison with the low temperature expansion systems. Both supercritical and subcritical reactant storage systems were considered in combination with a water evaporator heat sink, a deployed radiator with bumper meteoroid protection and a nondeployed radiator with bumper meteoroid protection. Product water was vented to space. The heat rejection system was sized to reject the heat represented by the electrical load plus the waste heat from the fuel cell.

In this analysis, 28-volt fuel cell systems were considered. Individual cell voltages were optimized to obtain minimum system weight.

Radiators considered were of the finned tube type using spaced bumper shielding for meteoroid protection. Information on optimum weights of deployed radiators using this type of construction was found in the literature[1]. Weights of nondeployed radiators which need shielding on only one side and radiate from only one side were estimated from this information. Radiator weights are given in Figure 28.

Radiator design was based on a 0.999 probability of no meteoroid puncture during the mission and an average coolant temperature of 330° K. A non-oriented radiator with high solar-reflectivity surfaces was assumed. One side was considered viewing space and the other viewing earth. Heat exchangers and thermal controls associated with the radiator system were estimated to weigh 2.5 kilograms per kilowatt of cell output.

Weights of water evaporators were calculated on the basis of storing water at room temperature and venting steam at fuel cell temperature. A heat capacity of 7.1 kilowatt-hours per kilogram of water resulted. The water evaporators were heavier than the assumed radiator designs for every mission studied. Hence, the use of evaporators is not considered in the results of this study.

Total weights for the various fuel cell systems considered are given in Figures 29 and 30. System volume for a representative 10 kilowatt system is shown in Figure 31.

Additional characteristics of these fuel cell power and vehicle cooling systems are:

a. Lightweight systems require radiators and this may be impractical for some missions.

DEPLOYED RADIATOR SYSTEM WEIGHT[2]

BUMPER - SHIELD TUBE - FIN TYPE
BOTH SIDES RADIATING
ALUMINUM CONSTRUCTION
AVERAGE COOLANT (WATER) TEMP. 330°K
PROBABILITY OF NO PUNCTURE 0.999
WT. OPTIMIZED SHIELDING DISTRIBUTION & FIN EFFECTIVENESS

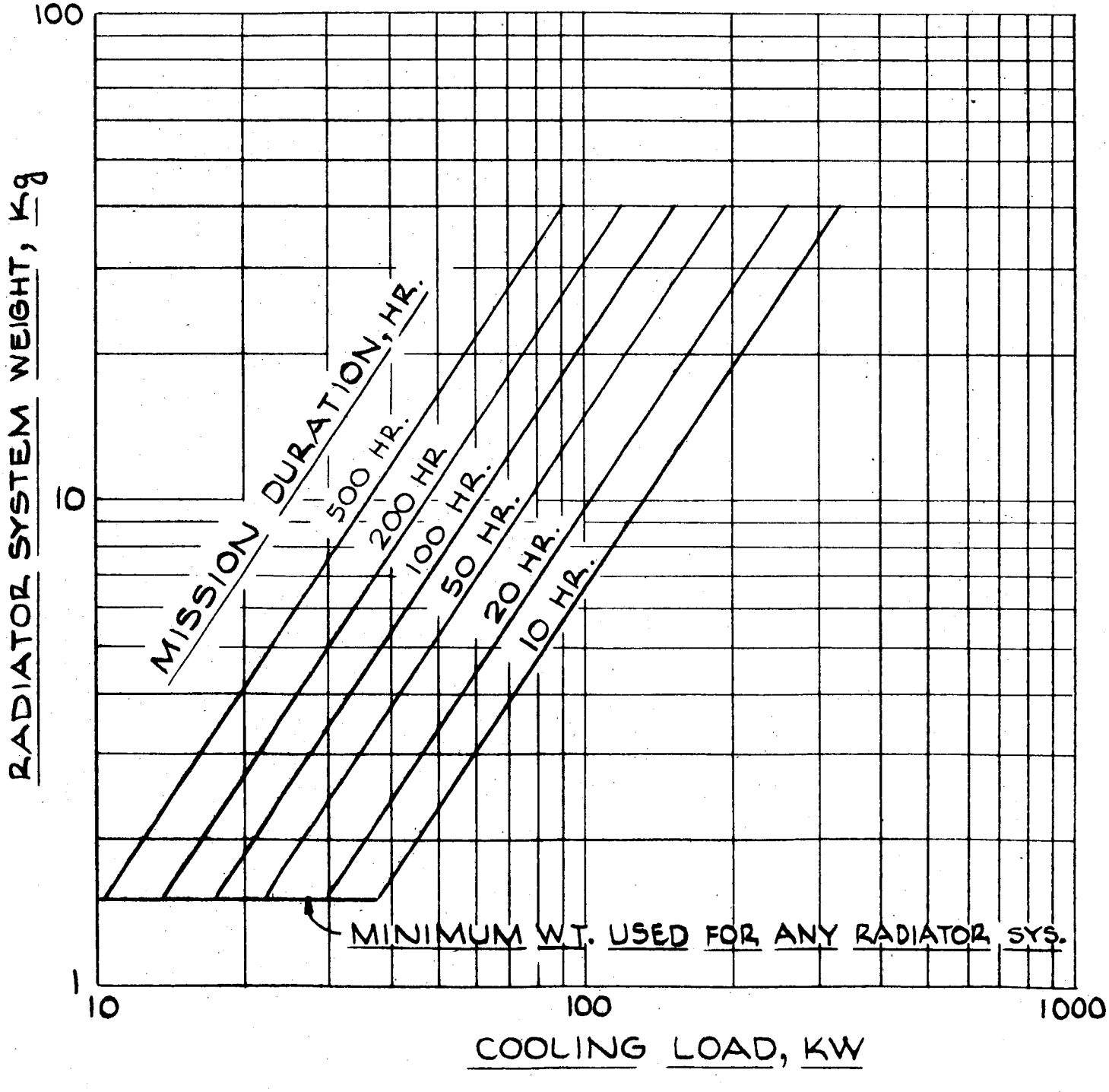

FIGURE 28

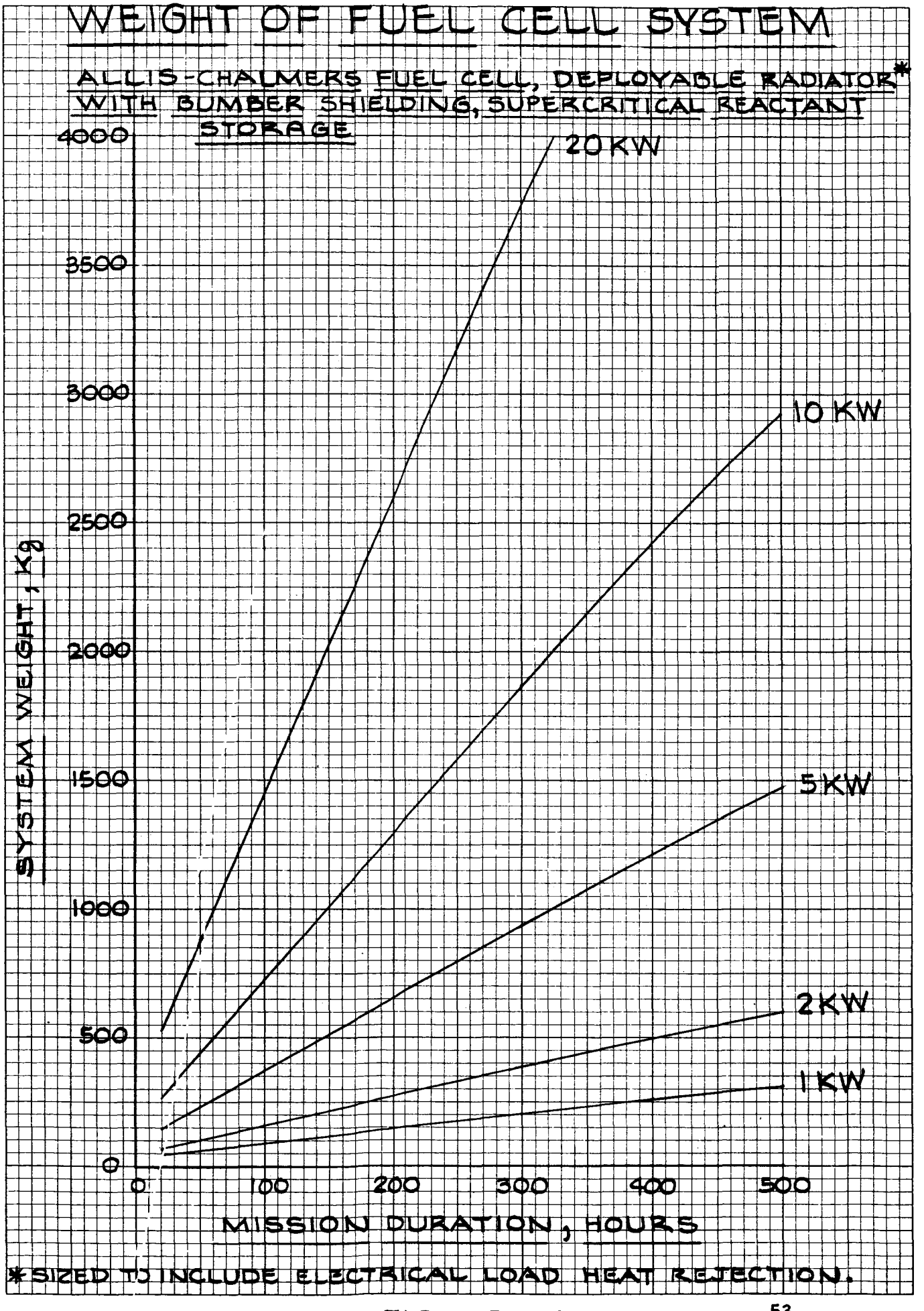
WEIGHT OF FUEL CELL SYSTEM
ALLIS-CHALMERS FUEL CELL, DEPLOYABLE RADIATOR* WITH BUMBER SHIELDING, SUPERCRITICAL REACTANT STORAGE
SYSTEM WEIGHT, KG
4000
3500
3000
2500
2000
1500
1000
500
0
20 KW
10 KW
5 KW
2 KW
1 KW
0
100
200
300
400
500
MISSION DURATION, HOURS
*SIZED TO INCLUDE ELECTRICAL LOAD HEAT REJECTION.

FIGURE 29

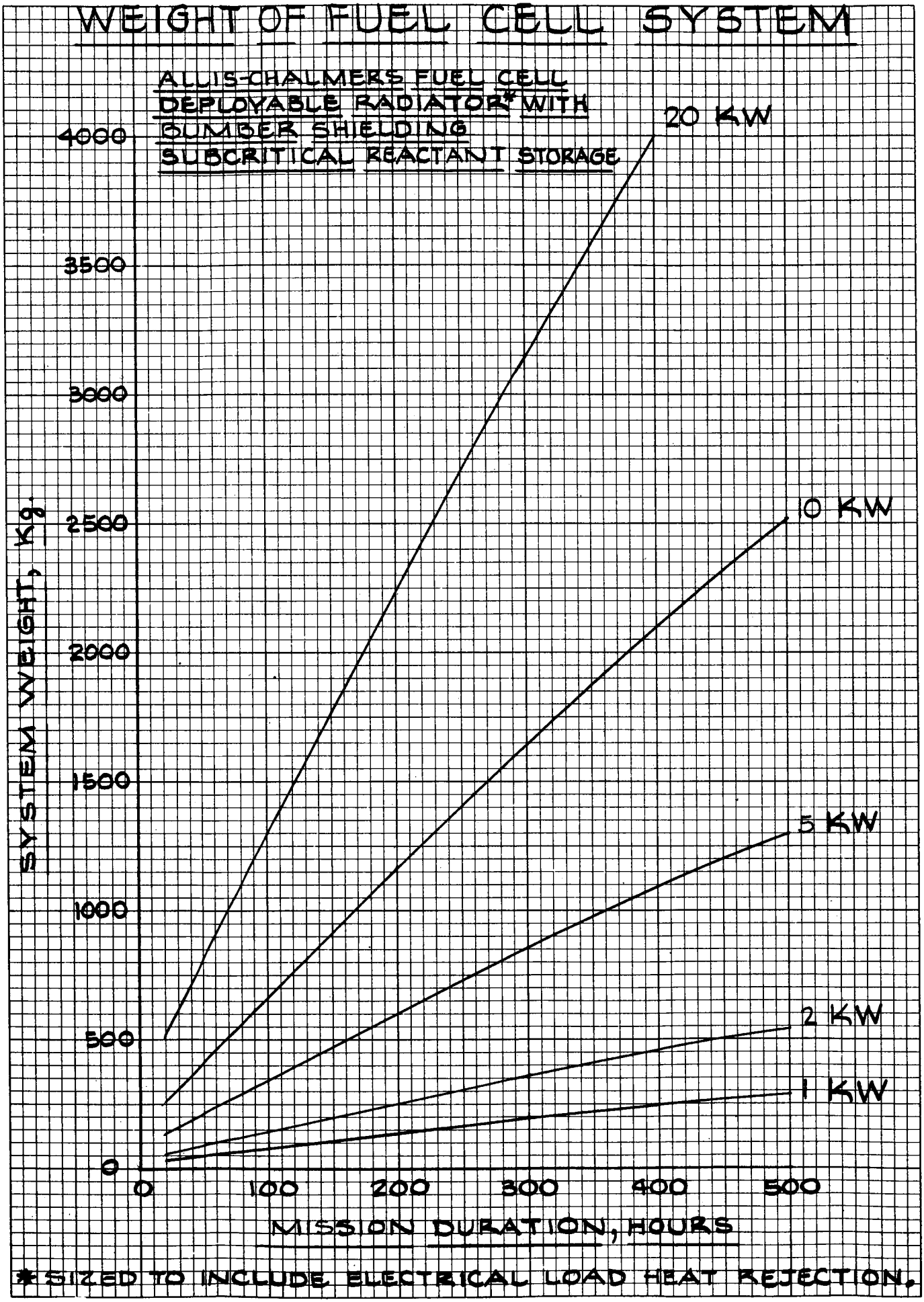
WEIGHT OF FUEL CELL SYSTEM
ALLIS-CHALMERS FUEL CELL
DEPLOYABLE RADIATOR* WITH
BUMPER SHIELDING
SUBCRITICAL REACTANT STORAGE
20 KW
10 KW
5 KW
2 KW
1 KW
SYSTEM WEIGHT, Kg.
4000
3500
3000
2500
2000
1500
1000
500
0
0
100
200
300
400
500
MISSION DURATION, HOURS
*SIZED TO INCLUDE ELECTRICAL LOAD HEAT REJECTION.

FIGURE 30

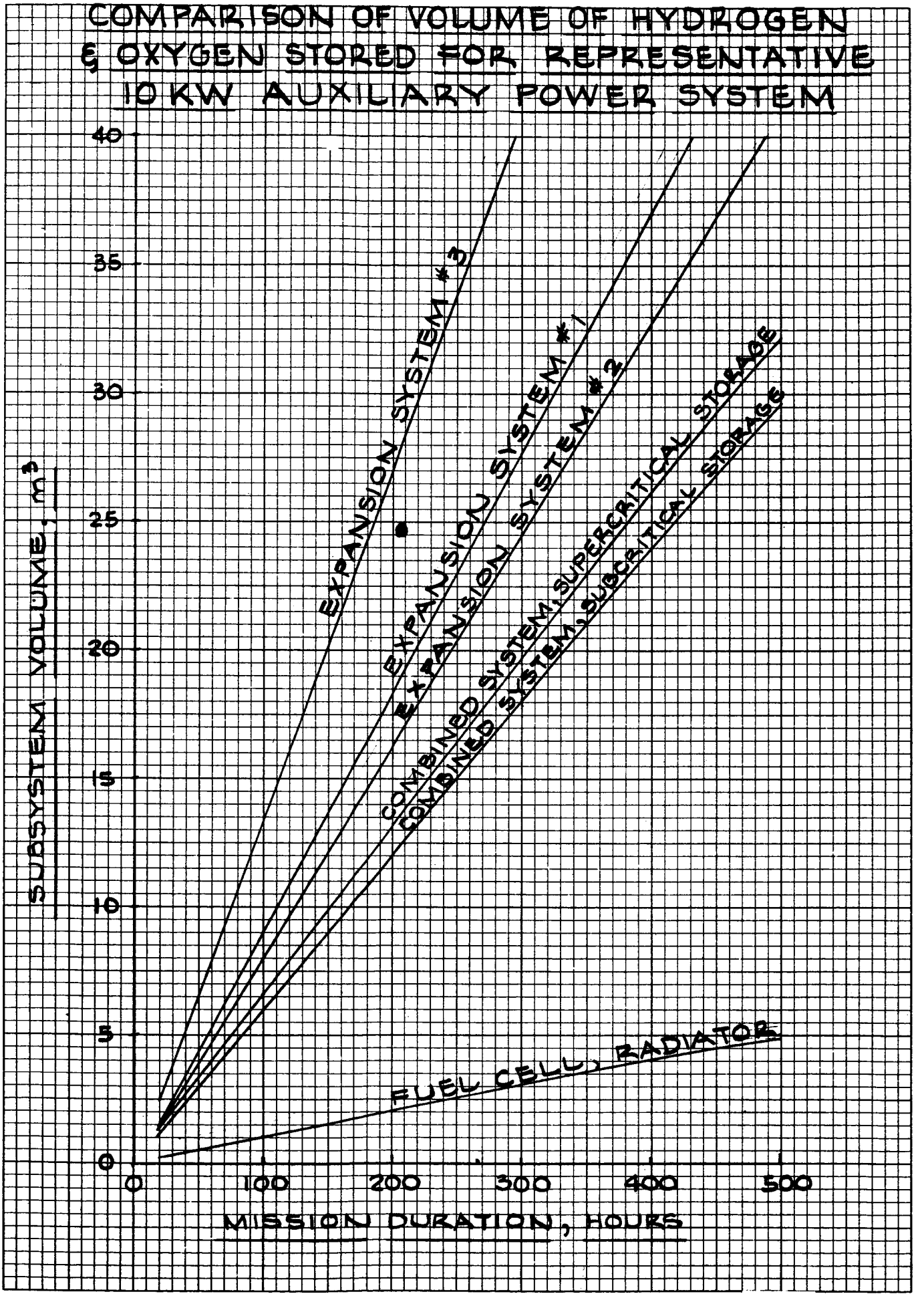
COMPARISON OF VOLUME OF HYDROGEN & OXYGEN STORED FOR REPRESENTATIVE 10 KW AUXILIARY POWER SYSTEM
SUBSYSTEM VOLUME, m³
40
35
30
25
20
15
10
5
0
0
100
200
300
400
500
MISSION DURATION, HOURS
EXPANSION SYSTEM #3
EXPANSION SYSTEM #1
EXPANSION SYSTEM #2
COMBINED SYSTEM, SUPERCRITICAL STORAGE
COMBINED SYSTEM, SUBCRITICAL STORAGE
FUEL CELL, RADIATOR

FIGURE 31

b. Moderately low fuel cell operating temperatures minimize materials problems.

c. These systems are largely static and are expected to require minimum redundancy.

d. Increased reliability can be obtained by partial system redundancy, as by supplying three units, any two of which can supply the required power.

5.2.4 Combined Systems

By properly combining the low temperature expansion system and the fuel cell system, a balanced system can be obtained for which no external heating or cooling is required. The waste heat from the fuel cell would eliminate the need for combustion of hydrogen in connection with the low temperature expansion system; the heat rejection capacity of the low temperature expansion system would eliminate the need for an additional heat sink system for the fuel cell.

Since low temperature expansion system vents unburned hydrogen, this hydrogen could conceivably be used in the fuel cell reaction. However, the pressure of the exhaust hydrogen is well below that desired for fuel cell operation and the flow rate for a thermally balanced system is about twenty times greater than fuel cell requirements. By adding a compressor to increase the pressure of a portion of the exhaust hydrogen for fuel cell use, a weight reduction on the order of 1 percent to 2 percent could be realized for long missions. The systems which were studied did not include this feature. A schematic of the combined fuel cell and low temperature expansion system which was used as the basis of this study is shown in Figure 32.

System Number 2 of the low temperature expansion systems was shown to be the lightest for missions longer than 30 hours (see Section 5.2.2). This system has an excess cooling capacity of about 0.65 kilowatt per kilowatt of load supplied by the system[2]. A combined system which supplies a maximum of 30 percent of the load with fuel cell power may be completely cooled with the exhaust hydrogen from the low temperature expansion cycle. A combined system in which more than 30 percent of the load is supplied by fuel cells will require additional hydrogen for cooling purposes.

Comparison of Figures 27 and 30 shows that the weight of a fuel cell system for a given power requirement is less than the weight of the corresponding expansion system. The weight of a combined system in which all cooling is supplied by the exhaust hydrogen from the expansion system varies with the load distribution as indicated in Figure 33. For missions longer than about 20 hours, a combined system is lighter than a straight expansion system. The combined system with minimum weight is obtained with the load shared on the basis of approximately 70 percent expansion system and 30 percent fuel cell system.

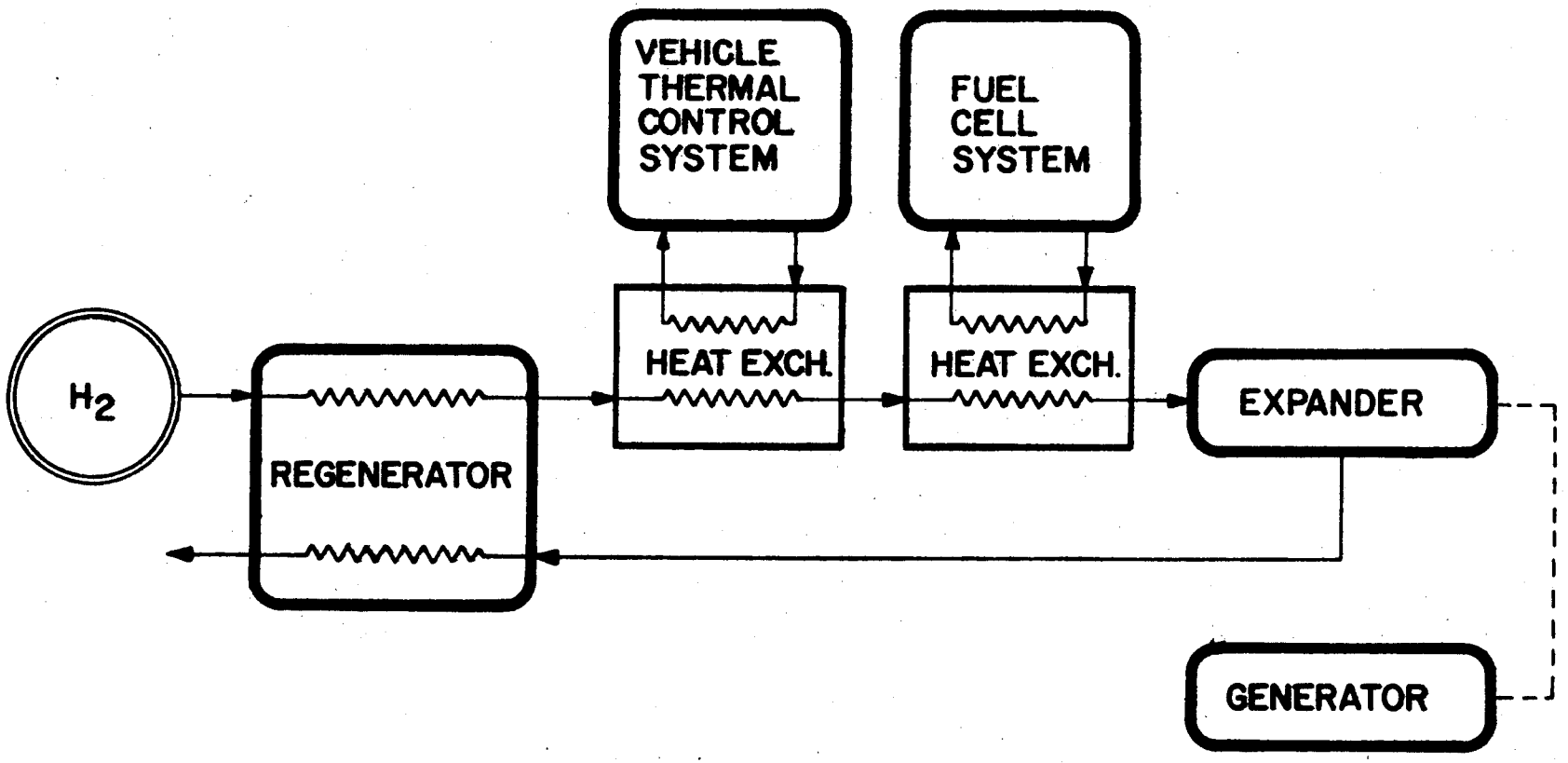

FIGURE 32

COMBINED FUEL CELL AND LOW TEMPERATURE EXPANSION SYSTEM

EFFECT OF LOAD DISTRIBUTION ON WEIGHT OF A COMBINED FUEL CELL & LOW TEMPERATURE EXPANSION SYSTEM

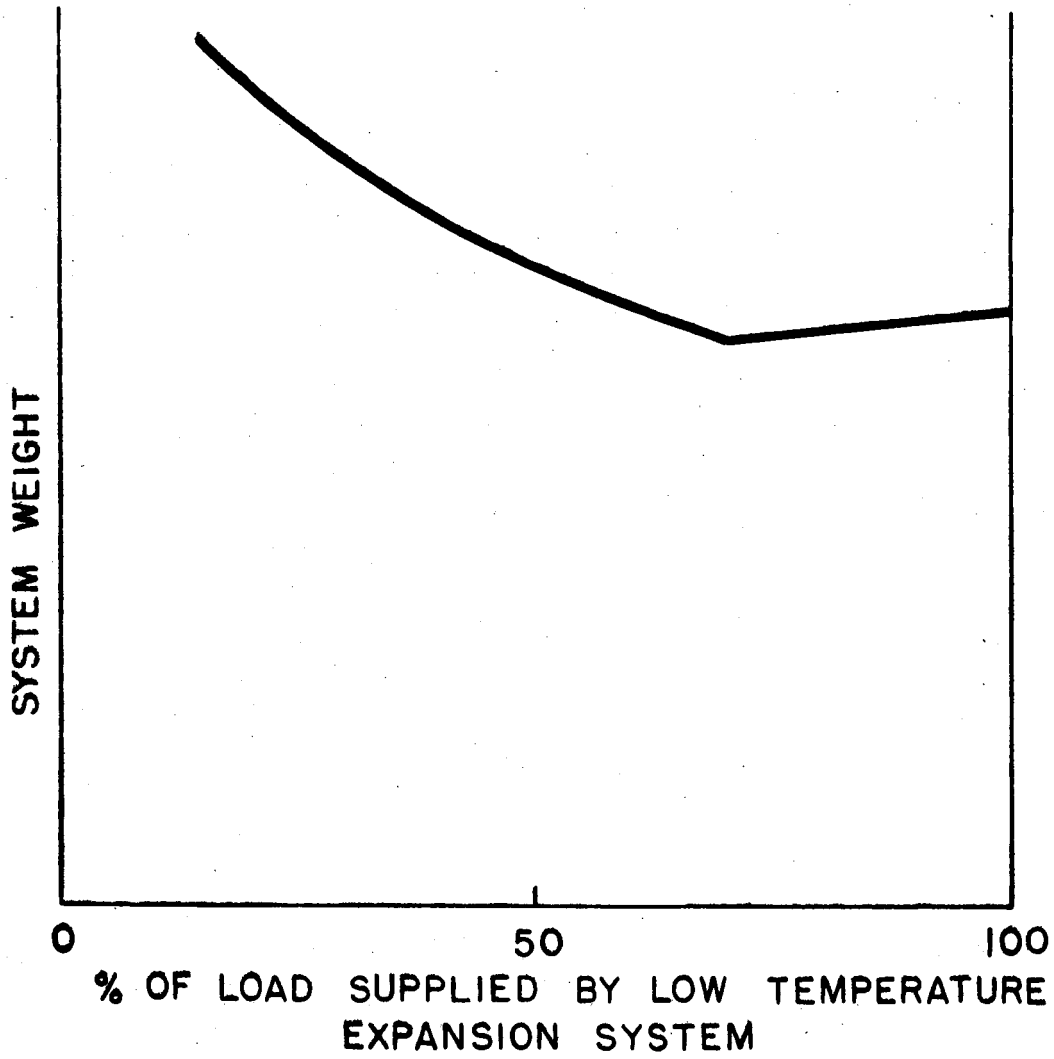

FIGURE 33

Weights of the lightest combined systems are given in Figure 34. Volumes of hydrogen and oxygen required for a representative 10 KW system are shown in Figure 31.

Additional characteristics of these combined systems are:

a. Ability to reject heat from the vehicle is not seriously affected by the vehicle thermal environment.

b. Low temperature operation avoids materials problems.

c. A larger number of components is required than for either separate system.

d. As many dynamic components are required as in a separate low temperature expansion system.

e. Redundancy for the fuel cell portion can be obtained on a partial system basis.

5.2.5 Comparison of Power Systems

The weight comparison of the low temperature expansion system, the fuel cell system and the combined system is shown in Figure 35. Two representative power levels (1 KW and 10 KW) are illustrated. A weight and volume comparison is given in Table II. In addition to providing auxiliary power, all systems compared are capable of providing complete cooling for the power supply unit and the vehicle electrical load.

The volume of hydrogen and oxygen stored, which is used as an indication of total system volume, is the least for the fuel cell system. The combined system has the next lowest volume, and the expansion system the highest. This is shown for a representative 10 KW power system in Figure 31.

Fuel cell systems lend themselves to modular construction and contain relatively few moving components. Low temperature expansion systems, on the other hand, contain a considerable number of dynamic elements and modular construction is not attractive. Inclusion of redundancy to meet a specified system reliability figure would therefore be expected to increase the weight of the expansion system proportionately more than the weight of the fuel cell system. As previously stated, the present analysis did not consider the use of redundant elements.

The main advantage of the expansion system lies in its relative freedom from the vehicle external thermal envrionment. The combined system also has this feature. Fuel cell systems require the use of radiators (or evaporators) to reject waste vehicle heat and the radiator effectiveness is limited by the vehicle environment. The radiator area depends upon operating temperature, fin effectiveness, radiator configuration and thermal environment, and for some missions, the necessary area may not be readily available.

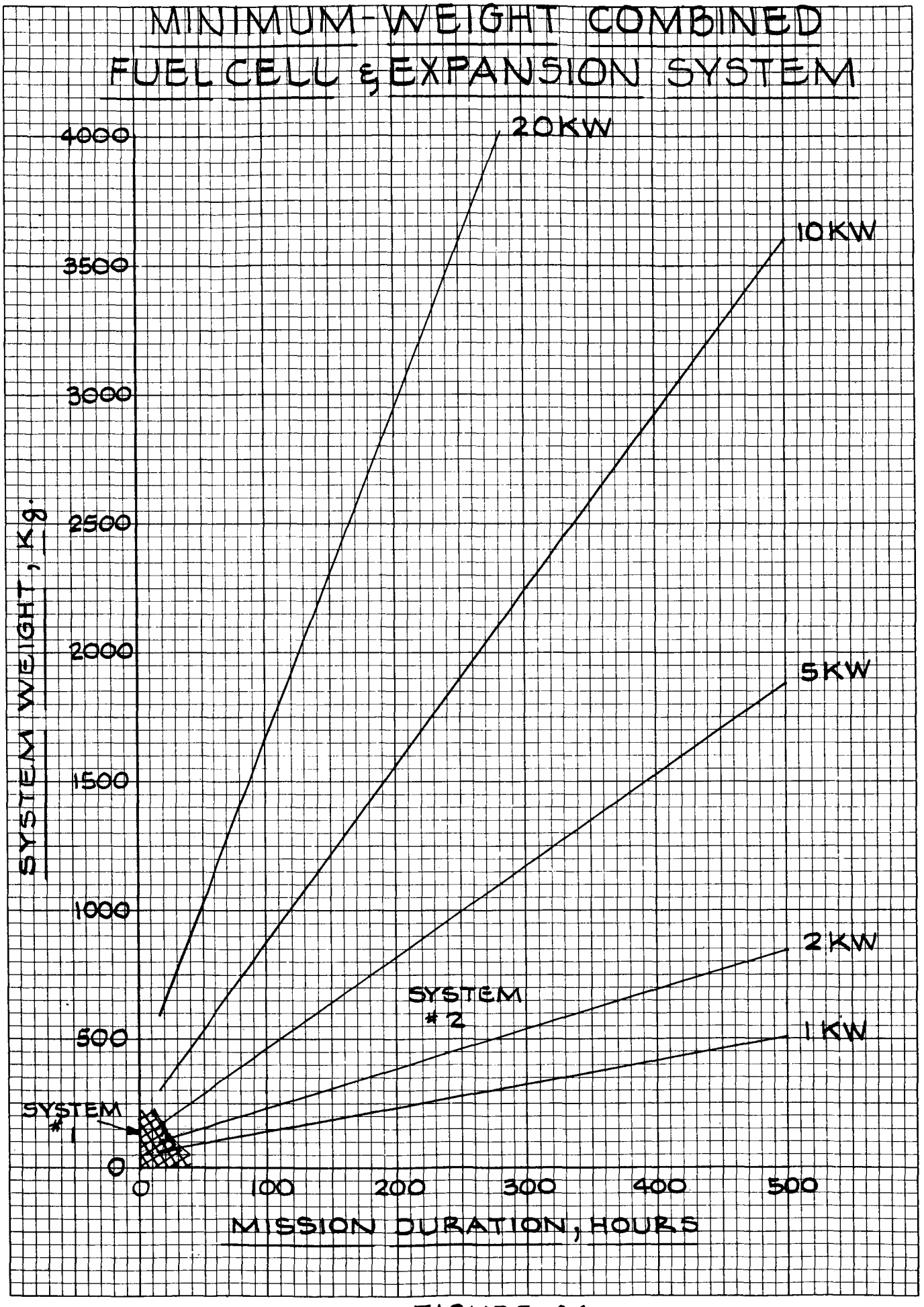
MINIMUM-WEIGHT COMBINED
FUEL CELL & EXPANSION SYSTEM
20KW
10KW
5KW
2KW
1KW
SYSTEM #2
SYSTEM #1
4000
3500
3000
2500
2000
1500
1000
500
0
0
100
200
300
400
500
SYSTEM WEIGHT, KG.
MISSION DURATION, HOURS

FIGURE 34

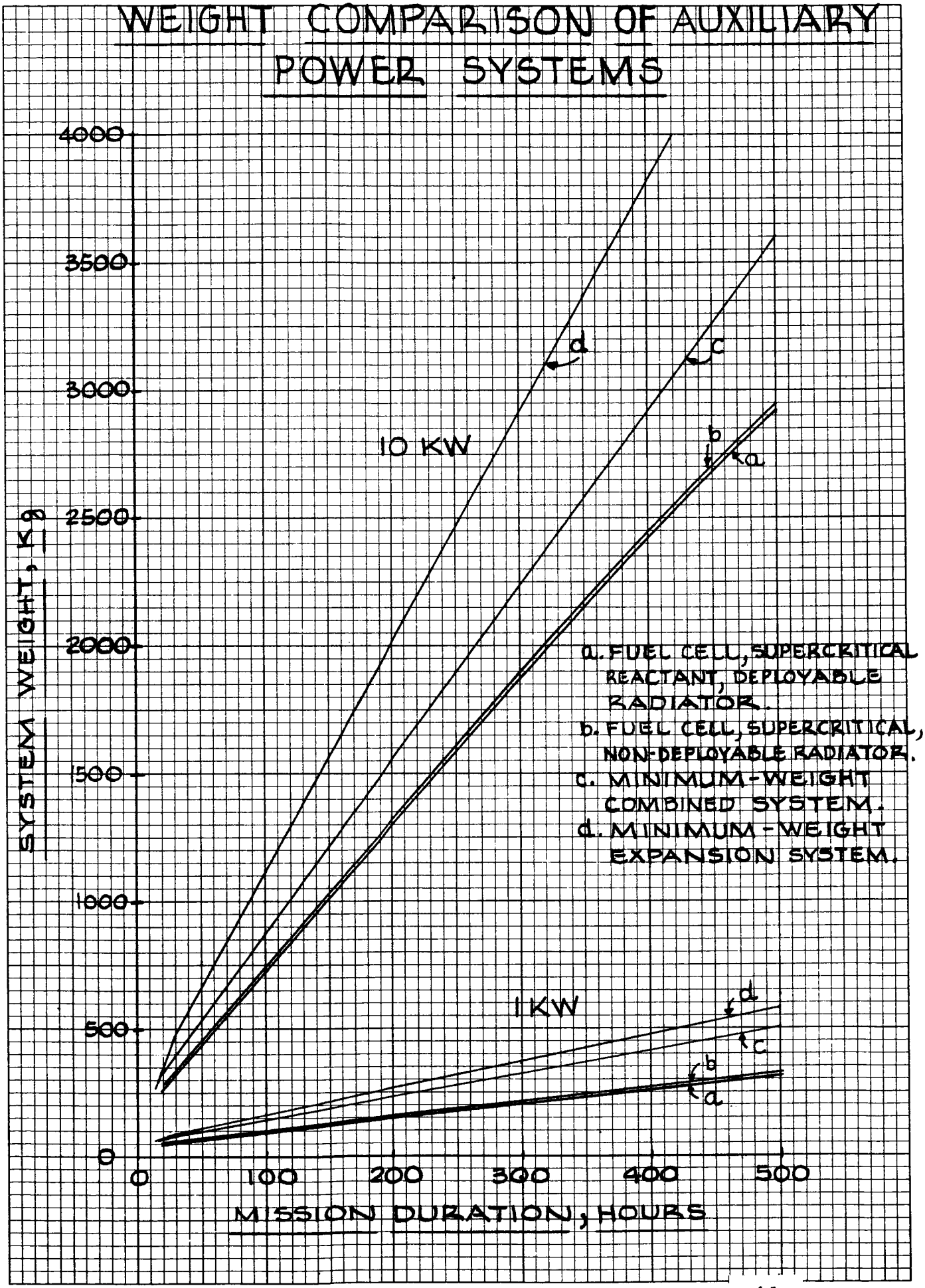
WEIGHT COMPARISON OF AUXILIARY POWER SYSTEMS
SYSTEM WEIGHT, Kg
4000
3500
3000
2500
2000
500
1000
500
0
0
100
200
300
400
500
MISSION DURATION, HOURS
10 KW
1 KW
a
b
c
d
a. FUEL CELL, SUPERCRITICAL REACTANT, DEPLOYABLE RADIATOR.
b. FUEL CELL, SUPERCRITICAL, NON-DEPLOYABLE RADIATOR.
c. MINIMUM-WEIGHT COMBINED SYSTEM.
d. MINIMUM-WEIGHT EXPANSION SYSTEM.

FIGURE 35

TABLE II

WEIGHT AND VOLUME COMPARISON OF POWER SYSTEMS FOR LUNAR LOGISTICS VEHICLE AND SIMILAR MISSIONS

Description of System	Weight Rank*	Volume Rank*
Fuel cell with deployed radiator heat sink	1	1
Fuel cell with nondeployed radiator heat sink	2	2
Combined fuel cell and low temperature expansion system	3	4
Low temperature expansion system	4	5
Fuel cell with water evaporator heat sink	5	3

* Weight and volume increase with increasing rank.

6.0 COMPARISON OF STATIC MOISTURE REMOVAL AND DYNAMIC VAPOR PRESSURE CONTROL SYSTEMS

A weight and feasibility comparison between fuel cell systems using the Dynamic and those which use Static Moisture Removal was conducted. Analysis of the dynamic system included design of the cell electrode holder plates for minimum weight and estimation of weights and parasitic power requirements for flyable versions of the components used in the dynamic system breadboard design.

The weight constants used in the weight optimizing computer program were evaluated for the dynamic system and the program was used to obtain minimum weight designs. Comparison between the static and dynamic systems was made on the basis of equal net power output. In general, the dynamic system has a shorter cell stack than the static system which incorporates a water removal plate associated with each cell. On the other hand, the dynamic system requires additional auxiliaries external to the cell stack and has a considerably greater parasitic load.

The weight comparison covered the range of 1 to 10 KW power requirements and mission durations from 0.5 to 500 hours. The dynamic system is heavier than the static system except for very short missions. The cross-over time is about three hours for a 10 KW system. Figure 36 shows a weight comparison of the two systems.

Comparison of the volumes required for the two systems for a representative range of missions is shown in Table III. The dynamic system has the smaller volume only for high power, short duration missions, such as the 10 KW 5 hour mission shown in the table.

The waste heat produced by the two systems has been calculated and compared as an indication of the relative radiator areas required. For a fixed voltage and power output, the dynamic system will produce a larger heat burden by virtue of its greater parasitic power requirement. When each system operates at its optimum voltage for a particular mission, the comparison of required radiator area is shown in Figure 37. The dynamic system generally requires more radiator area than the static system, but as the mission power levels increase, the required areas tend to become equal.

On the basis of the smaller number of components required, and on the trouble-free operation of large numbers of static cells in the laboratory, the static system is expected to attain a considerably higher reliability than the dynamic system.

For any of the Lunar Logistics Missions outlined in MTP-M-63-1 Volume V[3], the static fuel cell is the lighter, has the smaller volume and is the more feasible system.

SYSTEM WEIGHT COMPARISON, STATIC & DYNAMIC MOISTURE REMOVAL SYSTEMS

1965 FUEL CELL CAPABILITY
SUPERCRITICAL STORAGE (20% EXCESS)
DEPLOYABLE RADIATOR

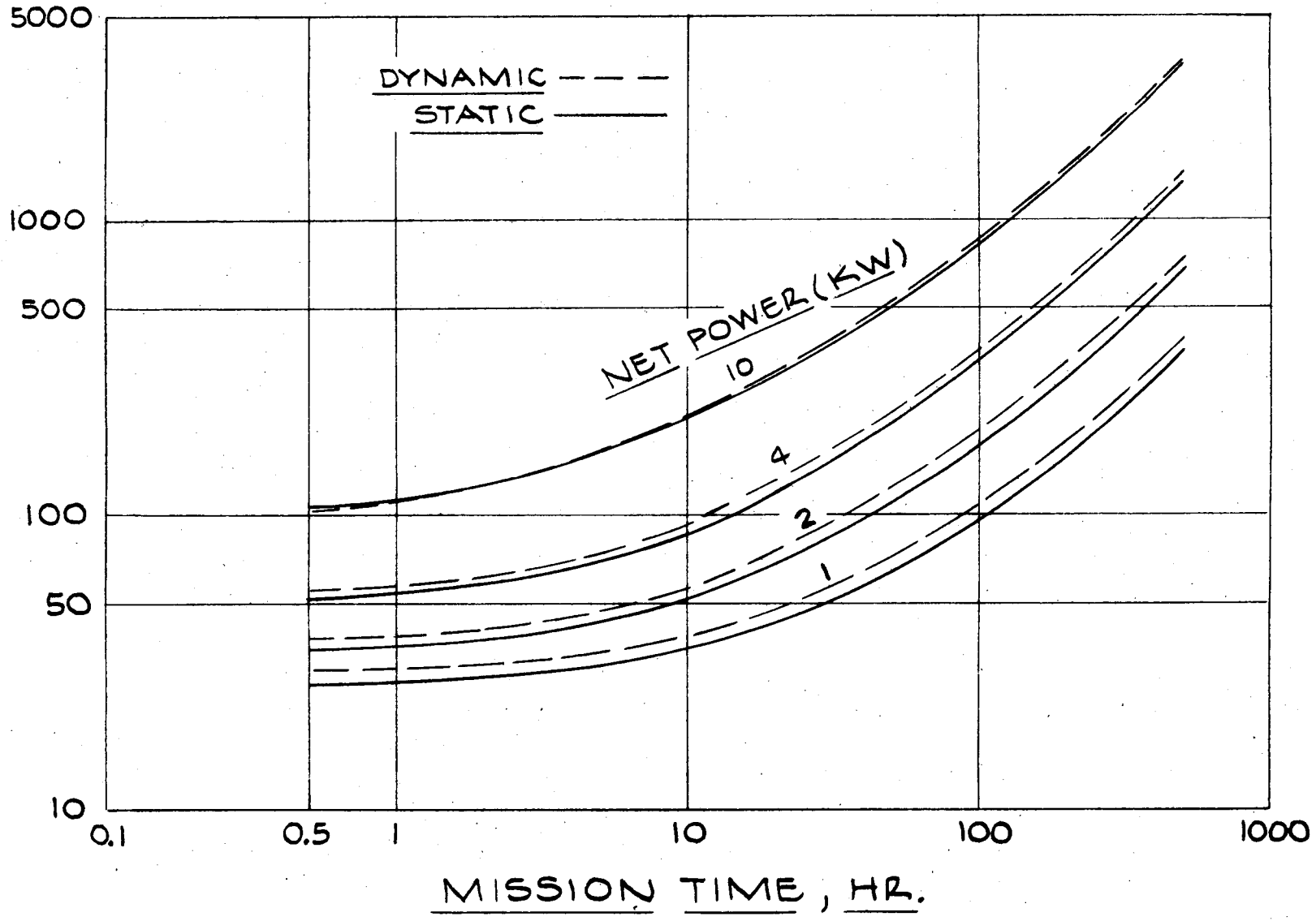

FIGURE 36

TABLE III

COMPARISON OF ESTIMATED VOLUMES OF STATIC AND DYNAMIC VAPOR PRESSURE CONTROL SYSTEMS

MISSION		SYSTEM VOLUME (m^3)	
POWER (WATTS)	MISSION DURATION (HR)	STATIC	DYNAMIC
1000	5	0.0267	0.0276
1000	500	0.716	0.786
2000	500	1.29	1.40
4000	500	2.42	2.57
10,000	5	0.168	0.158

COMPARISON OF RADIATOR AREA REQ'D. FOR STATIC & DYNAMIC SYSTEM

1968 FUEL CELL CAPABILITY
28 ±2 VOLT SYSTEM
OPERATION AT OPTIMUM VOLTAGE
SUPERCRITICAL H_2 & O_2 STORAGE
DEPLOYED RADIATOR

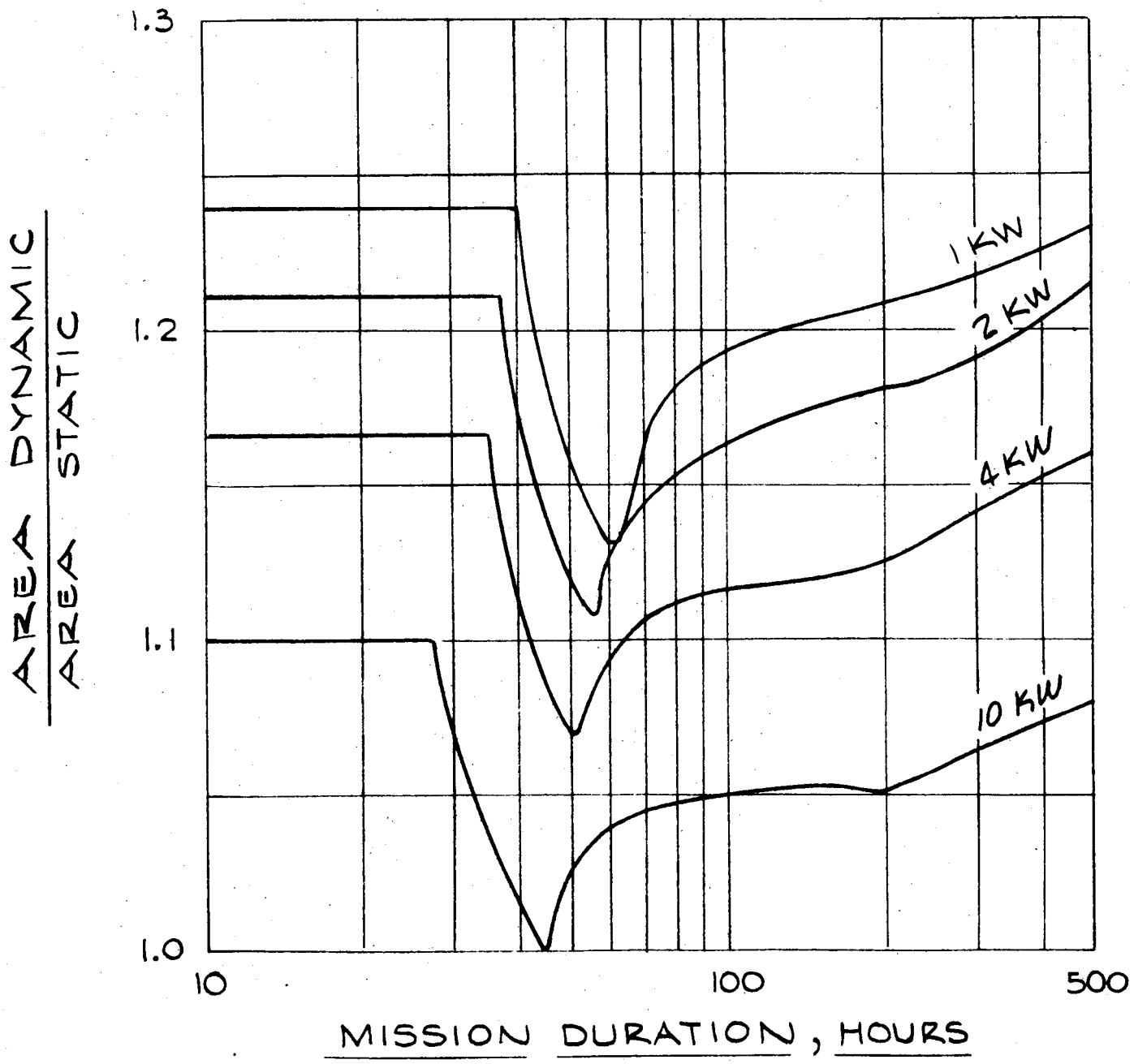

FIGURE 37

7.0 WEIGHT ANALYSIS OF A POWER SYSTEM FOR A LUNAR SURFACE VEHICLE

A weight and feasibility analysis was performed for the electrical power system of the Mobile Laboratory. This vehicle is intended for use in exploration of the lunar surface. The vehicle mission consists of a launch by an Apollo vehicle, a LEM truck landing on the moon, storage on the lunar surface for up to 5,000 hours and operation during a fourteen day exploratory excursion.

The conceptual design of the power system consists of:

a. Hydrogen-oxygen fuel cells as the primary power source.

b. Rechargable batteries for start-up and peak power.

c. Reactant storage and supply equipment.

d. Heat rejection equipment.

e. Potable water recovery and supply equipment.

f. All necessary controls and regulating equipment.

The power system is to supply all the electrical power required for operation of Molab, including the vehicle drive, environmental control and communications.

7.1 System Specifications

The system requirements which were significant in the weight analysis are:

7.1.1 The power system must have full operational capability on the lunar surface under all extremes of temperature, pressure and radiation.

7.1.2 The load profile for the fourteen day mission is summarized in Table IV.

7.1.3 The system must be capable of withstanding up to 5,000 hours storage on the lunar surface in a shut-down condition without experiencing depreciation of performance.

7.1.4 Voltage regulation for all load conditions defined in the power profile shall be within 28 ± 2 volts.

TABLE IV

TYPICAL POWER PROFILE

Mission Day	Average Power (KW)	Duration (Hours)	Consumption (kwh)
1	0.05	2.4	0.12
	4.5	8.4	3.78
	2.0	2.4	4.80
	8.0	momentarily	----
	4.0	3.6	14.40
	2.0	7.2	14.40
2	4.5	3.6	16.2
	3.5	6.0	21.0
	2.0	7.2	14.4
	9.0	momentarily	----
	6.0	2.4	14.4
	3.5	1.2	4.2
	2.0	3.6	7.2
3, 4, 5, 6 and 7	7.5	momentarily	---
	6.0	3.6	21.6
	3.5	6.0	21.0
	2.0	4.8	5.6
	6.0	3.6	21.6
	3.5	2.4	8.4
	2.0	3.6	7.2
8, 9, 10, 11 and 12	9.5	momentarily	---
	6.0	2.4	14.4
	4.0	6.0	24.0
	2.0	4.8	9.6
	8.5	1.2	10.2
	4.0	2.4	9.6
	2.0	7.2	15.4
13	6.0	2.4	14.4
	9.0	momentarily	---
	6.0	3.6	21.6
	2.0	9.6	19.2
	4.5	2.4	10.8
	8.5	momentarily	---
	4.5	2.4	10.8
	2.0	3.6	7.2
14	3.0	6.0	18.0
	2.0	6.0	12.0
	0.05	12.0	0.6

7.1.5 Batteries shall have a nominal set output voltage of 28 volts. As a minimum, the kilowatt-hour capacity of the batteries shall be capable of supplying all start-up power for the fuel cell subsystem.

7.1.6 Potable water shall be recovered from the fuel cell product water at a rate of 11.7 earth kilograms per 24 hours.

7.2 Battery Subsystem

Silver-cadmium batteries were selected for the battery subsystem. This couple appears to offer the best available combination of specific energy and reliability. Its electrical characteristics facilitate control of the charge cycle.

Electrical capacity of the battery subsystem was selected so that all loads in the power profile greater than 6.0 kilowatts was supplied by the batteries. This capacity, 3.0 kilowatt-hours, is also the amount required to supply start-up power for heating the fuel cell subsystem from 0° C to operating temperature.

The charge-discharge characteristics of the silver-cadmium cell are shown in Figure 38. System design was based on a maximum discharge of 35% of the battery capacity. This allowed operation entirely within the higher voltage range of the cell, resulting in better charge efficiency, higher reliability and more uniform operating voltage.

Assuming discharge of the batteries occurs at 26.4 volts, the ampere-hour capacity of the batteries will be

$$C = \frac{3000}{(26.4)\ (.35)} = 325 \text{ amp-hours}$$

Discharge during the 8.5 kilowatt peak will be at the rate of

$$I_D = \frac{8500 - 6000}{26.4} = 94.5 \text{ amps}$$

or, expressed in the terms usually used for batteries

$$I_D = \frac{2}{7} C$$

CHARGE - DISCHARGE CHARACTERISTICS OF A TYPICAL SILVER - CADMIUM CELL

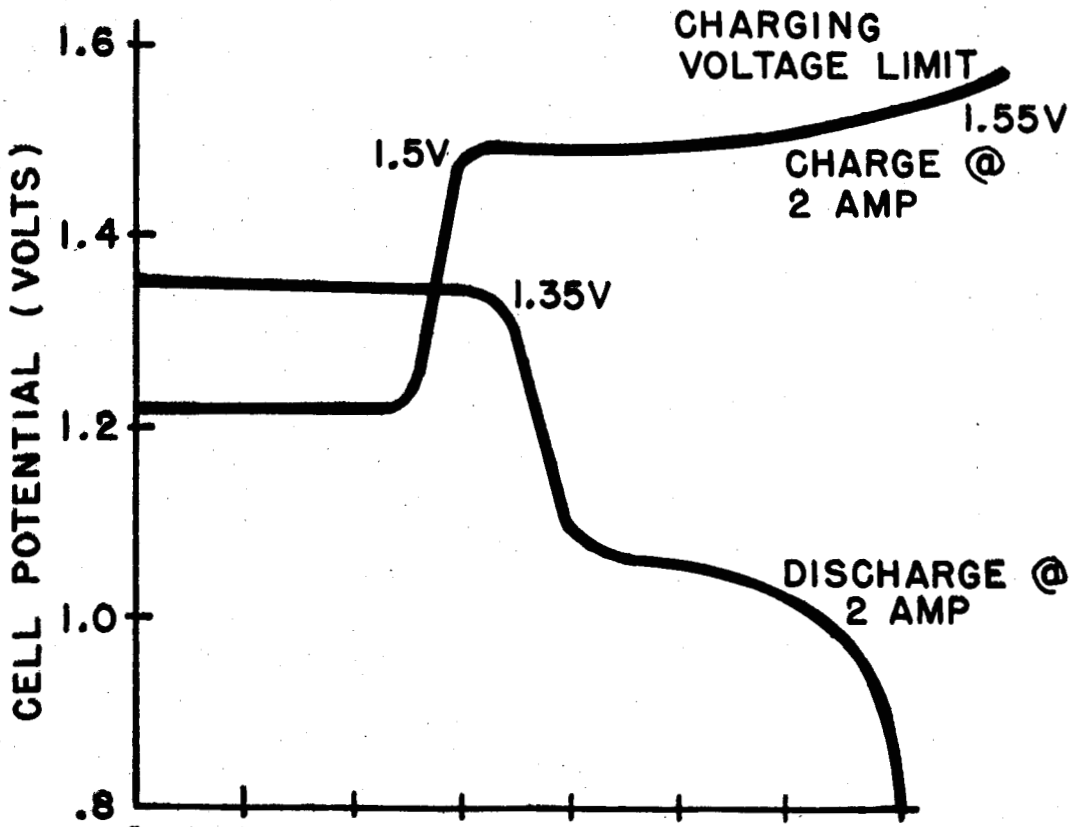

FIGURE 38

Recharge of the battery system will be accomplished during the 9.6 hour period following discharge. Charging is performed at a constant current which would return 110 % of the discharged ampere-hours during the time available for charging, with termination of the charge when 1.55 volts per cell is reached. Hence, the charging current is approximately

$$I_C = \frac{(.35)(325)(1.1)}{9.6} = 13.0 \text{ amps}$$

Charging is accomplished at about 1.5 volts per cell, or 30 volts for the battery. If the charging circuitry is assumed 85 % efficient, the power required for charging is

$$P_C = \frac{(13.0)(30.0)}{0.85} = 460 \text{ watts}$$

Charging power must be added to the power profile for the fuel cell subsystem.

Weight of the battery subsystem was estimated on the basis of projected specific energy for 1968. For a 80% discharge depth, the specific energy of silver-cadmium batteries is expected to be 53 watt-hours/kg. For a discharge depth of 35%, this corresponds to 24 watt-hours/kg. Hence, the weight of the battery subsystem is

$$W_B = \frac{3000}{24} = 125 \text{ kg.}$$

7.3 Fuel Cell Subsystem

Design of the fuel cell subsystem was based on the 1968 projected polarization curve shown in Figure 16. The chosen system configuration consisted of three modules, any two of which could supply all load requirements.

Requirements for fuel storage and heat rejection for this mission were completely different from those previously considered. The computer program for system weight optimization (see Section 4.0) was therefore useful to only a limited extent. The program was used to obtain a curve of fuel cell system weight as a function of cell operating voltage. The optimum parameters were determined manually.

The resulting fuel cell design supplies 6.0 kilowatts at 27.8 volts, and 2.0 kilowatts at 29.9 volts. The weight of a single module is 38 kg, and the weight of the subsystem, including the redundant module, is 114 kg.

7.4 Power Conditioning Equipment

Electrical characteristics of the battery and fuel cell are such that additional equipment is required to assure proper operation of the combined system. Figure 39 shows approximate characteristics of the fuel cell, battery, and combined system. If the fuel cell and battery were connected in parallel with the load, the following conditions would prevail:

a. With the load disconnected, the fuel cell would charge the batteries and would be capable of exceeding the maximum safe charging voltage of 1.55 volts/cell.

b. With vehicle loads in excess of 2 kilowatts, the fuel cell would not develop the necessary battery charge voltage of 1.5 volts/cell and, hence, the batteries could not be recharged.

c. If the battery system is designed so that no power is supplied by the batteries until the load exceeds 6.0 kilowatts, then at the 8.5 kilowatt level, the fuel cells will actually supply about 7.2 kilowatts.

The power conditioning equipment incorporates the circuitry and controls needed to supervise the distribution of the electrical load between the fuel cells and the batteries. It also contains voltage boosting and regulation equipment for charging the batteries. The electrical output from the power conditioning equipment will be as indicated by the broken lines in Figure 39.

Weight of the power conditioning equipment was estimated to be about 35 kg.

7.5 Radiator Subsystem

Design of the radiator was based on an armored tube-fin configuration with fins 90% effective. The radiator was assumed to be mounted atop the Molab vehicle with a horizontal orientation and a surface emissivity of 0.85 and absorptivity of 0.25. An average radiator temperature of 93° C was assumed with the fuel cell operating at 107° C. All the waste heat from the power supply, including parasitic power losses, was rejected by the radiator. Water produced by the fuel cell in excess of the specified potable water requirements was used as a heat sink during the periods of maximum heat rejection.

For the assumed conditions, the required radiator area will be about 1.9 square meters per kilowatt of heat rejected and the weight will be about 5.6 kilograms per square meter. Evaporation of water rejects about 560 caolories per gram of water evaporated.

A trial-and-error procedure was used to determine the minimum radiator size required when heat rejection is supplemented by evaporation of excess

POWER SYSTEM ELECTRICAL CHARACTERISTICS

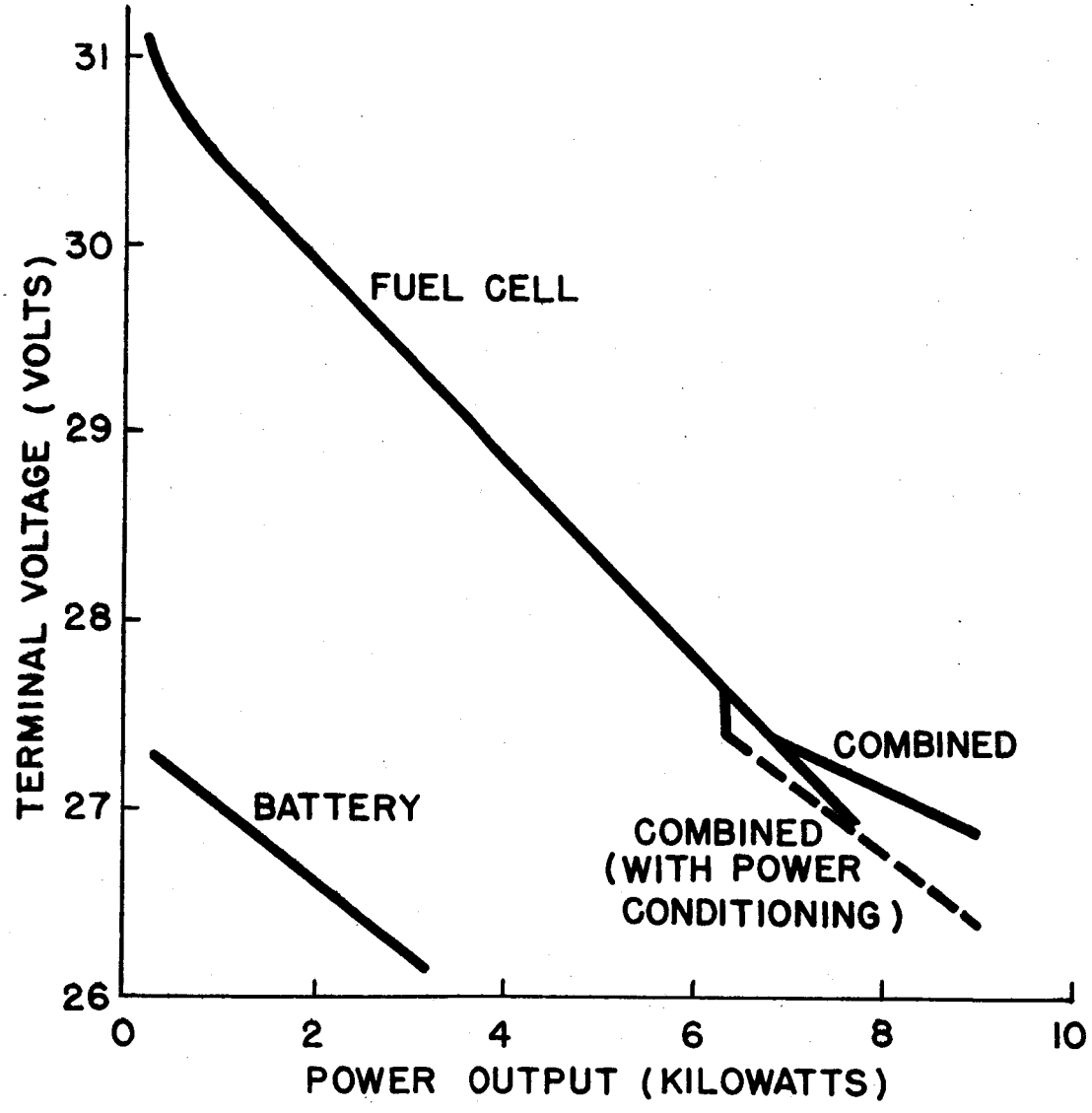

FIGURE 39

fuel cell product water. The result is a radiator capable of rejecting 2.1 kilowatts of waste heat. Water evaporation is required as indicated in Figure 40. As shown in the figure, evaporation of water at a rate exceeding the production of water in the cell is required only for the 6.0 and 8.5 kilowatt loads. At the other load levels which occur in the load profile, at least part of the water is condensed and collected.

The area of the radiator will be

$$A = (2.1)(1.9) = 4.0 \text{ square meters}$$

Weight of the radiator will be

$$W_R = 4.0\ (5.6) = 22 \text{ kilograms}$$

7.6 Fuel Storage and Supply Subsystem

Accurate data is not available for cryogenic tankage to store reactants for the specified 5,000 hours on the lunar surface. An extrapolation of the subcritical reactants tankage data given in Figures 24 and 26 was used. The values which were used are:

a. Hydrogen: 5 kilograms launch weight per kilogram consumed.

b. Oxygen: 1.15 kilograms launch weight per kilogram consumed.

Allowing reactants 10% in excess of stoichiometric requirements to provide for purge and a residual in the tanks, the weight of fuel storage and supply subsystem is 730 kilograms.

7.7 Summary of the Weight Analysis

The weight of the power supply for the Molab is estimated to be:

Battery subsystem	125 kg
Fuel cell subsystem	114 kg
Power conditioning equipment	35 kg
Radiator	22 kg
Fuel storage and supply subsystem	730 kg
TOTAL	1,026 kg

Radiator area: 4.0 square meters.

WATER EVAPORATION RATES FOR SUPPLEMENTAL COOLING

RADIATOR DESIGNED FOR 2.1 KILOWATTS OF HEAT REJECTION AT 93°C

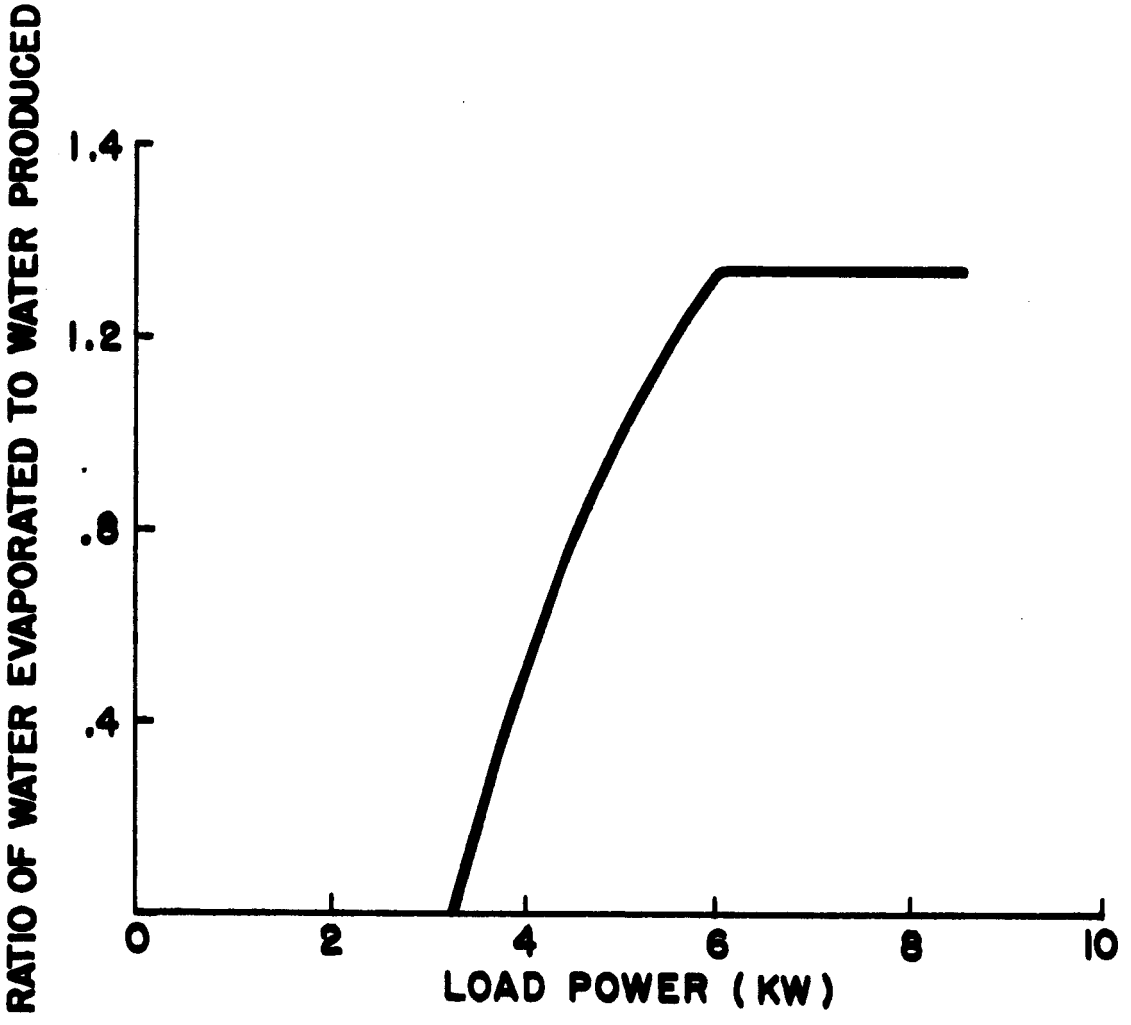

FIGURE 40

8.0 CONCLUSIONS

Hydrogen-oxygen fuel cells employing Static Moisture Removal were shown to be feasible and breadboard tests were conducted over a range of current densities up to 214 ma/cm^2. Results of tests on the breadboard system have further simplified the system by showing that water removal on only one side of the cell with a single cavity pressure setting for loads varying over a broad range is possible.

The static system is well suited for operation in a space environment since all fluid transport occurs in the gaseous state and all liquids in the system are contained in capillaries. When recovery of product water is not desired, a significant thermal advantage is realized with this system since approximately 35 % of the waste heat burden produced in the cell may be ejected directly to space vacuum as latent heat of vaporization of the product water. This reduces the heat burden imposed upon the space vehicle heat rejection system.

Static Moisture Removal eliminates the need for recirculating reactant pumps, condensers and gas-water separators. The absence of these components and their associated parasitic power requirements, valves, piping and connections makes Static Moisture Removal an inherently efficient and reliable system.

The mechanism of water removal from a cell with Static Moisture Removal is complicated by the existence of electrolyte concentration gradients in the direction of reactant flow. However, one of the primary purposes of this series of tests was the measurement of the diffusion coefficient for water in an aqueous KOH solution. It is now apparent that this is not practical with an operating cell.

Diffusion of hydrogen through the water removal membrane of a cell operated with Static Moisture Removal occurs at a low rate. For the range of cavity pressures normally used (corresponding to 35% to 40% KOH), the rate of diffusion would amount to about 0.1% of consumption at rated load for a 2 kilowatt unit. The rate of diffusion appears to be about 50% greater at a cavity pressure corresponding to 46% KOH than at a pressure corresponding to 33% KOH. This is attributed to the smaller volume of electrolyte through which diffusion must occur for the higher concentrations.

The weight of a fuel cell system for a general mission can be minimized by proper selection of cell operation voltages. The requirement of voltage regulation prevents a complete optimization of system weight in a large class of problems. Due to the large number of variables which are involved in describing such a system, it is not possible to draw completely general conclusions regarding optimum voltages or minimum system weights. However, for missions in which the power requirement is sufficiently uniform, an empirical equation has been derived which adequately reproduced the computer results.

For some missions, the minimum weight auxiliary power system will consist of fuel cells for some base load and batteries for peak loads. When a mission requires only two levels of power, the duration of peak power output for which the weight of a combined system equals the weight of a fuel cell system has been expressed in terms of the load power levels and mission duration.

For the Lunar Logistics Vehicle and other similar missions, the fuel cell power system with a radiator heat sink is lighter and more feasible than either the combination of a fuel cell and low temperature expansion system or the separate low temperature expansion system. For missions in which the effectiveness of a radiator is limited by the vehicle thermal environment, the combined system is lightest.

Static Moisture Removal allows fuel cell system weight reduction compared to the dynamic system for all mission requirements of 4 kilowatts or less, and for 10 kilowatt systems for missions greater than three hours.

REFERENCES

1. "Investigation of a 3 KW Sterling Cycle Solar Power System", (Volume VII, Space Radiator System Analysis) Technical Report Number WADD-TR-61-122, March 1962.

2. "The Cryhocycle", Sundstrand Aviation - Denver.

3. "Flight Astrionics Aspects of the Lunar Logistic Vehicle Study", by Astrionics Division of the George C. Marshall Space Flight Center, Huntsville, Alabama. MTP-M-63-1, Volume V.

4. "Combined Fuel Cell - Cryhocycle Weight and Feasibility Study: Terminal Report", F. J. Arnaud, Allis-Chalmers, 1962.